Spatial planning of a bulk power system with high residential heat pump adoption

Claire Halloran

Keble College

University of Oxford

A thesis submitted for the degree of

Doctor of Philosophy

Hilary 2024

Acknowledgements

This thesis would not be possible without 50 kilograms of coffee and the support of countless people.

Thank you to my supervisor, Prof. Malcolm McCulloch, for making time for a last-minute DPhil student in your busy schedule and for providing support and guidance for the past three and a half years.

I would also like to thank my informal supervisors, Dr. Fili Fele and Prof. Jesús Lizana. Fili, thank you for your mentorship and teaching during the first years of my DPhil. Jesús, thank you for your support and patience in the final years of my DPhil.

Thanks to my colleagues in the Energy and Power Group for their support and friendship throughout this process. I appreciated the company of my fellow DPhil students, Abdullah, Alycia, Amelia, Andris, Aniq, Becky, Chris, Daniel, Farhad, Flora, Jen, Kevin, Miriam, Mónica, Sarah, Thorston, Tonny, and Yifu. A special thanks to Mallory for keeping the group running smoothly and answering all of my frantic emails.

Thanks to the Rhodes Trust for financially supporting this work and my time in Oxford. Thank you to Kim for guiding me through the Rhodes application process and for helping me figure out what I want to be when I grow up.

I am grateful for my friends that made Oxford home: Jenny, Josh, Miriam, Sara, Taylor, and the rest. You all kept me sane throughout this process.

I could not have made it through this degree without the support and love of my family. Thank you, Mom and Dad, for always supporting my aspirations without question, even when they involved more years of school. You both made me who I am today. Sophia, thank you for being a lifelong friend and for inspiring me with your strong sense of justice. Grace, thank you for your willingness to move to a strange island with me. I can never thank you enough for the past five years of love, support, and joy.

Abstract

This thesis investigates the impact of widespread residential heat pump use on bulk power system planning at high spatial resolution.

The electrification of residential heating offers a challenge for power systems in drastically increased peak demand. At the same time, flexible heating could reduce demand peaks and increase use of renewable generation. While studies have identified spatial variation in heating demand and flexibility potential, these differences have not yet been incorporated into bulk power system planning. By incorporating spatial heating data and projections into capacity expansion planning, this thesis accounts for spatial variation in a future with high residential heat pump adoption. The research contributions are divided into four chapters. The first two research chapters focus on heating demand, and the final two research chapters focus on heating flexibility.

Reanalysis weather data is used to scale limited heat pump demand data from field trials to regional hourly demand projections. A power system planned with regional hourly heat pump demand is compared to a system planned with conventionally used, spatially uniform heat pump demand. Cost-optimal placement of generation and storage capacity requires regional hourly heat pump demand data, and using spatially uniform heat pump demand for planning leads to load shedding.

Space heating flexibility potential in the current residential housing stock is quantified using a top-down, data-driven method based on historical weather data and sub-national annual gas demand. This heating flexibility potential is incorporated into a capacity expansion model to assess where flexibility offers the most value to the bulk power system. Heating flexibility is most valuable in regions with moderate thermal energy storage losses near demand centers; in low-carbon scenarios, heating flexibility is most valuable in regions with the lowest thermal energy storage losses. A wide range of regional flexibility participation can achieve at least 95% of optimal flexibility savings.

This thesis demonstrates the importance of considering regional differences in heating demand and flexibility potential when planning bulk power systems. While this thesis focuses on the case study of Britain, the methods can be applied across cold and temperate countries transitioning from fossil fuel-based heating systems to electric heat pumps.

Contents

List of Figures

List of Tables

List of Abbreviations

AC . . . . . alternating current

ASHP . . . . . air-source heat pump

BDEW . . . . Bundesverband der Energie- und Wasserwirtschaft (German Association of Energy and Water Industries)

CCC . . . . . Climate Change Committee

COP . . . . . coefficient of performance

DESNZ . . . . Department for Energy Security and Net Zero

DHW . . . . . domestic hot water

DNO . . . . . distribution network operator

DZ . . . . . Data Zone

ECUK . . . . . Energy Consumption in the UK

ENTSO-E . . European Network of Transmission System Operators for Electricity

EPC . . . . . energy performance certificate

ESO . . . . . electricity system operator

EU . . . . . European Union

EV . . . . . electric vehicle

ERA5 . . . . . ECMWF (European Centre for Medium-Range Weather Forecasts) Reanalysis v5

EDRP . . . . . Energy Demand Research Project

FOM . . . . . fixed operations and maintenance

GSHP . . . . . ground-source heat pump

GSP . . . . . grid supply point

HDD . . . . . heating degree days

HVDC . . . . high voltage direct current

IEA . . . . . International Energy Agency

LSOA . . . . . Lower layer Super Output Area

LV . . . . . low-voltage

MGA . . . . . modeling to generate alternatives

NCA . . . . . National Comprehensive Assessment

PV . . . . . photovoltaics

RHPP . . . . . Renewable Heat Payment Plan

SPF . . . . . seasonal performance factor

TAE . . . . . total absolute error

TAPE . . . . . total absolute percent error

UK . . . . . United Kingdom

US . . . . . United States

VoLL . . . . . value of lost load

VOM . . . . . variable operations and maintenance

WSHP . . . . water-source heat pump

Nomenclature

$A_{n,s}$	number of households at each bus n heating with air-source or ground-source heat pumps s (unitless)
A_r	number of households in region r (unitless)
$a_{n,s}$	number of households heating flexibly at bus n with either air-source or ground-source heat pumps s (unitless)
$C*$	minimum power system cost (€)
C_{lc}	cycle incidence matrix for cycles c and edges l (unitless)
C_r	average heat capacity of residential buildings in region r (kWh/℃)
CAP_{CO2}	carbon dioxide emissions budget (Mt CO_2e)
$COP_{r,s,t}$	coefficient of performance for region r at time t for heat pump type s (unitless)
c_l	capital cost of branch l (€/MW)
$c_{n,s}$	capital cost of technology s at bus n (€/MW)
D_t^{ASHP}	normalized hourly ASHP demand at time t (unitless)
$D_t^{HH,ASHP}$	hourly ASHP demand per household at time t (kW)
D_t^{GSHP}	normalized hourly GSHP demand at time t (unitless)
$D_t^{HH,GSHP}$	hourly GSHP demand per household at time t (kW)
$d_{n,s,t}$	load of type s at bus n at time t (MW)
$d_{n,ground,t}$	ground-source heating demand at bus n at time t (MW_{th})
$d_{n,air,t}$	air-source heating demand at bus n at time t (MW_{th})
E_s	carbon dioxide emissions intensity of generation source s (kg CO_2e/MWh)
$\bar{e}_r$	total thermal energy storage capacity in region r (kWh)
$\bar{e}_{n,s}$	store energy capacity at bus n for store type s (MWh)
$\bar{e}_{n,s}*$	optimal store energy capacity at bus n for store type s (MWh)
$\bar{e}_{n,s}^{min}$	near-optimal minimum store energy capacity at bus n for store type s (MWh)

$\bar{e}^{max}_{n,s}$	near-optimal maximum store energy capacity at bus n for store type s (MWh)
F_l	capacity of branch l (MW)
$\hat{F}_l$	maximum possible capacity of branch l (MW)
$\tilde{F}_l$	existing capacity of branch l (MW)
$\bar{f}_l$	AC line security margin (p.u.)
$f_{l,t}$	power flow on branch l at time t (MW)
$f_{n,s,t}$	charge of storage unit s at bus n at time t (MW)
$\bar{g}_{n,s}$	capacity of generator s at bus n (MW)
$\tilde{g}_{n,s}$	existing generation capacity of technology s at bus n (MW)
$\hat{g}_{n,s}$	maximum installable generation capacity of technology s at bus n (MW)
$g_{n,s,t}$	dispatch of generator s at bus n at time t (MW)
$\bar{g}_{n,s,t}$	time-dependent per-unit maximum generation dispatch of technology s at bus n at time t (p.u.)
H_r	average heat loss rate for residential buildings in region r (kW/℃)
HDD_r	annual heating degree days in region r (days ℃)
$\bar{h}_{n,s}$	nominal power of storage unit s at bus n (MW)
$\tilde{h}_{n,s}$	existing storage unit capacity of technology s at bus n (MW)
$\hat{h}_{n,s}$	maximum possible capacity of storage unit s at bus n (MW)
$h_{n,s,t}$	dispatch of store or storage unit s at bus n at time t (MW)
$inflow_{n,s,t}$	inflow into storage unit s at bus n at time t (MW)
K_{nl}	incidence matrix for branches l and buses n (unitless)
L_l	length of line l (km)
$o_{n,s,t}$	operation cost of technology s at bus n and time t (€/MWh)
P	share of British households participating in heating flexibility (unitless)
Q_r	average domestic annual heating consumption in region r (kWh)
$Q^{HH}_{r,d}$	total daily heating demand per household in region r in day d (kWh)
$Q^{ASHP,space}_{r,d}$	total daily space heating demand per household with ASHP in region r in day d (kWh)

$Q_{r,d}^{GSHP,space}$ . . . total daily space heating demand per household with GSHP in region r in day d (kWh)

$Q_{r,d}^{DHW}$ . . . . . total DHW demand per household in region r in day d (kWh)

$r_{n,s}$ . . . . . ratio between maximum state of charge and nominal power of store or storage unit s at bus n (h)

S . . . . . self-sufficiency share for all countries (unitless)

$spillage_{n,s,t}$ . . . spillage from storage unit s at bus n at time t (MW)

$soc_{n,s,t}$ . . . . . state of charge of storage unit s at bus n at time t (MWh)

T_r^{air} . . . . . outdoor air temperature in region r (℃)

$T_{r,d}^{air}$ . . . . . outdoor air temperature in region r on day d (℃)

$T_{r,t}^{air}$ . . . . . outdoor air temperature in region r at time t (℃)

T_r^{ground} . . . . . ground temperature in region r (℃)

T_r^{ground} . . . . . ground temperature in region r on day d (℃)

$T_{r,t}^{ground}$ . . . . . ground temperature in region r at time t (℃)

$T_{r,t}^{in}$ . . . . . indoor air temperature for homes in region r at time t (℃)

T_t^{in} . . . . . indoor air temperature at time t (℃)

T^{mean} . . . . . mean daily temperature (℃)

T^{min} . . . . . minimum daily temperature (℃)

T^{max} . . . . . maximum daily temperature (℃)

$T_{r,t}^{sink}$ . . . . . heating sink temperature for region r at time t (℃)

$T_{r,s,t}^{source}$ . . . . . heating source temperature for region r at time t for heat pump type s (℃)

$\bar{T}^{air}$ . . . . . time-averaged outdoor air temperature (℃)

t_r^c . . . . . comfortable heat-free hours for homes in region r (h)

V . . . . . volumetric increase in line and link capacities (unitless)

w_t . . . . . duration of time t (h)

x_l . . . . . series reactance of branch l (Ω)

$\Delta T_{r,s,t}$ . . . . . temperature difference between heat source and sink for region r at time t for heat pump type s (℃)

ΔT^{flex} . . . . . heating flexibility temperature window (℃)

$\eta_{n,s}$ . . . . . efficiency of generator type s at bus n (unitless)

$\eta_{n,s}^{stand}$ . . . . . standing efficiency of storage unit s at bus n (unitless)

$\eta_{n,s}^{charge}$ . . . . . charging efficiency of storage unit s at bus n (unitless)

$\eta_{n,s}^{discharge}$ . . . . discharging efficiency of storage unit s at bus n (unitless)

$\eta_{l,s,t}$ . . . . . efficiency of branch l of type s at time t (unitless)

$\theta_{n,t}$ . . . . . voltage angle at bus n at time t

κ . . . . . average thermal heat pump capacity (MW_{th})

τ_r . . . . . thermal time constant of residential buildings in region r (h)

τ_n . . . . . thermal time constant of residential buildings at bus n (h)

Indices

c . . . . . cycle index

d . . . . . day index

l . . . . . branch index

n . . . . . bus index

r . . . . . region index

s . . . . . technology index

t . . . . . time index

1 Introduction

Contents

This thesis aims to answer the research question:

How will widespread residential heat pump adoption impact spatial planning of bulk power systems?

This question is divided into two spatially varying aspects of the heating transition and their impact on the power grid: heat pump demand and heating flexibility.

1.1 Context and motivation

Heating buildings accounts for 10% of carbon dioxide emissions globally [1]. This share is even higher in regions with cold and temperate climates: for instance, in

the United Kingdom (UK), 17% of emissions came from heating in the residential sector alone in 2019 [2]. In the European Union (EU), space and water heating for households accounted for 22% of final energy consumption in 2020, and more than half of this energy came from fossil fuels [3]. Decarbonizing heating is therefore critical for meeting the targets set out in the Paris Climate Agreement. Heating decarbonization is also urgent to meet net zero targets: the International Energy Agency (IEA) Roadmap to Net Zero by 2050 includes no new fossil fuel boiler sales after 2025 [4].

The primary technology for decarbonizing heating is expected to be electric heat pumps. In 2050, the IEA envisions that 55% of energy demand for heating will come from 1.8 billion heat pumps worldwide in their Roadmap to Net Zero [4]. In the UK, the Climate Change Committee (CCC) includes 12 million heat pumps in residential buildings by 2035 and 27 million by 2050 in their central Balanced Net Zero Pathway [5]. While gas lobbyists have promoted the use of hydrogen boilers instead of heat pumps [6], the UK National Infrastructure Commission estimates that an energy system with hydrogen heating would be 20% more expensive than an energy system without and found that "... there is no public policy case for hydrogen to be used to heat individual homes or other buildings" [7].

Heat pumps collect heat from a source, such as outdoor air in the case of an air-source heat pump (ASHP) or outdoor ground for a ground-source heat pump (GSHP), and transfer heat to a sink, typically indoor air or radiator water. Because heat pumps use electricity to transfer heat, rather than generate it, they can be highly efficient. The temporal efficiency of heat pumps is expressed as a coefficient of performance (COP): for instance, a COP of 3 indicates that 3 units of heat are transferred for every unit of electricity used at a given time. COP values decrease as the source temperature decreases. For example, in a recent UK residential heat pump trial, a median COP value of 2.44 was observed for ASHPs on the coldest day of the year when the outdoor air temperature was -0.4℃ [8].

Because of their high efficiency and use of electricity as a fuel, heat pumps can reduce emissions from heating compared to fossil fuel boilers or furnaces. Based on

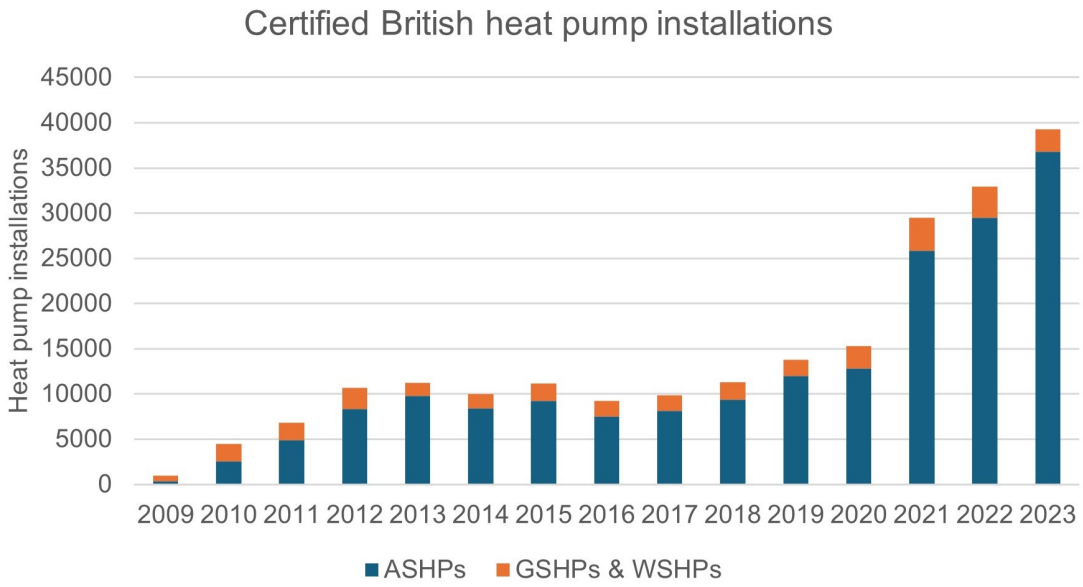

Figure 1.1: Certified British ASHP and GSHP & WSHP (water-source heat pump) installations from 2009 to 2023 based on data from MCS [11].

the 2018 and 2019 British electricity generation mix, switching from a gas boiler to a heat pump can already reduce greenhouse gas emissions from heating a household by at least 65% [9]. As the electricity supply decarbonizes, the emissions reduction from replacing a fossil fueled boiler with a heat pump will grow. For all states in the contiguous United States (US), switching to ASHPs is projected to reduce average greenhouse gas emissions per household under a broad range of future grid scenarios for 2022 to 2038 [10]. Because of their high efficiency, heat pumps can even reduce emissions compared to heating with electric resistance heaters, which use electricity to generate heat at about 100% efficiency.

Heat pump sales have grown rapidly in cold and temperate countries. Global heat pump sales growth in 2021 was 15%, with 35% growth in the EU [1]. In the US, ASHP shipments (an approximation of sales) have nearly doubled in the past decade to 4.3 million units in 2022 [12]. As shown in Figure 1.1, certified annual heat pump installations in Britain have quadrupled over the past decade to nearly 40,000 [11]. Because certification is required to qualify for government incentives, these figures are likely to capture the vast majority of heat pump installations in Britain. The majority of these certified installations are ASHPs, with a few thousand GSHPs and

water-source heat pumps (WSHPs) installed each year. Heat pump installations approximately doubled from 2020 to 2021 and have continued to grow since.

1.1.1 Power systems

The power system can be divided into the bulk power system and the distribution system. The bulk power system is the high-voltage (400 and 275 kV in Britain) system for generating and transmitting large amounts of electricity. The distribution system includes the medium- and low-voltage (LV) networks used primarily for delivering electricity to domestic and commercial end-users, as well as distributed resources that are connected to these networks, such as rooftop solar.

The bulk power system must balance supply and demand on a sub-second level across the entire network. Electricity generation needs to meet demand at all times to maintain the alternating current (AC) frequency as well as voltage level and phase angle. The transmission system ensures that demand is matched spatially by transporting power from where it is generated to where it is consumed. Matching supply and demand in space and time is becoming increasingly challenging as both supply and demand are increasingly weather-dependent [13].

Electricity systems are incorporating increasing capacities of weather-dependent renewable generation, particularly wind and solar. The unsubsidized levelized cost of electricity from onshore wind and utility-scale solar photovoltaics (PV) is now competitive with the marginal cost of existing conventional generators, including nuclear, coal, and combined-cycle gas [14]. While the levelized cost of electricity does not capture generation availability and reliability or transmission expansion costs, this difference is a rough indication that it can be cheaper per kilowatt-hour to build new wind and solar to generate electricity than to generate electricity from existing, fully depreciated conventional generators. However, these renewable technologies rely on the weather, which varies daily and annually and can be difficult to forecast.

At the same time, moving heat load to the power system will increase the weather sensitivity of electricity demand. Widespread adoption of heat pumps in regions where fossil fuels are the primary heating fuel is expected to dramatically

increase electricity load, particularly at times of peak demand in the winter. In Britain, where gas is the dominant heating fuel, heating all homes with heat pumps is postulated to increase peak demand by up to 78 GW in a cold year in the 2020s [15]. In the contiguous US, electrification of residential and commercial space and water heating along with cooking without efficiency improvements is expected to increase winter daily average net peak demand (electricity demand minus renewable generation) by 231 GW (49%) by 2050 [16][1]. In some US census tracts, 100% heat electrification could increase peak demand by 4 times or more [17]. Because both this growing heating demand and renewable generation vary in space and time, meeting this new, weather-dependent demand with larger shares of renewable generation poses a challenge for the bulk power system.

1.1.2 Spatial energy transitions

The transition to low-carbon energy systems will impact regions differently, even within the same country. Globally, geographical location is an important contributor to energy poverty [18], and power outages disproportionately affect vulnerable regions in the US [19]. During the transition to low-carbon energy systems, regional equity has been highlighted as a major concern [20]. As the land use footprint of the electricity system expands with increasing renewable generation, there has been increased awareness of local impacts in power systems planning. Because renewable potential varies spatially, energy system optimization models are adopting increasing spatial granularity on the supply side [21].

In the UK, the National Grid Electricity System Operator (ESO), which operates the transmission system, has introduced regionalization into their Future Energy Scenarios (FES). National Grid ESO is shifting from a top-down to bottom-up modeling approach due to the importance of local factors in the energy transition and to improve coordination with distribution network operators (DNOs), which own and operate portions of the distribution system [22]. The first bottom-up

[1]Hourly residential and commercial demand are calculated based on building energy modeling of a single-family home residential archetype and 5 commercial building archetypes for a typical meteorological year in 14 different locations across the US. Hourly wind and solar generation are calculated with the same weather data based on projections for 2050 renewable penetration.

modeling included in the FES regionalization was the Spatial GB Clean Heat Pathway Model [23], which models the adoption of clean heating technologies (including ASHPs, GSHPs, hydrogen boilers, and district heating) in residential and non-residential buildings in different regions of Britain. This FES also included regional electricity demand projections to 2050 for 250 grid supply points (GSPs), the connections between the transmission and distribution systems [24]. These projections included heat pump demand as well as residential, EV, commercial, industrial, district heat, and electrolyzer demand.

While National Grid ESO has shown concern about impact of the spatial differences in the heating transition on the power system, academic research on spatial demand-side changes has primarily focused on electric vehicles (EVs) to date [25, 26]. Spatial variation in these demand-side changes may be equally as important to bulk power systems planning as supply-side spatial variation.

1.1.3 Heating demand

Thermal heating demand is determined by three factors: weather conditions, occupant behavior, and building stock characteristics. Because each of these factors vary spatially, heating demand varies among regions.

The primary weather determinant of heating demand is outdoor air temperature, but wind speed, humidity, and solar irradiance also have secondary effects [27]. The American Society of Heating, Refrigerating and Air-Conditioning Engineers (ASHRAE) divides the world into 19 climate zones for building design standards based on heating degree days, cooling degree days, and monthly averaged daily precipitation [28]. Britain contains three of these climate zones: 4A Mixed Humid in the south of England, East of England, and East Midlands; 5A Cool Humid in the West Midlands, north of England, Wales, and most of Scotland; and 6A Cold Humid in the highlands of Scotland.

Occupant behavior determines comfortable indoor temperature ranges at different times of day and thus drives sub-daily heating demand. When a home is occupied, the World Health Organization recommends a minimum indoor temperature of

18℃ in cold and temperate climates [29], but indoor temperatures may fall below that level when the home is unoccupied. In Britain, people typically heat their homes to higher temperatures in the morning and evening, allowing the temperature to drop during the day while they are out of the house and at night when they are asleep. The timing of this behavior can vary regionally: for instance, in December, most people in South West England are asleep from 11:30 pm until 6:30 am. In contrast, most people in the East of England are asleep from 10:30 pm until 7:30 am in December [30].

The residential building stock determines the magnitude and timing of thermal heat demand needed to maintain a comfortable indoor temperature. More energy-efficient buildings require less thermal energy to maintain the same indoor temperature, and buildings with higher thermal capacities can maintain the same indoor temperature longer without heating. In England and Wales, the age of a home is the strongest predictor of its energy efficiency [31]. The age of homes varies dramatically among regions: 22% of homes in London and 23% of homes in Wales were built before 1900, compared to just 10% in the East of England [31]. Larger homes also tend to have higher gas consumption, primarily for heating [32], and home size also varies among regions: in England, average floor areas range from 84 m^2 in London to 102 m^2 in the South East, and homes in rural areas tend to be larger on average (123 m^2) than those in urban areas (80 m^2) [33].

Because of spatial variation in each of these factors, thermal heating demand varies among regions. While occupant behavior and building stock differ within Britain, weather has the largest regional variation. Understanding this weather-driven regional variation in heating demand is key for planning a power system that can accommodate growing heat pump demand to support heat decarbonization.

The quantity of interest for the power system is the electrical heat pump demand needed to meet a certain thermal heating demand profile. Heat pump load depends on the ratio of thermal heating demand to the COP. COP values depend on temperature difference between the heat source (air for ASHP, ground for GSHP) and the heat sink, such as radiators or underfloor heating. Heat pumps are less

efficient and COP values are lower when there is a larger difference between the heat source and sink temperatures. The heat sink supply temperature depends on the outdoor air temperature: lower outdoor air temperatures require higher sink supply temperatures to maintain comfortable indoor air temperatures.

Thermal energy storage can also desynchronize thermal heating demand and electrical heat pump demand. In the ongoing Electrification of Heat trial in Britain, 81% of homes that had a heat pump installed also had thermal energy storage installed [34]. The most common form of thermal energy storage installed was a hot water cylinder, with new cylinders installed in 39% of homes and replacement cylinders in 37% of homes. These cylinders allow water to be pre-heated and stored to meet hot water demand at a later time, thus increasing heat pump demand prior to the thermal energy demand for hot water. In the remaining 4% of homes with thermal energy storage, phase change material heat batteries were installed due to space constraints. The next section discussed the use of building envelopes as thermal energy storage for shifting space heating demand.

1.1.4 Space heating flexibility

Heating flexibility has the potential to reduce the impact of new heat pump demand on the power system and facilitate renewable adoption. Heating flexibility involves shifting the consumption of heat pumps in time to benefit the power system through reduced peak demand, increased renewable generation consumption, or decreased fossil-fueled generation consumption. Households' temperatures are adjusted within a comfortable temperature range for occupants to shift heating demand. For instance, a home's building envelope may be pre-heated to the highest comfortable temperature prior to peak demand times or during a time with high renewable generation. During peak demand times or times with high fossil-fueled generation, heating may be turned off and homes cool to the lowest comfortable temperature.

Academic studies project that heating flexibility could reduce the added electricity demand from heat pump adoption. In Britain, peak heat pump demand could

be reduced by 16% if 100% of hot water demand and 20% of space heating demand were flexible [15]. In the US, the combination of building efficiency improvements (e.g. high-performance heat pumps and improved building insulation) and heating flexibility could nearly halve the projected increase in net demand from heating electrification [16]. These reductions in peak demand could reduce the impact of heat electrification on the power system.

Real-world trials have also explored the potential for heating flexibility in Britain. The Smart Systems and Heat Phase 2 field trial from 2017 to 2018 explored Heat as a Service, a business model in which customers pay for "warm hours" rather than the fuel used to heat their homes that would allow a heating provider to heat homes flexibly [35]. The ongoing EQUINOX (Equitable Novel Flexibility Exchange) trial is exploring business models for residential heat pump flexibility to reduce the need for distribution system network reinforcement as well as the cost of heat pump ownership [36]. While not heat pump specific, the Demand Flexibility Service also introduced the opportunity for residential customers to be rewarded for shifting electricity consumption away from peak demand times in winter 2022/23 [37]. The median demand reduction from households that opted to reduce electricity use for 1 to 2 hours was 45% [38]. Each of these trials is a step towards commercial viability of heating flexibility.

1.2 Research questions

This thesis investigates the impact of the residential heating transition to electric heat pumps on bulk power system planning. Incorporating spatial differences in this heating transition into capacity expansion planning, this thesis focuses on a high residential heat pump adoption future.

Given the impending challenge of balancing spatial and temporal variation in power generation and demand, the overarching research question of this thesis is: *How will widespread residential heat pump adoption impact spatial planning of bulk power systems?* This thesis includes 4 research chapters, following an introduction and a literature review. The following research questions will be addressed in these chapters:

1. How will residential heat pump demand vary in space and time?
2. How will spatiotemporal differences in residential heat pump demand impact bulk power system planning?
3. What is the regional heating flexibility potential from residential building thermal inertia?
4. Where will residential heat pump flexibility be most valuable to the bulk power system?

The findings of this research can improve bulk power system planning by more accurately siting new capacity to meet heat pump demand and focusing heating flexibility procurement in areas where it will offer the most benefit to the bulk power system.

1.3 Case study: Britain

Due to the availability of high spatial resolution heat and electricity data and open-source power system models, the mainland British power system is chosen as a case study for this research.

The British electricity grid includes England, Wales, and Scotland and has undersea high voltage direct current (HVDC) interconnections to Northern Ireland, Ireland, France, Belgium, the Netherlands, Denmark, and Norway, as shown in Figure 1.2. An additional connection to Germany is currently under construction. The UK has historically been a net importer of electricity from these countries but was a net exporter for the first time in 40 years in 2022 [39]. Because of the growing importance of HVDC interconnections with other European countries in the British power system, this thesis adapts a European-wide power system model to focus on Britain and interconnected countries.

Following electricity market liberalization under the Electricity Act 1989 [40], a number of actors are involved in the ownership and operation of the British power system. Generators sell large amounts of electricity in a competitive market.

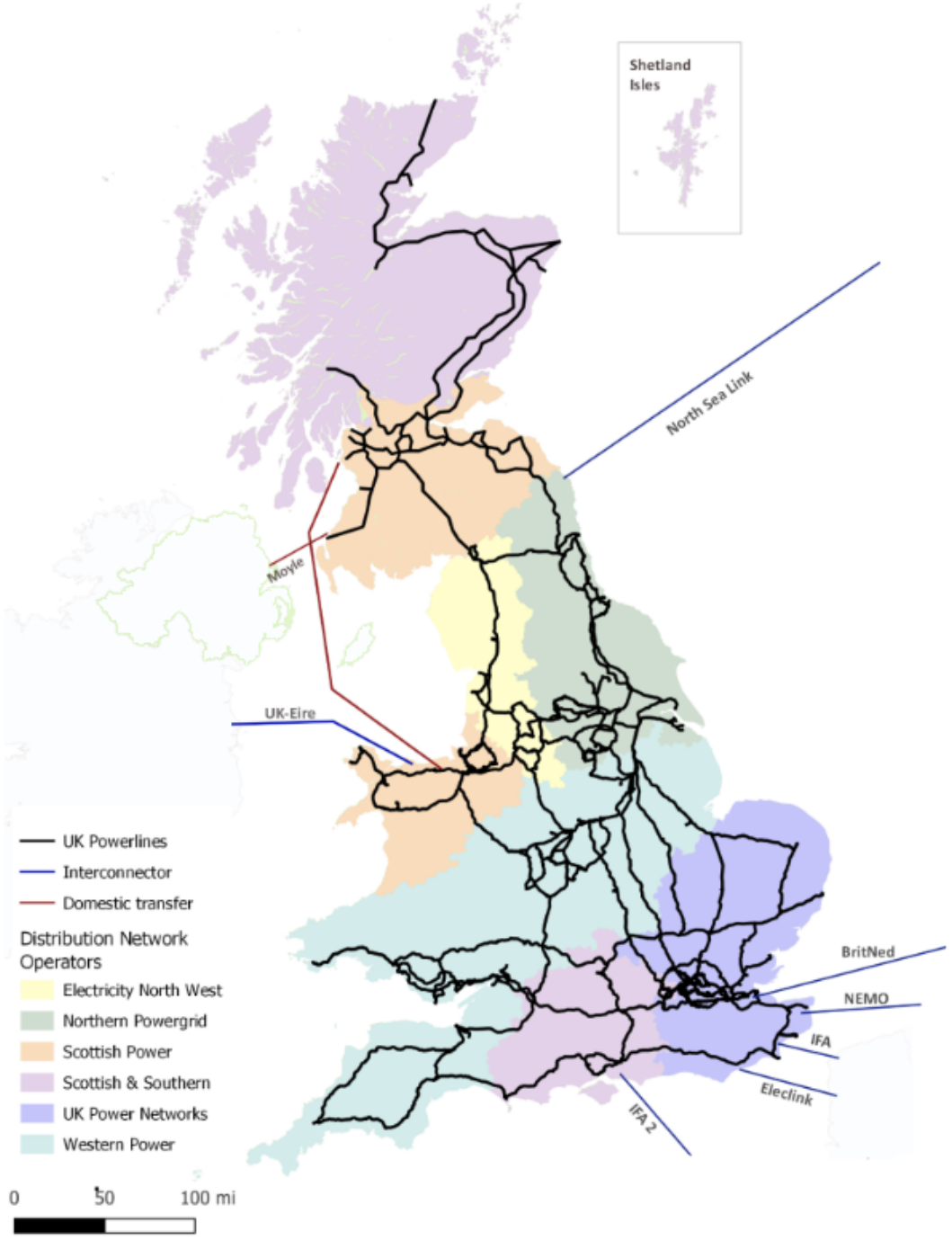

Figure 1.2: Map of the British power system, including transmission lines, interconnectors, and distribution network operators. Note that this figure predates completion of the Viking Link between Britain and Denmark. Contains UK Department for Energy Security &Net Zero [39] information licensed under the Open Government Licence v3.0. Crown Copyright 2023.

The high-voltage transmission system is operated by National Grid ESO, which ensures that supply and demand are balanced on the bulk power system [41]. National Grid plc owns the transmission system in England and Wales [42]. In Scotland, SP Transmission plc [43] owns the transmission system in the south and SSEN Transmission owns the transmission system in the north [44]. DNOs own and operate the distribution networks in different parts of the UK, as shown in Figure 1.2. Energy suppliers sell electricity to small end users, such as residential customers and small businesses.

In the last decade, the British power system has rapidly transitioned to renewable generation. Electricity generation from renewable sources increased by five times from 2010 to 2022, and electricity generation from fossil fuels decreased by 54% in the same time period [39]. Low-carbon sources, including renewable and nuclear generation, produced 56.2% of electricity in 2022. The share of electricity from renewable sources surpassed the share from fossil fuels in both 2020 and 2022 [39].

Residential electric heat pumps could reverse the decades-long trend of decreasing peak demand in Britain. The British power system is a winter-peaking system, and peak demand has decreased in recent decades from a maximum of 60.1 GW in 2002 to 47.1 GW in 2022 [45]. Domestic users accounted for the largest share of electricity demand at 30% in 2022 [39]. Because gas dominates domestic heating in Britain, replacing gas boilers and other fossil-fueled heating with electric heat pumps is expected to drastically increase winter electricity demand. From 2017 to 2020, an annual average of 225 TWh of gas was used for domestic space heating and 67 TWh for domestic water heating in the UK [46]. In the 2021 Census, 74% and 72% of households in England and Wales, respectively, reported that gas was their only central heating source [47]. In Scotland, 74% of households reported that they only had gas central heating in the 2011 Census [48]. Just 5% of households in Wales, 9% in England, and 13% in Scotland reported using electric central heating in the same censuses. Thus, a widespread shift from gas boilers to electric heat pumps in the residential building stock is expected to dramatically increase electricity demand in the winter.

The UK has a temperate climate: the mean annual temperature from 2013 to 2022 was 10.3℃ in England, 9.7℃ in Wales, and 7.9℃ in Scotland. Since the 1980s, mean temperatures have increased at about 0.25℃ per decade [49]. Heating degree days (HDDs), which measure how long outdoor temperature is below the indoor temperature and by how much and approximately correlate with total heating demand, have decreased: there were 12% fewer annual HDDs on average from 2013 to 2022 than 1961 to 1990.

Despite the temperate climate of the UK, heat decarbonization is a significant challenge because of the housing stock. The UK has the oldest housing stock in Europe [50]: in England, 20.3% of homes were built prior to 1919, and just 11.9% were built from 2002 onward [51]. A large share of the English housing stock was also built in the middle of the twentieth century, with 18.1% built from 1945 to 1965 and 18.6% built from 1965 to 1980 [51]. Because of their age and poor energy efficiency, homes in the UK lose heat up to 3 times faster than homes in cold and temperate European countries such as Germany, Austria, Denmark, Sweden, and Norway [52]. Initial British heat pump adopters are likely to have newer, and thus more energy efficient, homes: for instance, just 8% of the homes selected as suitable for heat pumps in the Electrification of Heat trial were built prior to 1919 [34]. However, widespread residential heat pump adoption, particularly installing heat pumps in the highly inefficient homes of late adopters, could drastically increase peak electricity demand.

1.4 Scope

Because the domestic sector accounted for 69% of space heating energy end use in the UK from 2016 to 2021, the scope of this thesis is limited to residential heating electrification [46]. In the same time period, the commercial and industrial sectors only accounted for 26% and 5% of space heating energy end use respectively, so changes in commercial and industrial heating are not considered.

To assess the maximum possible impact of residential heat pumps on the bulk power system, this thesis focuses on a high-adoption end state. While Eyre and

Baruah [53] highlighted the uncertainty about the evolution of the UK heating transition in 2015, projections have coalesced around individual heat pumps as the primary heating technology for residential heat decarbonization. The CCC central Balanced Net Zero Pathway includes 27 million residential heat pumps in the UK by 2050, which corresponds to 80% of households having a heat pump [5]. The National Grid ESO high-electrification Consumer Transformation scenario includes 9 million GSHPs and 15 million ASHPs[2] in 2050, which corresponds to 46% of households having an ASHP and 27% having a GSHP [54]. This thesis assesses the impact of 26.5 million households (all households in the UK as of 2011) adopting heat pumps, which is consistent with the CCC central scenario and slightly higher than the National Grid ESO high-electrification scenario for 2050. Although district heating is projected to heat 18% of homes in 2050 in the CCC Balanced Net Zero Pathway and 19% in the National Grid ESO Consumer Transformation scenario, this thesis focuses on heat pumps in individual homes, which are expected to be the dominant technology for heating decarbonization, and does not consider district heat networks.

The bulk power system is a complex system undergoing simultaneous supply-side and demand-side changes. To assess the impact of heat pumps on this complex system, this thesis uses a capacity expansion model from the perspective of central planner. When modeling liberalized electricity markets, which are present across the EU, the UK, and most of the US, these models assume that minimizing the system cost from the perspective of a central planner approximates the development of the power system. However, Trutnevyte [55] shows that cost minimum capacity expansion modeling poorly approximates the historical UK generation mix after market liberalization, with differences of 9% to 23% between the modeled minimum cost scenario and actual total system costs. These differences are explained by several factors. During the "dash for gas" in the early 1990s, combined-cycle gas turbine developers overbuilt capacity because they did not anticipate the increase in gas prices after 2000. Climate policies also drove renewable capacity expansion beyond

[2]Both the CCC and National Grid ESO figures include hybrid ASHPs, which have a backup hydrogen or biomass boiler or electric resistance heater.

cost-optimal levels after 2005. Finally, generation developers did not anticipate the decrease in electricity demand following the 2008 economic crisis. Each of these differences between the cost-optimal expansion and historical generation mix demonstrates that the energy system is subject to uncertainties that can be difficult to anticipate in capacity expansion modeling. Therefore, following the guidance of DeCarolis et al. [56], this thesis utilizes capacity expansion modeling to gain insight about the spatial nature of the heating transition, rather than attempting to make exact predictions about the future of the power system. The conclusions of this thesis are primarily drawn based on differences between cost-optimal models.

To demonstrate the impact of high spatial resolution heating data, this thesis focuses on the impact of heat pumps alone. Because a single weather-year of data reveals spatial differences in heating demand caused by geographically-driven climate differences that are expected to be persistent, only a single weather-year of heating demand and renewable generation data is used to demonstrate this impact. Robust power system planning for investment decisions should consider multiple weather years of data to capture a wider array of interactions between renewable generation and heating demand. Other growing electricity loads, such as EV charging, are outside the scope of this analysis but should be considered in power systems planning.

1.5 Publication outline

Table 1.1 presents the papers based on this thesis and the corresponding thesis chapters.

1.6 Thesis structure

The remainder of this thesis is structured as follows. To contextualize the contributions of this thesis, Chapter 2 reviews the relevant literature and identifies the research needs in integrated modeling of the heating and power systems.

The impact of residential heat pumps on the bulk power systems will depend on when, where, and how much people heat their homes, so Chapter 3 introduces

Table 1.1: Thesis papers

Paper	Chapter
C.E. Halloran, F. Fele, and M.D. McCulloch, "Impact of Spatiotemporal Heterogeneity in Heat Pump Loads on Generation and Storage Requirements," In. Proc. IEEE Power & Energy Society General Meeting 2022. [57]	3 & 4
C. Halloran, J. Lizana, F. Fele, M.D. McCulloch. "Data-based, high spatiotemporal resolution heat pump demand for power system planning." Applied Energy, 2024. [58]	3 & 4
C. Halloran, J. Lizana, M. McCulloch. "Quantifying national space heating flexibility potential at high spatial resolution with heating consumption data." (*Under review.*) [59]	5
C. Halloran, J. Lizana, F. Fele, M. McCulloch. "Where residential heating flexibility will offer the most value to electricity systems." (*In preparation.*)	6

a method for projecting heating demand at high spatiotemporal resolution. This novel method combines high temporal accuracy daily demand patterns from a recent heat pump trial with high spatial resolution heating projections from reanalysis weather data. Because simultaneous power system decarbonization and heating electrification makes it difficult to predict the impact of heating demand changes, Chapter 4, incorporates both high spatiotemporal resolution heating demand and spatially uniform heating demand into bulk power system planning. The capacity expansion results for each demand projection are compared to demonstrate the importance of using high spatial resolution demand data for spatial bulk power systems planning.

The ability of residential customers to heat flexibly depends on the regional housing stock, so Chapter 5 quantifies regional heating flexibility potential. A novel top-down method for quantifying heating flexibility potential at high spatial resolution using regularly updated gas demand data, historical weather data, and census data on home size is introduced and validated. Because of the complex interactions between heating flexibility and the bulk power system, Chapter 6 assesses where heating flexibility offers the bulk power system the most savings. To account for structural uncertainty about regional heating flexibility participation, the near-optimal locations for heating flexibility are also explored.

Finally, Chapter 7 presents the conclusions of this thesis. Appendix A presents the technology cost projections used in power systems planning.

2
Literature review

Contents

This chapter reviews existing literature on integrated modeling of the heating and power systems, with a particular focus on spatial fidelity. While Bloess et al. [60] provide a review of power and heat sector coupling studies, this review focuses on decentralized heat pumps, in line with the scope of this thesis. The spatial focus of this review is also unique.

2.1 Overview

The first part of this chapter focuses on heat sector modeling, and the second part focuses on power sector modeling. Section 2.2 evaluates approaches for modeling heat pump demand and heating flexibility. Section 2.3 discusses bulk power systems

planning studies and their consideration of the impacts of heat pumps. Finally, Section 2.4 discusses the research gaps at the intersection of heating and power sector modeling, which are highlighted in **boldface** throughout this chapter.

2.2 Heat sector modeling

This section discusses approaches for modeling heat pumps in sector-coupled studies. Modeling approaches in these studies must balance computational complexity, spatial resolution, and accuracy. Heat pump demand models are evaluated in Section 2.2.1, and heat pump flexibility models are reviewed in Section 2.2.2.

2.2.1 Heat pump demand

As larger shares of renewable generation are connected to the bulk power system, hourly regional heat pump demand profiles are necessary for systems planning. For power systems dominated by dispatchable generation, such as fossil-fueled and nuclear power plants, peak demand is the key quantity for planning. However, the spatial and temporal variation in renewable generation potential requires hourly regional demand profiles. Despite this requirement for higher temporal resolution, the National Grid ESO only provides projections for peak heat pump demand and minimum summer afternoon and morning demand at 250 GSPs from 2020 to 2050 [24]. These projections are based on hourly heating demand projections from the Spatial GB Clean Heat Pathway Model based on bottom-up heating demand calculations calibrated with historical energy use, but these hourly profiles are not publicly available [23, 61]. Therefore, alternative approaches for projecting regional hourly heat pump demand are needed to assess the impact of heat pump adoption on the bulk power system in the coming decades.

While the first projections of heat pump demand relied on historical gas demand patterns for a given year [62], more sophisticated models have been developed to examine multiple weather-years of heating demand and renewable potential patterns in power systems planning. The most common approaches for modeling heat pump

Table 2.1: Approaches for modeling heat pump demand in power system planning.

Model	Computational intensity	Spatial resolution	Hourly profile accuracy
Physics-based	✗	✓	✓
Degree-day	✓	✓	✗
Statistical	✓	✗	✓

demand at the sub-daily resolution necessary for power system planning can be divided into physics-based modeling, degree-day models, and statistical models [27]:

- Physics-based models use detailed building parameters, historical weather data, and energy balance equations to calculate building energy consumption.
- Degree-day models use regressions of historical HDDs to model daily heating demand.
- Statistical models typically use machine learning to derive relationships between measured heating demand and other variables, such as outdoor air temperature.

Each of these approaches projects heating electricity load at different spatial and temporal resolutions; however, they all have important limitations for high spatial resolution power system planning, as summarized in Table 2.1.

Physics-based models

While physics-based modeling can model heating demand at high spatial resolution with high hourly profile accuracy, it requires large amounts of data for calibration and is computationally intensive. A simple physics-based approach for modeling heat pump demand for a semi-detached single family home in the UK based on outdoor temperature was applied by Tassou et al. [63] in 1986 to compare the life cycle costs of heat pumps to other heating systems. Recently, more complex physics-based models of multiple building archetypes have been used to project large-scale spatial variation in heating demand in Italy [64] and Texas [65]. Protopapadaki and Saelens [66] use physics-based modeling to assess the impact of heat pump adoption

on both urban and rural LV residential distribution grids in Belgium. However, physics-based modeling for integration with bulk power systems requires a large amount of data about different regional building archetypes and is computationally intensive. In Britain, the government provides an in-depth Standard Assessment Procedure including all the data required for analyzing the energy needs of homes [67]. Moreover, calibrating these models using historical energy demand requires a large amount of data, as demonstrated in the ResStock project in the US [68]. For these reasons, spatiotemporally granular heat demand profiles from physics-based modeling are rarely incorporated into bulk power system planning. Heinen et al. [69] use a physics-based model in an investment planning problem for Ireland. However, they consider only 2 building archetypes (new and existing detached houses in Dublin, Ireland) and only use weather data from Dublin, where one-third of the Irish population lives. Clegg and Mancarella [70] combine a physics-based modeling of half-hourly heating demand for 12 residential building archetypes and 12 commercial and industrial building archetypes in 3 weather zones with a degree-day-like model to scale to 404 heating nodes in Britain. For a wider variety of housing stock and weather conditions, the data requirements for physics-based modeling of heat pump demand of a national building stock with high spatial granularity quickly become prohibitive for power system planning.

Degree-day models

Degree-day models offer a computationally lightweight method for projecting heating demand at high spatial resolution, but the hourly heating profiles used to disaggregate daily heating demand do not accurately reflect geographically-specific heat pump demand patterns driven by occupancy schedules in different cultures as well as building stock differences. Reanalysis data, including hourly values of outdoor air temperature, are available globally at high spatial resolution for several decades [71, 72]. Thus, HDDs offer a globally applicable approach for projecting daily heating demand for a variety of weather-years at high spatial resolution, given a correlation between HDDs and heating consumption. In Britain, annual domestic

gas consumption is available for regions with 500 to 1,500 residents [73], so HDDs can be correlated with annual gas demand at high spatial resolution.

Since occupancy and behavioral patterns, rather than weather, tend to dominate heating consumption patterns at sub-daily temporal resolutions, HDD models that project hourly heating demand must temporally disaggregate daily heating demand using hourly heating profiles. Many degree-day models use standard German gas profiles from Bundesverband der Energie- und Wasserwirtschaft (BDEW), a German energy industry association [74], to generate hourly heat pump demand profiles for capacity expansion studies. For instance, the BDEW model is used to develop the When2Heat model [75], which only provides one profile for each European country. Similarly, the sector-coupled PyPSA-Eur model [76] uses hourly gas demand profiles from BDEW. These gas-based profiles tend to overestimate peak heat pump demand because gas boilers typically have higher thermal capacities than heat pumps: in the UK, gas boilers typically have a capacity of 20 to 30 kW, but the median heat pump capacity in a British trial was just 8 kW [77]. This capacity difference leads to peakier gas demand profiles compared to more continuous heat pump demand profiles, and Watson et al. [77] found that using gas demand overestimates peak heat pump demand by 8% compared to using empirical data from British heat pump trials. Eggimann et al. [78] use population and HDDs to spatially and temporally disaggregate heating demand and use half-hourly heat pump profiles from Love et al. [79] based on field trials. However, this set of profiles is limited to just 4 day types: a medium winter weekday, medium winter weekend, cold winter weekday, and cold winter weekend. Recently, Staffell et al. [27], introduced a global model for hourly heating and cooling demand at regional resolution. Because they use globally representative heating demand profiles for temporal upscaling of heating demand, this approach is likely to lead to less accurate daily heating profiles than models based on geographically-specific heat pump trials that reflect national heating patterns.

Statistical models

Although statistical models provide a low computational intensity approach for projecting hourly heating demand with increasing accuracy as relevant heating trial data becomes available, they do not yet account for spatiotemporal heating demand variation.

The first statistical models of heat pump demand in the UK were developed using heating demand data from the Carbon Trust's Micro Combined Heat and Power (CHP) Accelerator [80], assuming that micro-CHP would resemble typical heat pump installations because of their smaller thermal capacity compared to gas boilers. Sansom [81] develops the first statistical model of national heat pump demand in the UK using weekend and weekday heating demand profiles from this trial and a regression of commercial and domestic daily gas demand versus daily temperature. Navarro-Espinosa and Mancarella [82] use demand profiles from the same trials to develop a model of 5-minutely individual heat pump demand to assess the impact of electrified heating on the LV distribution network.

Following the release of data from the UK Renewable Heat Payment Plan (RHPP) trials [83], which monitored 700 homes with heat pumps from August 2011 to March 2014, increasingly accurate statistical models of heat pump demand were developed. Anderson et al. [84] use RHPP data to develop a statistical model of heat pump demand at 2-minutely temporal resolution based on local outdoor temperature for use in LV distribution network models. Using RHPP data, Watson et al. [77] and Watson et al. [15] develop temperature-based statistical models of diversified half-hourly heat pump demand; however, they do not spatially disaggregate demand below the national level. Similarly, Ruhnau et al. [85] model hourly heating demand and COP based on temperature and other weather variables in Britain at the national level. While Canet et al. [86] provide annual heating demand for 35,000 Lower layer Super Output Areas (LSOAs) in England and Wales to downscale their statistical model of half-hourly heat pump demand, they only provide a single heating profile for air-source and ground-source heat pumps for the entire region.

While these studies accurately represent hourly variation in heating demand, none of them capture sub-national differences in temporal heating demand.

Heat pump demand modeling research gap

Although several studies have modeled heat pump load, existing models either do not accurately capture hourly heat pump usage patterns or do not represent sub-national heating demand variation (research gap 1).

2.2.2 Heating flexibility

While some studies model flexibility as lossless demand shifting within a certain time window, this approach is inappropriate for heating because it does not account for losses that can lead to demand increases before and after demand reductions. The approaches used to model the interactions between heating flexibility and the power system that capture losses can be divided into transient simulation models, reduced-order models, and steady-state models:

- Transient simulation models (also known as dynamic simulation models or white-box models) are "fundamentally based on conservation of energy, mass, and momentum" [87] and include detailed information about building structure, occupancy schedules, and heating systems.

- Reduced-order models (also called lumped-parameter, resistance-capacitance, or gray-box models) represent only the main building components from transient simulation models with 5 or fewer thermal masses to reduce computational complexity [87].

- Steady-state models model heating flexibility analogously to a battery, with limits on the charging and discharging power of thermal storage as well as its state of charge, usually represented as an internal temperature within a range of comfortable temperatures.

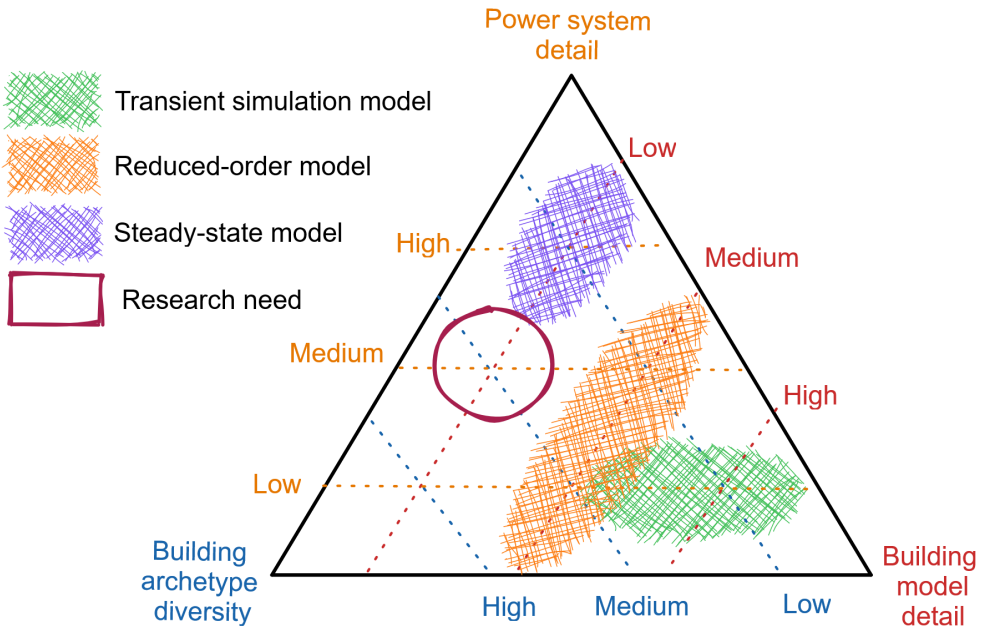

Figure 2.1: Heating flexibility model trade-offs between power system detail, building model detail, and building archetype diversity. The trade-off space for each model type is shaded in the corresponding color, and the research need is circled in red.

Each approach attempts to maximize insight into different aspects of heating flexibility under the constraint of computational requirements. Thus, each modeling approach is a trade-off between building system model detail, energy system model detail, and the diversity of buildings represented, as summarized in Figure 2.1. Computational requirements prevent any modeling approach from including a high level of detail for all three components, so a more detailed representation of one component requires a simplified representation of the others. While an approach could include a low level of detail for all three components, it would not provide as much insight as including at least a medium level of detail on at least one component.

Incorporating heating flexibility into bulk power systems planning requires capturing the national building stock diversity among regions. Because of the computational intensity of capacity expansion planning and the large diversity of building archetypes that need to be included, only a low level of building model detail can be included, as highlighted in the research need in Figure 2.1. Because bulk power systems planning is concerned with the aggregated load of all customers

that share a connection to the high-voltage grid, this level of building model detail should be sufficient to capture the aggregate behavior of residential heating. While steady-state models could be used in bulk power systems planning, they have not yet been used to capture even a moderate diversity of building archetypes due to limited data availability about the spatial distribution of different building archetypes.

Transient simulation models

While transient simulation models can represent heating flexibility from a variety of building types, the computational intensity of such high building thermal detail requires low energy system detail for grid integration studies. These models can represent a variety of building types, from a single archetype of a detached Irish house [88] to 144 configurations of Danish single-family homes [89]. However, transient simulation models tend to be too computationally intensive to couple with energy system models. A few studies [89, 90] use dynamic electricity prices to account for building interactions with the power system. Similarly, Langevin et al. [16] use net load (hourly load minus renewable generation) in 22 regions in the US as a proxy for marginal electricity costs and quantify the change in annual electricity use and daily net peak load from energy efficiency and demand response measures. More commonly, transient simulation models are used to quantify flexibility metrics of interest such as solar photovoltaic self-consumption [88, 91]; peak heating demand [91]; flexibility energy capacity [88, 90, 92, 93], power capacity [92, 93], and duration [90, 92, 93]; flexibility recovery time [93]; and thermal energy storage efficiency [88, 92].

Reduced-order models

Because of their reduced building thermal behavior detail, reduced-order models can allow either more building diversity to be represented or more detailed power system models to be used. Reduced-order models represent the temperature of a small number of components, ranging from 2 to 3 [94], 4 [69], and 5 thermal masses [95, 96]. These studies trade off between the details of the power system model and the diversity of building types considered. At one extreme, Hedegaard

and Balyk [94] represent 10 archetypes of Danish single-family homes in a linear energy system investment optimization model considering five representative weeks at hourly temporal resolution. In contrast, Heinen et al. [69] consider only 2 building archetypes (new and existing detached houses in Dublin, Ireland), and include hourly weather data for an entire year at a time in their electricity system planning model. Similarly, Patteeuw et al. [95] only include a single building archetype due to the computational complexity of the mixed-integer linear unit commitment and economic dispatch problem power system model. Patteeuw et al. [96] later consider 36 building types and 3 heating systems in this model, but each combination is considered individually due to computing constraints. Modeling only a single building archetype at a time does not capture the differences in heating flexibility operations due to building stock diversity, such as the distribution of heating flexibility duration and power capacity.

Steady-state models

While they have the lowest level of detail about building thermal behavior, steady-state models of heating flexibility can incorporate a diversity of building types into complex power systems models. Self-discharge heat losses to the environment are commonly included based on a thermal time constant that includes a single thermal mass and a single thermal resistance [76, 97–100]. This approach has also been used to model thermal energy storage in hot water tanks [101]. As power system models increase in complexity [21], considering higher spatial and temporal resolution, thermal storage models offer an opportunity to include the variety of the building stock in these models without compromising computational tractability. Despite the opportunity to represent a large diversity of buildings, many of these models do not account for heterogeneity in the building stock in large geographies [76, 99, 100] while others only consider a few building parameter variations [98, 102]. Considering 7 building archetypes to represent the German building stock, Papaefthymiou et al. [103] use a transient simulation model to derive the parameters of a thermal storage model. Mathieu et al. [97] consider regional

weather differences to quantify flexibility potential from heat pumps and other thermostatic loads for 13 climate zones in California, but they assume a uniform distribution of thermal parameters for the entire state.

Heating flexibility modeling research gap

Despite the variety of approaches, none accurately represents the diversity of a national building stock at high spatial resolution and its flexibility duration in complex power system models. Recently, Canet and Qadrdan [104] used energy performance certificate (EPC) data to parameterize a steady-state model that quantifies heating flexibility potential at high spatial resolution in England and Wales. In this model, heating flexibility duration decreases with increasing annual heating demand. Because of its basis in EPCs, which overestimate heating demand, this method is likely to underestimate heating flexibility duration in the current residential building stock. Previous works have shown that EPCs are based on standard occupancy procedures that overestimate energy consumption [105, 106] and assume default heating losses based on the year of construction that fail to capture retrofit improvements to the building fabric [107]. Moreover, comparing EPC-modeled energy use with smart meter-measured gas use in British households, Few et al. [108] find that differences between the two for lower bands persist even in homes where occupant behavior matches EPC assumptions. These differences are likely to be particularly pronounced in rural areas, where Canet et al. [86] found that an EPC-based method overestimated heating demand compared to gas consumption by a median of 61% in the most rural LSOAs in England and Wales, which the authors suggest could be due to changes in building stock and household composition as well as unallocated gas demand data.

Thus, **although many methods have been applied to quantify heating flexibility, none accurately represent the geographic diversity of a national building stock with sufficiently low computational requirements to be incorporated with complex power system models (research gap 3).** The only study that represents the variety of flexibility duration potential in British

homes is likely underestimating that potential because of its basis in EPCs [104], which are known to overestimate heating demand.

2.3 Bulk power systems planning

In the past decade, the spatial resolution of capacity expansion models has increased to account for regional differences in renewable potential [21]. Despite growing industry concern about the impact of regional demand differences on power system planning, as evidenced by National Grid ESO incorporating regionalization into the FES [22], few academic capacity expansion studies account for regional differences in demand-side changes, particularly in the heating sector.

2.3.1 Spatiotemporal demand diversity

Several studies have projected regional differences in heating demand that seem likely to affect power systems planning for the heating transition, but none have investigated the grid impact of this regional variation. Previous studies have demonstrated spatial variation in demand growth from residential heating electrification in the UK [78], Italy [64], US [17], and Texas [65]. Clegg and Mancarella [109] incorporate high spatiotemporal resolution heating demand [70] into a combined operational optimization for the bulk power and gas systems. However, none of these studies investigate the impact of these spatiotemporal variations on bulk power system planning.

Spatiotemporal variation in heat pump demand seems likely to impact energy systems planning models given the implications of spatial and temporal resolution highlighted in other studies. Several studies on the energy transition have demonstrated the importance of high spatial and temporal resolution for energy system planning models. For power systems with high shares of renewable generation, Frysztacki et al. [110] have demonstrated that capacity expansion models with low spatial resolution that ignore network congestion can underestimate costs by up to 23%. Similarly, Heuberger et al. [25] find that using a high spatial resolution network model to plan investments to meet EV loads reduces the need for dispatchable

power capacity and increases the value of energy storage. Crozier et al. [26] explored spatiotemporal variation in EV use and electricity demand in analyzing how EV charging will impact the transmission and distribution systems. Jalil-Vega and Hawkes [111] have demonstrated the importance of using high spatial resolution demand and network topology in an investment model considering different heat supply technologies and gas, electricity, and heat network infrastructure.

These recent studies have demonstrated that accounting for spatial and spatiotemporal variation is crucial in energy systems planning models. Despite regional variation in heat pump demand driven by weather, occupancy patterns, and building stock, **no previous study has analyzed the implications of these spatiotemporal variations for bulk power systems planning for an entire grid region (research gap 2).**

2.3.2 Impact of flexibility

Studies assessing the potential benefits of demand-side flexibility for the power system can be divided into market and central planning models [112]. These studies are summarized in Table 2.2, which distinguishes between market and central planning models. The system considered in each study describes which markets are included in market studies an which energy systems are included in central planning studies. For all studies, electrification of technologies (heat and EVs) and sectors (residential, commercial, and industrial) and spatial resolution in nodes per country are included.

Market models

Market models quantify the impact of flexibility participation in capacity [112, 113, 120, 124], energy [112, 119–121, 125, 128], and ancillary markets [112, 116, 119, 120]. Most studies consider futures with higher shares of renewable generation [112, 119–121, 124] as well as electrification of heat [116, 121, 124] and transportation [119, 125]. These market models show that flexibility can contribute to system reliability through frequency regulation [116, 119, 120], energy balancing [112, 119, 125, 128],

Table 2.2: Studies on the impact of flexibility on large-scale energy systems. M = market model, C = central planner. H2 = hydrogen. Res. = residential, Ind. = industrial, Com. = commercial.

Study	Year	Model	System	Electrification	Nodes per country
Earle et al. [113]	2009	M	Capacity	None	1
Kiviluoma and Meibom [114]	2010	C	Power & heat	Res. & Ind. heat, Res. EVs	1 electric, 3 heat
Hedegaard and Balyk [94]	2013	C	Power	Res. heat	2 electric, 20 heat
Hedegaard and Münster [115]	2013	C	Power & heat	Res. heat	2 electric, 20 heat
Hao et al. [116]	2015	M	Ancillary	Res. heat	5
Krakowski et al. [117]	2016	C	Power	Res. EVs	1
Gils [118]	2016	C	Power	None	6
Teng et al. [119]	2016	M	Energy & ancillary	Res. heat, Res. & Com. EVs	1
Heinen et al. [69]	2017	C	Power & heat	Res. heat	1
Aryandoust and Lilliestam [120]	2017	M	Energy & ancillary	None	1
Olkkonen et al. [121]	2017	M	Energy	Res. & Com. heat	1
Li and Pye [122]	2018	C	Power, heat, transport, & agriculture	Res., Com., & Ind. heat, Res., Com., & Ind. EVs	1
Brown et al. [123]	2018	C	Power, heat, transport, H2, & methane	Res. & Com. heat, Res., Com., & Ind. EVs	1
Bloess [100]	2019	C	Power & heat	Res., Com., & Ind. Heat	1
Lynch et al. [124]	2019	M	Capacity, energy, & ancillary	Res. heat	1
Guminski et al. [125]	2019	M	Energy	Res., Com., & Ind. heat, Res. EVs	∼100s
Schill and Zerrahn [126]	2020	C	Power	Res. heat	1
Zeyen et al. [76]	2021	C	Power, heat, transport, H2, methane, & biomass	Res. & Com. heat, Res., Com., & Ind. EVs	
Bernath et al. [127]	2021	C	Power, heat, & H2	Res. heat & Res. EVs	1
Zhou et al. [112]	2022	M	Capacity, energy, & ancillary	None	22
Savelli and Morstyn [128]	2023	M	Energy	None	∼2,000
Göke et al. [129]	2023	C	Power, heat, transport, methane, & H2	Res. & Ind. heat, Res., Com., & Ind. EVs	1-5

and capacity reserves [113, 119, 124]. By matching renewable generation and load, flexibility can reduce the cost of renewable integration and the need for thermal generation [119, 121, 124, 125].

Central planning models

Central planning models assess the impact of demand flexibility on the cost-optimal design of an energy system. Compared to market models, central planning models often include extensive sector-coupling, including the heat [69, 76, 100, 114, 115, 122, 123, 127, 129], transport [76, 122, 123, 129], agricultural [122], hydrogen [76, 123, 127, 129], biomass [76], and methane [76, 123, 129] sectors. Many of these studies demonstrate that flexibility can reduce the need for firm generation [69, 94, 115, 118], wind curtailment [69, 114], storage [122, 123], and transmission expansion [123, 130].

Flexibility impact research gap

In both market and central planning models, little consideration has been given to the impact of location on the value of flexibility. As shown in Table 2.2, most flexibility studies to date consider only 1 spatial node per country. Gils [118] considers 6 regions in Germany and Guminski et al. [125] considers the full-resolution transmission network of Germany and Austria, but neither study explicitly discusses the impact of location on flexibility value. While Zhou et al. [112] investigate differences in flexibility value among 22 grid regions in the contiguous US, they do not consider the impact of flexibility location within these large grid areas. Only Hao et al. [116] and Savelli and Morstyn [128] consider the effect of location within a power system on the value of flexibility, but they consider neither increasing renewable generation nor large-scale demand-side changes. Thus, **determining where demand-side flexibility will be most valuable within a high-renewable electricity system with high residential heating electrification is a research gap (research gap 4).**

2.3.3 Near-optimal spatial planning

Two approaches have been used to explore near-optimal spatial planning of power systems in the last decade: regional self-sufficiency and modeling to generate alternatives (MGA). Both approaches have shown that a wide variety of spatial configurations of generation and storage technologies are possible without increasing power system cost significantly.

Regional self-sufficiency

Regional self-sufficiency studies compare the cost of power systems designed with self-sufficiency constraints to those designed without. Self-sufficiency constraints require that the total electricity generated in a region must be at least the total electricity demand in that region. Two studies have shown that regional self-sufficiency at the national level in Europe results in 4% [131] to 7% [132] higher system costs than the optimal spatial allocation for a fully renewable power system.

However, sub-optimal renewable allocation on smaller spatial scales leads to higher costs. Tröndle et al. [132] found that regionally net self-sufficient fully renewable systems with continental trade have 22% higher costs than continental systems. Similarly, Neumann [131] found that nodal equity costs 18% more than system optimum balanced on a continental scale. This trend can be explained by the finding of Tröndle et al. [133] that regional electricity autarky is impossible in densely populated areas of Europe because of land-use constraints. These studies suggest that different spatial distributions of renewable generation among countries do not significantly increase system cost.

Modeling to generate alternatives

MGA accounts for structural uncertainty by providing alternative feasible solutions that keep system costs within some distance of the optimum [134]. As opposed to parametric uncertainty, which arises from uncertainty about parameter values such as technology cost projections in models, structural uncertainty arises from the incomplete representation of complex systems in models. Once the cost-minimum system design is found, a budget is set that constrains near-optimal solutions to be within some percent of the minimum cost. The new MGA objective typically seeks to maximize the difference in the values of a subset of decision variables.

First applied to energy systems planning by DeCarolis [135] in 2011, MGA has recently gained popularity in energy system studies, as summarized in Table 2.3. The vast majority of these studies focus on the power sector alone, although DeCarolis et al. [136] consider both power and transport and Price and Keppo [137] and Pickering et al. [145] consider the entire energy system. The most common MGA objective is maximizing the diversity of the generation capacity mix, with recent studies including transmission and storage [135, 141–143, 145–147]. Some studies instead explore diversity in the energy mix [136, 137, 140, 148] or both the energy and capacity mix [55, 138, 139, 144]. Among energy system models, budgets are relatively consistent, ranging from up to 8% to 25% of the minimum

Table 2.3: Large-scale energy systems studies that use MGA.

Study	Year	Sector	MGA objective	Budget	Demand
DeCarolis [135]	2011	Power	Capacity	<25%	Historical
DeCarolis et al. [136]	2016	Power & transport	Energy	<10%	Exogenous power, endogenous transport fuel choice
Trutnevyte [55]	2016	Power	Energy & capacity	<23%	Historical + Monte Carlo
Price and Keppo [137]	2017	Energy	Energy	<10%	Exogenous final energy demand projection, endogenous final energy consumption
Li and Trutnevyte [138]	2017	Power	Energy & capacity	<15%	2 projections
Berntsen and Trutnevyte [139]	2017	Power	Energy & capacity	N/A	13 scenarios
Sasse and Trutnevyte [140]	2019	Power	Energy	<20%	1 projection
Sasse and Trutnevyte [141]	2020	Power	Capacity & regional distribution	<20%	1 projection
Lombardi et al. [142]	2020	Power	Capacity & regional distribution	<20%	3 projections
Neumann and Brown [143]	2021	Power	Capacity, country distribution	<10%	Historical
Pedersen et al. [144]	2021	Power	All	<10%	2011 historical
Pickering et al. [145]	2022	Energy	Capacity & regional distribution	<10%	2018 demand, endogenous fuel choice
Neumann and Brown [146]	2023	Power	Capacity	<8%	2013 historical
Lombardi et al. [147]	2023	Power	Capacity & regional distribution	<10%	Historical + electrified heat, transport, & industry
Patankar et al. [148]	2023	Power	Energy & regional distribution	<10%	High electrification + 2 EV flexibility scenarios

system cost. Within these budgets, all of these studies identify a wide range of options for future energy systems.

In recognition of the structural uncertainty arising from political, land-use, and social dynamics that energy system models capture poorly, MGA has recently been used to explore near-optimal spatial distributions of renewable generation infrastructure as well as technology mixes. A few of these studies consider near-optimal spatial distribution of generation among countries [143, 144] and many more consider spatial distribution among subnational regions [141, 142, 145, 147, 148].

While these studies have revealed a diversity of options for energy supply decarbonization, few consider structural uncertainty about demand-side changes in detail. Most studies either rely on historical power demand [55, 135, 143, 144, 146] or a small number of demand projections [137–142, 147]. Trutnevyte [55] applies Monte

Carlo sampling to historical demand but only considers ±2% variation. Berntsen and Trutnevyte [139] consider 13 different scenarios for the evolution of electricity demand in Switzerland. Patankar et al. [148] consider both high and moderate EV demand flexibility but do not include demand flexibility in their MGA objective.

Those studies that do consider endogenous demand-side changes do not consider regional differences in demand. DeCarolis et al. [136] consider endogenous transport fuel choice, including electrification, but do not differentiate between regions in the US. Price and Keppo [137] endogenously determine the primary energy consumption mix to meet a final energy demand projection for 16 global regions but do not discussion regional differences. Pickering et al. [145] endogenously determine the fuel mix to meet 2018 energy demand across all energy sectors in Europe and highlight a near-optimal range of 4% to 100% heat electrification, 53 to 100% transport electrification, and 52% to 92% EV flexibility; however, they do not explicitly discuss regional differences in electrification and flexibility.

Near-optimal spatial planning research gap

To date, near-optimal spatial planning studies have focused on supply-side structural uncertainty. But demand side changes, such as heat and transport electrification, are occurring rapidly, and there is evidence that consumers' willingness to participate in demand response varies regionally. In Britain, there are regional differences in time-of-use tariff participation [149]. During Demand Flexibility Service events in winter 2022/23, National Grid ESO reported that customers in Southern England, the East of England, and the East Midlands shifted the largest amount of electricity [37]. National Grid ESO notes that regional differences in Demand Flexibility Service participation reflect that not all energy suppliers participated and do not necessarily imply lower consumer interest in some regions [150]. However, Li et al. [151] confirm regional variation within the UK in consumer willingness to shift their activities to provide demand response based on survey data. **Despite this observed regional variation in residential consumers' participation in demand response, no studies assessing near-optimal spatial planning of**

bulk power systems include this structural uncertainty in demand-side flexibility participation (research gap 5).

2.4 Research gaps

Based on this chapter's literature review, the following research gaps have been identified:

1. **Spatiotemporal accuracy of heat pump demand.** Existing models of heat pump load that are computationally lightweight enough to be incorporated into power systems planning either do not accurately capture hourly heat pump usage patterns or do not represent sub-national heating demand variation. Chapter 3 addresses this research gap.

2. **Spatiotemporal heat pump demand grid impact.** No study has analyzed the implications of spatiotemporal variations in heat pump demand within a grid for bulk power systems planning. Chapter 4 addresses this research gap.

3. **Spatial heating flexibility potential.** No existing methods for quantifying heating flexibility potential accurately represent the geographic diversity of a national building stock with sufficiently low computational requirements to be incorporated into complex power system models. The only study that represents the geographic variation of flexibility duration potential in British homes is likely underestimating that potential because of its basis in EPCs [104], which are known to overestimate heating demand. Chapter 5 addresses this research gap.

4. **Optimal flexibility locations.** No studies assess where demand-side flexibility will be most valuable within a bulk power system with high residential heating electrification. Chapter 6 addresses this research gap.

5. **Near-optimal flexibility locations.** No studies assessing near-optimal spatial planning of bulk power systems include structural uncertainty in demand-side flexibility participation. Chapter 6 addresses this research gap.

3

Heat pump demand projection

Contents

This chapter addresses the research question: *How will residential heat pump demand vary in space and time?* A data-based, hourly regional model of heating electrification is compared to a spatially uniform hourly model of heat pump demand.

3.1 Introduction

This chapter presents a novel method for generating hourly regional heat pump demand profiles to support power system planning. This method utilizes the accurate hourly profiles and low computational requirements of a statistical model based on heat pump field trial data. This high temporal resolution model is scaled for multi-regional spatial analysis using weather reanalysis data that is globally available at high spatial and temporal resolution. The results are compared to a uniform national-level hourly profile to understand the effect of high spatial resolution heat pump demand projection.

The primary research contribution of this chapter is a regional hourly model of residential heat pump demand. This model combines a statistical model based on field trial data with high spatiotemporal resolution weather data. This method represents heat pump demand profiles more accurately than existing degree-day models at higher spatial resolution than existing statistical models, addressing research gap 1 identified in Section 2.4. This model is also computationally lightweight enough to be incorporated into power systems planning.

This chapter is structured as follows. First, the methods and data are described in Section 3.2. Section 3.3 discusses the projected heat pump demand. Finally, key outcomes are presented in Section 3.4.

3.2 Methods and data

The methods and data used in this chapter are summarized in Figure 3.1. The method is divided into four steps: (1) temperature regions, (2) temperature profiles, (3) heating demand, and (4) COP. These methods are detailed in Sections 3.2.2 through 3.2.5, and the case study data are further described in Section 3.2.1.

3.2.1 Case study data

This section describes the data used in British case study in this chapter, as summarized in Figure 3.1.

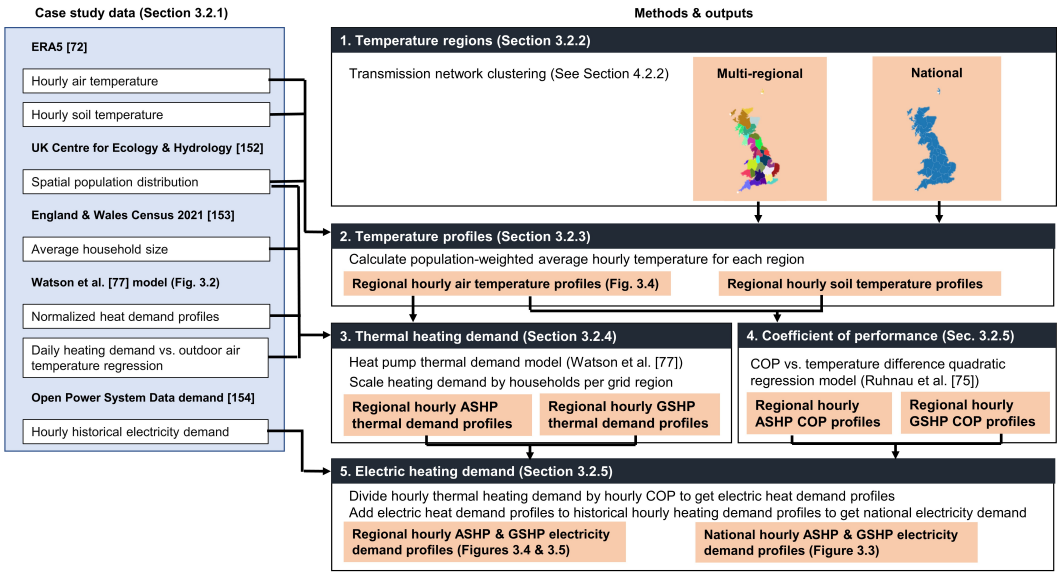

Figure 3.1: Summary of data sources, methods, and outputs for Chapter 3. Outputs for each step are highlighted in orange.

Reanalysis weather data

ECMWF (European Centre for Medium-Range Weather Forecasts) Reanalysis v5 (ERA5) provides hourly estimates of climate variables at 0.3 degree (approximately 30 km) spatial resolution from January 1940 to present [72]. In this chapter, the 2 m air temperature and the soil temperature level 4 variables are used to calculate heating demand and heat pump COP as described in Section 3.2.5. These parameters represent the air temperature 2 m above the surface and the temperature of the soil between 1 and 3 m below the surface, respectively.

Population layout

High-resolution spatial UK population data is used from the UK Centre for Ecology and Hydrology to determine the layout of households within the British Grid [152]. This 1 km × 1 km population data is based on the 2011 Census and 2015 Land Cover Map.

A constant occupation of 2.4 people per household is assumed across the whole of Britain, thus neglecting regional differences in household size. This assumption is based on a population-weighted average of the average household

size in England and Wales in both the 2011 and 2021 Census, which was 2.4 people per household [153]. This assumption is validated by comparing modeled annual heating demand with historical national heating demand and modeled regional heating demand in Section 3.3.2.

Heating demand

The Watson et al. [77] model, a statistical model of half-hourly British residential heat pump demand based on heat pump trials and gas boiler operation data, is used to generate half-hourly heat pump thermal demand profiles for British households based on average daily outdoor air temperature from ERA5. This model has two components shown in Figure 3.2: (a) and (b) normalized half-hourly heating demand profiles for different temperature ranges for ASHP and GSHP, respectively, and (c) a piecewise linear regression of outdoor air temperature and total heating demand.

The hourly thermal heating demand profiles shown in Figure 3.2(a) and (b) are based on data from the RHPP. The RHPP monitored 700 homes with heat pumps across Britain that were not connected to the gas grid from August 2011 to March 2014. The exact location of these homes is not given. Low-income households are disproportionately represented in this dataset, as Registered Social Landlords accounted for over 40% of the heat pumps installed under the RHPP. Despite the limitations of this data, discussed in Section 3.3.5, it is critical to use thermal heating profiles based on heat pump trials, rather than half-hourly gas demand data. The main reason for this is that heat pumps tend to be sized at a lower heating capacity than boilers: this capacity difference leads to more continuous demand profiles from heat pumps compared to peakier gas demand profiles, which in turn leads to overestimating the peak thermal demand from heat pumps by about 8% when using gas boiler demand data [77].

These hourly thermal heating demand profiles demonstrate that behavioral patterns and heat pump type determine hourly heating demand across a wide range of temperatures. For both ASHPs and GSHPs, heating demand is characterized by peaks in the morning and evening, when many people wake up for work and

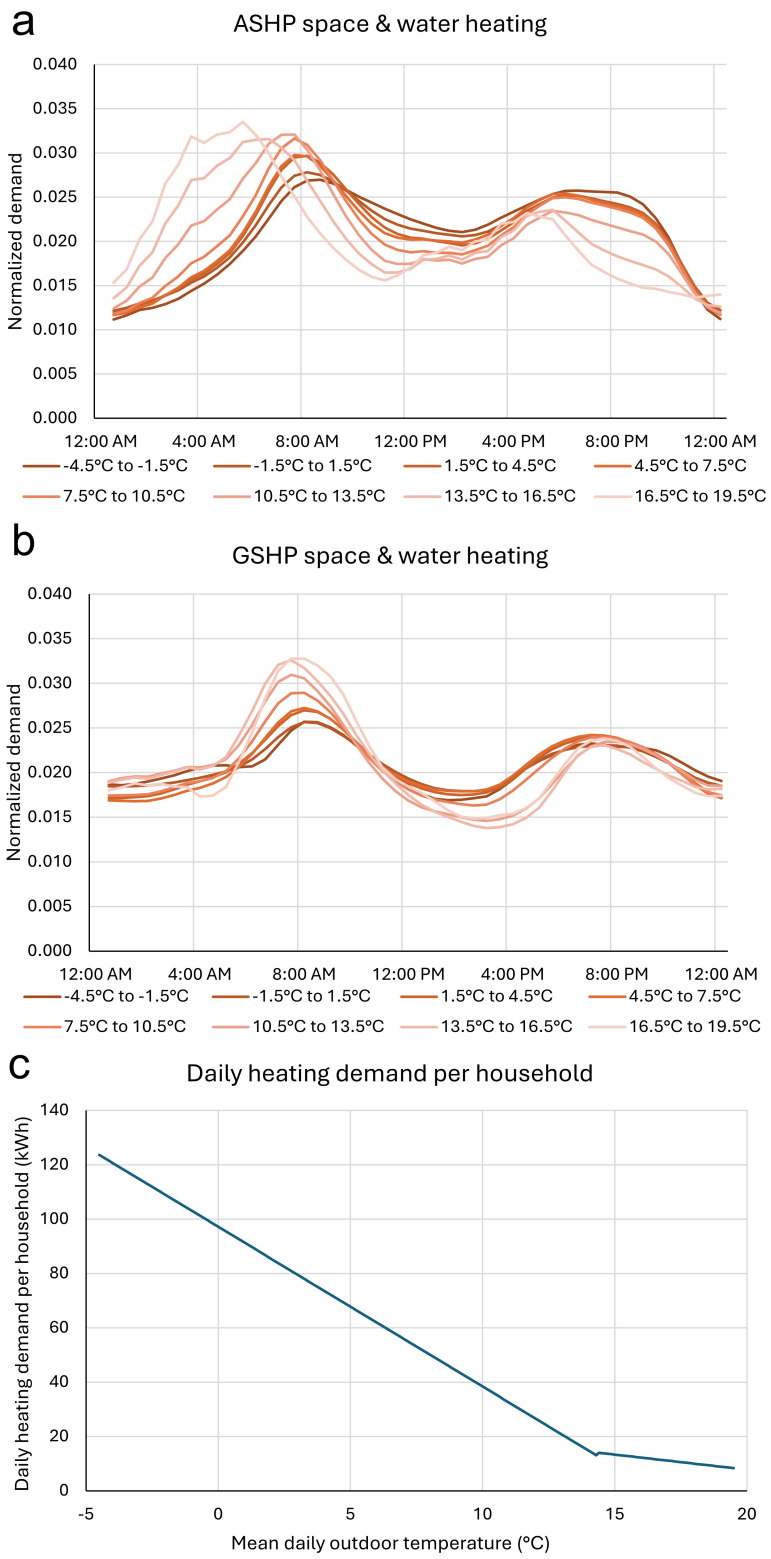

Figure 3.2: Aggregated half-hourly thermal heating demand profiles for households with (a) ASHP and (b) GSHP, normalized to sum to 1 unit-day, and (c) daily heating demand per household and daily mean temperature piece-wise linear regression model from Watson et al. [77] based on British heat pump trials and gas boiler operation data.

return home from work, respectively. These peaks are more pronounced at higher temperatures, when water heating predominates over space heating. Heat pump type also plays a role in heating demand at night and in the middle of the day. At colder temperatures, heating demand at midday is much higher than at night for ASHPs. In contrast, GSHP heating demand is relatively consistent between midday and at night at low temperatures. The consistency of these daily patterns across temperatures suggests that behavioral patterns are the predominant factor in determining hourly heating demand profiles.

The daily temperature and heating demand regression from Watson et al. [77] is shown in 3.2(c). To address the limitations of the RHPP dataset in representing the British housing stock and distribution of household characteristics, Watson et al. [77] use additional data from the Energy Demand Research Project (EDRP) in this regression. The EDRP dataset includes half-hourly heating demand between May 2009 and July 2010 from over 6600 single-family homes with gas boilers. The households in this dataset are also labeled with the socio-economic status of their postcode, so Watson et al. [77] weight data from each household category to create a representative regression. The heating demand regression assumes a heating pattern breakdown consistent with 25% GSHPs and 75% ASHPs, as observed in the RHPP trials. This ratio of ASHPs to GSHPs represents a middle ground between current British heat pump installation trends, in which ASHPs vastly outnumber GSHPs (see Figure 1.1), and the National Grid ESO high-electrification scenario, which includes GSHPs in 37% of households with heat pumps and ASHPs in 63% [54].

Historical electricity demand

Historical hourly electricity demand data is obtained from an open-source compilation of data from the European Network of Transmission System Operators for Electricity (ENTSO-E) transparency platform [154].

3.2.2 Temperature regions

To assess spatiotemporal differences in heating demand, two approaches are considered for analysis: (1) a novel method for generating hourly regional heat pump demand profiles for 30 temperature zones within Britain[1]; and (2) an approach for generating a single, countrywide heating demand profile, similar to the data provided in Ruhnau et al. [75]. The analysis performed using 30 temperature zones is referred to as "multi-regional," and the analysis using the single, national temperature region is referred to as "national." The boundaries of these two sets of regions are shown in the temperature regions box of Figure 3.1.

3.2.3 Temperature profiles

For each temperature region in the national and multi-regional approaches, population-weighted hourly air and ground temperatures T_r^{air} and T_r^{ground} are calculated. Specifically, assuming that more populous areas have a larger impact on heating demand, a population-weighted spatial average of the soil and air temperatures from ERA5 [72] for each region is taken using 1 km by 1 km population data based on 2011 Census and 2015 Land Cover Map [152]. This results in 30 regional hourly temperature profiles for the multi-regional approach and a national hourly temperature profile for the national approach.

3.2.4 Heating demand

The Watson et al. [77] model is used to calculate hourly thermal heating demand for each region using its mean daily air temperature $T_{r,d}^{air}$. The total heating demand per household $Q_{r,d}^{HH}$ for day d in each region r is calculated using the following piece-wise linear regression:

$$Q_{r,d}^{HH} = \begin{cases} 97.2 - 5.88 \cdot T_{r,d}^{air} \text{ kWh} & T_{r,d}^{air} < 14.3℃ \\ 30 - 1.11 \cdot T_{r,d}^{air} \text{ kWh} & T_{r,d}^{air} \geq 14.3℃ \end{cases} \tag{3.1}$$

[1]In anticipation of incorporating these heating demand profiles into power systems planning in Chapter 4, the multi-regional temperature regions are the grid regions resulting from hierarchical agglomerative clustering of the transmission network based on renewable generation potential, detailed further in Section 4.2.2.

While Watson et al. [77] identify slight differences in daily heat demand between households with ASHPs and those with GSHPs[2], this regression assumes uniform daily demand across households with GSHPs and ASHPs in the same region. This regression is based on a mix of 75% ASHPs and 25% GSHPs, as observed in the RHPP trials.

Hourly regional thermal heating demand is calculated by multiplying regional daily heating demand with a temperature-dependent hourly demand profile for either GSHPs or ASHPs from Watson et al. [77]. Figures 3.2(a) and (b) show the normalized profiles for ASHP and GSHP, respectively. To reflect the different use patterns observed in the RHPP trials, separate normalized hourly[3] daily-temperature-dependent profiles for GSHPs $D_t^{GSHP}(T_{r,d}^{air})$ and ASHPs $D_t^{ASHP}(T_{r,d}^{air})$ from Watson et al. [77] are used:

$$D_{r,t}^{HH,ASHP} = Q_{r,d}^{HH} \cdot D_t^{ASHP}(T_{r,d}^{air}) \; \forall \; t \in \{1, ...24\} \tag{3.2}$$

$$D_{r,t}^{HH,GSHP} = Q_{r,d}^{HH} \cdot D_t^{GSHP}(T_{r,d}^{air}) \; \forall \; t \in \{1, ...24\} \tag{3.3}$$

These hourly household demand profiles are multiplied by the number of households in each temperature region to give hourly regional heating demand profiles, $d_{n,air,t}$ for ASHPs and $d_{n,ground,t}$ for GSHPs in location n at time t.

Thermal heating demand and COP are modeled separately rather than modeling electric heating demand directly; this enables adjustment of the COP model to reflect heat pump efficiency improvements and analyzing different sink temperature assumptions such as the effect of high-temperature radiators or underfloor heating. For the national heating demand approach, demand is distributed to each region proportionally to its population. To establish the impact of widespread heat pump

[2]The separate ASHP and GSHP regressions shown in Equations 6.3 and 6.4 are found to decrease modeled heating demand error relative to historical total annual heating demand to -0.05% in Chapter 6 compared to +0.7% using a single regression with multi-regional temperatures, as discussed in Section 3.3.2.

[3]While Watson et al. [77] provide half-hourly demand profiles, this work resamples these demand profiles to hourly based on the maximum normalized demand in each hour to match the hourly reanalysis weather data used in power system planning.

adoption on the power system, it is assumed that 26.5 million British households use heat pumps for space and water heating, consistent with the CCC central scenario in which 80% of households have a heat pump in 2050 [5].

While the Watson et al. [77] model is based on a limited heat pump demand dataset, as discussed in Section 4.2.1, high spatial granularity weather reanalysis data from ERA5 [72] for each region is leveraged to obtain high spatiotemporal granularity heating demand data. Watson et al. [77] suggest that their model can be used for either national or regional projections of heat pump demand within Britain by using the appropriate population-weighted temperature. Furthermore, Anderson et al. [84] have already demonstrated good agreement between a temperature-based model trained on the RHPP trial data and local heat pump demand profiles from a small trial in London.

This spatial interpolation of demand profiles based on local temperature requires that each region has sufficient households for load diversification to occur. The least populous region used in the multi-regional analysis has 10,880 households, which is well above the threshold for heat pump load diversification of 275 households identified by Love et al. [79].

3.2.5 Coefficient of performance

COP is calculated based on the hourly temperature difference between the source and sink. The source temperature $T^{source}_{r,s,t}$ for region r at time t depends on the heat pump type s:

$$T^{source}_{r,s,t} = \begin{cases} T^{air}_{r,t} & s = \text{ASHP} \\ T^{ground}_{r,t} & s = \text{GSHP} \end{cases} \tag{3.4}$$

All sinks are assumed to be radiators, and their outlet temperature is calculated based on the outdoor air temperature, following Ruhnau et al. [75]:

$$T^{sink}_{r,t} = 40\ ^{\circ}\text{C} - 1.0 \cdot T^{air}_{r,t} \tag{3.5}$$

This equation reflects that higher radiator temperatures are required to maintain a comfortable indoor temperature at lower outdoor air temperatures. Because

the plurality (41%) of heat pumps installed in the ongoing Electrification of Heat Demonstration were low-temperature (<65℃) ASHPs, this equation seems likely to represent the radiator temperatures in most British households with heat pumps [34].

As in Ruhnau et al. [75], a minimum temperature difference of 15 ℃ is imposed to avoid unrealistically small temperature differences at warm outdoor temperatures.

$$\Delta T_{r,s,t} = \begin{cases} 15\ ℃ & T_{r,t}^{sink} - T_{r,s,t}^{source} < 15℃ \\ T_{r,t}^{sink} - T_{r,s,t}^{source} & \text{otherwise} \end{cases} \tag{3.6}$$

Regional COP $COP_{r,s,t}$ for region r and heat pump type s at each time t is calculated based on quadratic regressions of the hourly temperature difference $\Delta T_{r,s,t}$ between the heat source and sink [75]:

$$COP_{r,s,t} = \begin{cases} 6.08 - 0.09 \cdot \Delta T_{r,s,t} + 0.0005 \cdot \Delta T_{r,s,t}^2 & s = \text{ASHP} \\ 10.29 - 0.21 \cdot \Delta T_{r,s,t} + 0.0012 \cdot \Delta T_{r,s,t}^2 & s = \text{GSHP} \end{cases} \tag{3.7}$$

For an outdoor air temperature of -0.4℃, this model provides a COP value of 3.24 for ASHPs and 3.71 for GSHPs; both values are higher than the mean COP of 2.44 observed at this temperature in the ongoing Electrification of Heat Demonstration between 2020 and 2022 [8]. Because of its basis in manufacturer measurements of heat pump performance, this model can thus be taken as a realistic projection of future heat pump performance.

Note that these COP values do not account for auxiliary systems such as defrosters for ASHPs or potential backup heaters. It is also assumed that ground thermal energy is restored on an annual basis for GSHPs. Any energy that may be used in a reverse cycle to replenish thermal energy in the ground over the course of the year is neglected.

3.2.6 Heating electricity demand

Hourly heating electricity demand $d_{r,s,t}^{elec}$ for region r and heat pump type s at time t is calculated based on the ratio of hourly thermal heating demand $d_{r,s,t}$ (calculated in Section 3.2.4) and hourly $COP_{r,s,t}$ (calculated in Section 3.2.5):

$$d^{elec}_{r,s,t} = \frac{d_{r,s,t}}{COP_{r,s,t}} \; \forall r,\; t,\; s \in \{\text{ASHP, GSHP}\} \tag{3.8}$$

The heat pump electricity demand projections are added to historical hourly electricity demand data to quantify the change in total electricity demand.

3.3 Results and discussion

This section discusses the projected heat pump demand. Section 3.3.1 discusses the change in national electricity demand based on both models, and Section 3.3.2 validates the projected national and multi-regional heat demand. Section 3.3.3 connects spatial differences in temperature and heating demand differences between the national and multi-regional approach, and Section 3.3.4 analyzes spatiotemporal differences in electric heating demand between the two approaches. Finally, Section 3.3.5 discusses the limitations of this chapter.

3.3.1 National electricity demand

Widespread adoption of heat pumps will dramatically increase electricity demand, as shown in Figure 3.3. This figure compares the additional electricity demand from heat pumps calculated based on national and multi-regional temperature regions using Equation 3.8. While national heating demand is calculated based on a single population-weighted temperature for Britain, multi-regional heating demand is calculated using 30 regional population-weighted temperatures and summing heating demand in each region. Historical electricity demand for 2019 is included to demonstrate how heat pumps would increase electricity demand in both projections.

Whether a spatially homogeneous or heterogeneous heating demand profile is used, switching all current British households to heat pumps nearly doubles the 2019 historical peak electricity demand of 51.4 GW. Despite regional differences in peak demand, discussed in Section 3.3.3,these two approaches lead to little difference in the total peak demand: peak demand is 91.0 GW with the national heating profile and 91.9 GW with the multi-regional heating profile. This difference emerges because of regional differences in heating demand at the peak time. No matter the

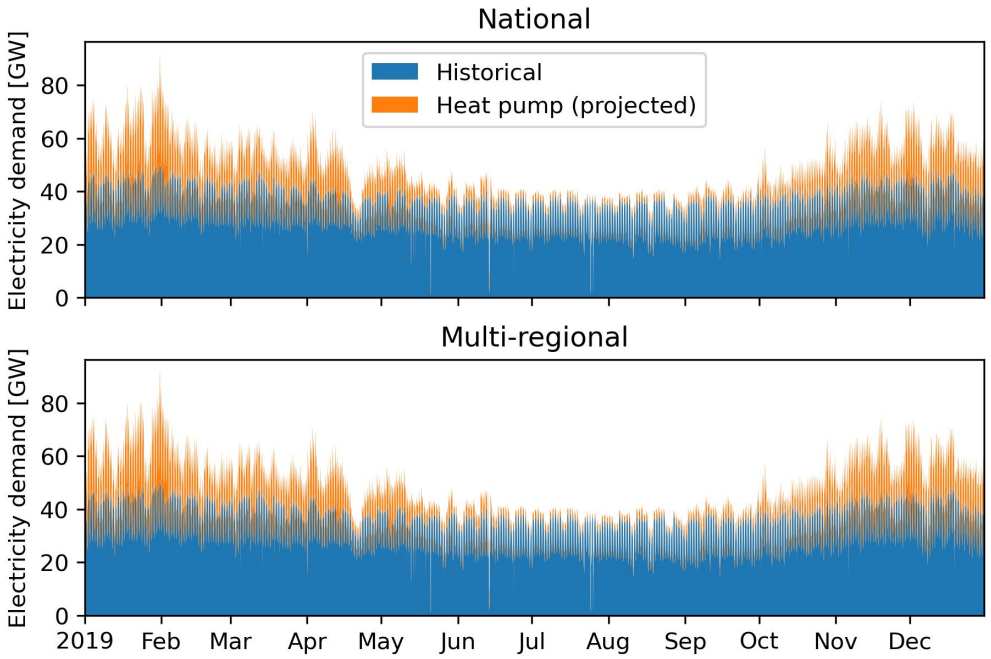

Figure 3.3: Hourly historical electricity demand and projected heat pump demand for 2019 based on national (top) and multi-regional (bottom) projections.

spatial resolution of the heating demand used, the total electricity demand peaks at 8 am on 31 January 2019. This peak time is one hour earlier than the historical electric peak demand, which occurred at 9 am on 31 January 2019. At the new peak time, there is 49.6 GW of historical electrical demand as well as 41.4 GW of heating demand when using national heating demand profiles and 42.3 GW of heating demand when using multi-regional heating demand.

In addition to nearly doubling peak demand, switching all current British households to heat pumps will increase annual electricity demand by about one-quarter. Because of the non-linearity of the daily heating demand regression in Equation 3.1, total heating demand slightly differs between the two approaches: because of the slope differences around the break point, regions with temperatures just above 14.3℃ have superlinearly higher heating demand than those with temperatures just below 14.3℃. National heating demand projections add 75.7 TWh of electricity demand, and multi-regional heating demand projections add 77.7 TWh of electricity demand to the 2019 total historical electricity demand in Britain of 298.6 TWh. The addition of heat pump demand increases seasonal

variation in electricity demand as much of this additional demand occurs between November and April. Although both approaches lead to similar annual heating demand, they lead to significant regional differences in annual heating demand, as discussed in Section 3.3.3.

3.3.2 Heating demand validation

To validate the use of national and multi-regional temperature profiles in the Watson et al. [77] model, the total annual heating demand, regional annual heating demand, and peak electrical heating demand are compared with other sources. The historical annual heating demand is only available in thermal terms because the majority of heating in Britain currently uses thermal fuels. However, the peak electrical heating demand is a key quantity for planning the power system and has been estimated in several papers.

Total annual heating demand

The total annual heating demand for all of Britain is compared with the historical demand for space and water heating. The Energy Consumption in the UK (ECUK) dataset [46] gives the total annual final energy consumption for domestic space and water heating for different fuels. This final energy consumption is converted to thermal demand using typical efficiencies of different heating technologies from the IEA [155]. The prevalence of different boiler types in England from the English Housing Survey Headline Report [156] is used to calculate a weighted average efficiency for boilers. The average efficiency of 95% is applied to natural gas and oil final energy consumption. The solid fuel and bioenergy and waste categories are assumed to be burned in pellet stoves with 85% efficiency, and both electricity- and heat-based heating systems (such as district heating) are assumed to have have 100% efficiency. This approach gives a historical thermal energy demand of 337.9 TWh for domestic space and water heating in 2019. The total annual thermal demand calculated from the national approach (335.5 TWh) and multi-regional approach (340.3 TWh) only deviate by -0.7% and +0.7%, respectively.

Regional annual heating demand

To validate the improved accuracy of the multi-regional heating demand model compared to the national model, regional annual residential heating demands are compared with estimates from two other models. To facilitate comparison, both the national and multi-regional models are applied to 11 NUTS-1 (Nomenclature of Territorial Units for Statistics) regions in Britain [157][4] rather than 30 grid regions. The resulting regional annual heating demand is compared with the the National Comprehensive Assessment (NCA) geospatial model and the HotMaps model.

The NCA geospatial model uses an energy demand benchmark approach based on building floor areas and types to estimate the spatial distribution of heating demand across the UK [158]. For buildings on the gas grid, the heat demand estimates are calibrated based on subnational gas consumption data to reflect regional differences in weather, building efficiency, and heating practices. Notably, this model overestimates total domestic heating demand for 2020 by 19% compared to the ECUK-derived 2020 total. The regional annual domestic demand estimates for 2020 for NUTS-1 regions are compared with the methods introduced in this chapter.

The HotMaps model uses a top-down approach to estimate final energy demand for space heating and domestic hot water on a hectare scale for all EU 28 countries, plus Iceland, Norway, and Switzerland [159, 160]. This top-down approach downscales national-level energy consumption data to smaller regions based on population, weather, and building stock characteristics; these downscaled data are further downscaled to the hectare level based on population, land use, and gross domestic product data. This hectare-level heating demand is aggregated to the NUTS-1 level for comparison with the methods introduced in this chapter.

Table 3.1 compares residential annual heating demand estimates from the multi-regional and national models introduced in this chapter to the NCA and HotMaps models. While there is variation in regional heating demand estimates between these models, the multi-regional model generally provides an estimate of residential

[4]Source: Office for National Statistics licensed under the Open Government Licence v.3.0. Contains OS data © Crown copyright and database right 2022.

Table 3.1: Regional annual residential heating demand from different models

NUTS-1 region	NCA (TWh)	HotMaps (TWh)	Multi-regional (TWh)	National (TWh)
North East England	17.0	16.0	14.0	12.9
North West England	43.9	40.9	39.0	37.0
Yorkshire & The Humber	33.9	30.5	32.9	29.9
East Midlands	28.7	26.0	31.8	30.6
West Midlands	34.3	31.5	34.6	33.7
East of England	36.1	31.7	39.3	41.1
London	50.1	40.9	29.2	30.6
South East England	53.1	45.5	50.6	53.5
South West England	32.1	29.4	24.0	25.8
Wales	18.9	19.2	15.0	15.0
Scotland	35.1	35.2	32.1	27.6

heating demand that is in closer agreement with estimates from other sources than the national model. In particular, the multi-regional heating model is more consistent with other sources for regions in northern Britain (Scotland, North East England, North West England, and Yorkshire and the Humber) than the national model. Because the temperature-based models introduced in this chapter do not account for regional housing stock differences, some significant differences emerge: heating demand is overestimated compared to the NCA and HotMaps models in the East of England, which has the lowest share of homes built before 1900 in England and Wales and thus the most efficient housing stock [31]. Conversely, the national and multi-regional models underestimate heating demand in London and Wales, which have the highest shares of homes built before 1900 in England and Wales at 22% and 23%, respectively. A portion of the difference between the national and multi-regional models for London and the NCA model could be because the NCA model overestimates residential heating demand compared to ECUK. Overall, the multi-regional method is more consistent with other models of regional heating demand than the national model.

Peak electricity demand

To further validate the use of different temperature profiles in the model, the peak electricity demands for both approaches are compared to previous projections. Using national temperature profiles leads to a peak electric heating demand of 41.4 GW and using multi-regional temperature profiles leads to 42.3 GW. These peak values agree with those of the When2Heat model [75] for 2019 with a COP weighted as

75% ASHP with radiators and 25% GSHP with radiators for space heating and a COP weighted as 75% ASHP to water and 25% GSHP to water for hot water. Using this approach gives a peak heating demand of 40.4 GW, which is just 1.0 GW lower than the peak obtained using the national approach and 1.9 GW lower than that obtained using the multi-regional approach. These figures are much lower than the peak demand projections from Watson et al. [15] of 62 GW for a cold year in the 2020s with very good heat pump performance (seasonal performance factor (SPF)$>$ 3). This difference arises from the use of different weather-years and different heat pump performance assumptions. Both winter 2018/19 and winter 2019/20 were milder than average [161, 162], so it is expected that the 2019 peak demand to be less than that of a cold year in the 2020s. Moreover, the SPF for both GSHPs and ASHPs is above 4 in every region, so heat pump performance is much better than that considered in Watson et al. [15] based on the RHPP trials. Overall, the peak electricity demand used in this chapter is in line with recent estimates for a mild winter with high performance heat pumps in the When2Heat model [75].

3.3.3 Spatial differences in temperature & heating demand

The spatial differences in temperature and heating demand profiles between the national and multi-regional approaches are illustrated in Fig. 3.4.

Figure 3.4(a) and (b) shows the spatial differences in mean temperature and temperature standard deviation used in the multi-regional analysis. Although both approaches are consistent with total historical thermal heating demand, temperature differences across regions are notable.

Using the national approach, the hourly temperature profile for 2019 has a population-weighted mean temperature of 10.5℃ and a standard deviation of 5.3℃. With the multi-regional approach, the mean annual temperature by region, shown in (a), ranges from 8.0℃ in the north of Britain to 11.4℃ in the south. Generally, the mean temperature increases from the northwest to the southeast. Figure 3.4(b) shows the standard deviation in hourly temperature, which ranges from 3.9℃ on the northeast coast to 5.9℃ inland in the south. The hourly temperature standard

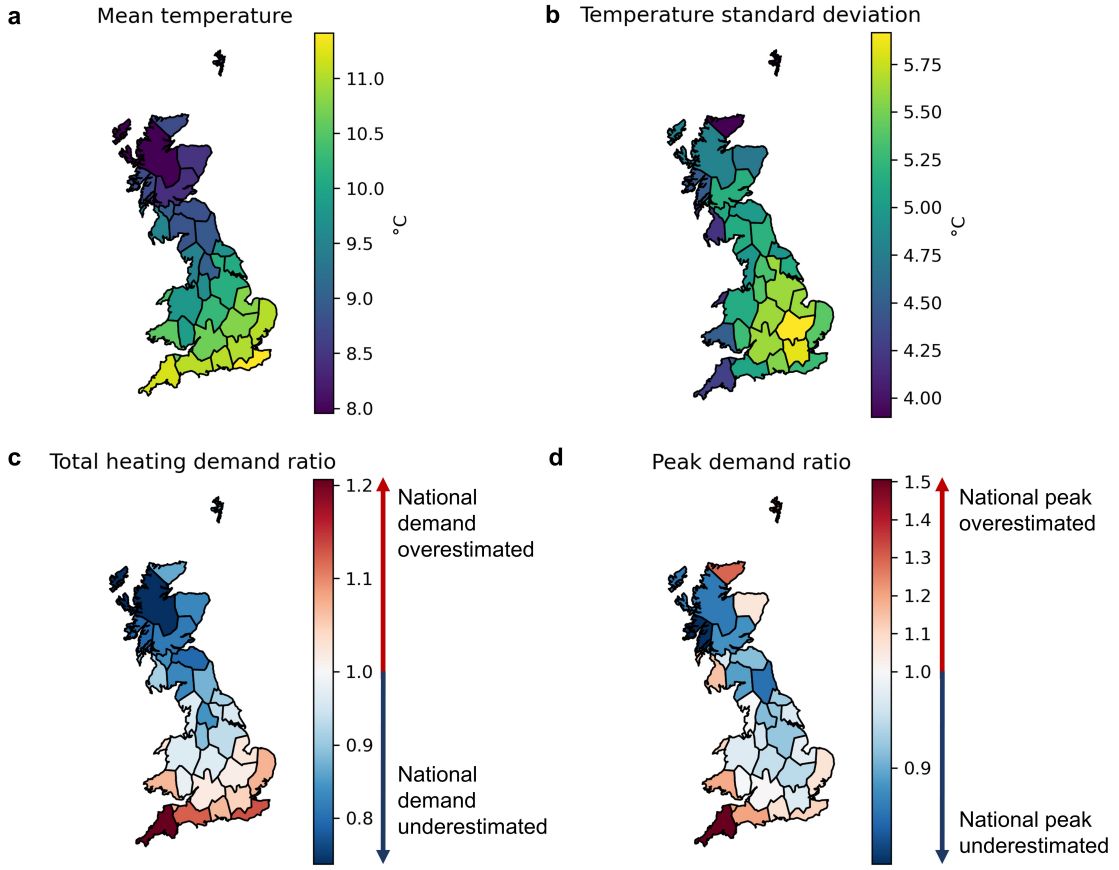

Figure 3.4: Maps summarizing spatial differences in temperature data and comparing spatially homogeneous and heterogeneous heating demand profiles in each region. Maps of (a) the mean and (b) standard deviation of hourly temperature in 2019. Map (c) displays the ratio of total heating demand using the national approach compared to the multi-regional approach. Map (d) shows the peak demand ratio comparing the regional heating demand at the peak system demand time when using the national approach compared to the multi-regional approach. Reproduced from Halloran et al. [58] under a CC BY 4.0 license.

deviation is generally lower in coastal areas and the north and higher inland and south. This result is explained by the high thermal capacity of oceans and seas, which keeps coastal temperatures steady when the temperature varies inland.

Figures 3.4(c) and (d) compare the heat pump load differences in total heating demand (c) and peak heating demand (d) when using the national approach. This analysis highlights the significant spatial differences in the heat pump demand.

The results in Figure 3.4(c) demonstrate that using a national temperature region overestimates annual electrical heating demand by up to 26% in the south

of Britain and underestimates by up to 21% in the north compared to the multi-regional approach. Because temperature is the basis of the multi-regional model, these errors are closely correlated with mean temperature: regions with lower mean temperatures have their demand overestimated when using a homogeneous heating demand profile. Temperature standard deviation has a secondary effect on the total heating demand estimate ratio: coastal regions in the south with low standard deviation in temperature have consistently higher temperatures, so they have some of the highest overestimates in homogeneous heating demand.

Figure 3.4(d) displays the ratio of the regional heating demand at the peak system demand time. Using national temperature to model heating demand overestimates the peak consumption in regions with large area shares near the coast, particularly in the south, by up to 51% and underestimates peak consumption inland (regions with low area shares near the coast) by up to 20%. This result is explained by the lower temperature standard deviation in coastal areas, which suggests that the temperature in those regions will drop less than the temperature inland on cold days.

This chapter only compares the multi-regional and national heating demand models for the 2019 weather-year; however, the differences between the models observed for this weather-year are based on geographically-driven weather patterns, such as colder temperatures in the north than the south and lower temperature variation in coastal areas than inland. Therefore, similar differences between the multi-regional and national heating demand models are expected across weather-years.

3.3.4 Spatiotemporal differences in heating demand

Using a spatially homogeneous heat demand profile leads to spatiotemporal inconsistencies with local temperature-based heating demand in different regions throughout the year, as illustrated in Figure 3.5. This figure shows hourly electric heating demand per household in 4 sample regions from 28 January to 2 February 2019, which includes the peak heating demand at 8 am on 31 January. Regions are labeled based on their clustered electrical bus number, as described in Section 4.2.2.

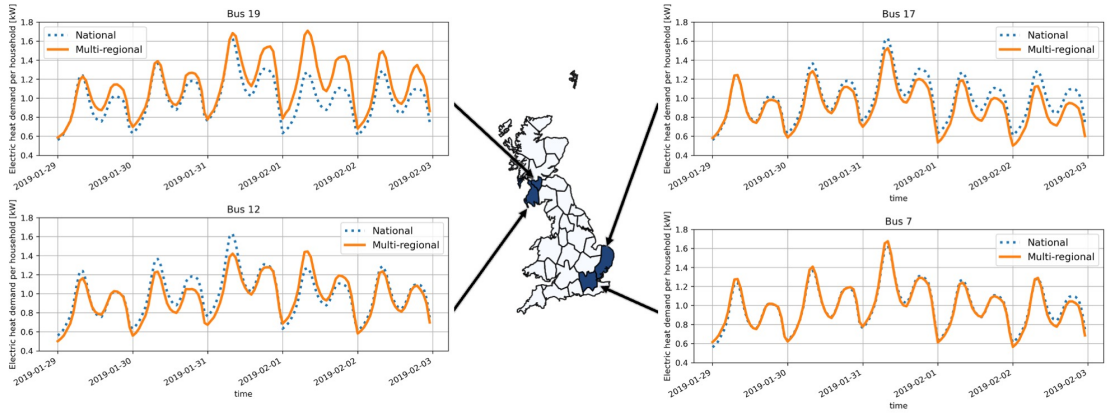

Figure 3.5: Map illustrating the spatiotemporal inconsistencies between uniform heating demand per household based on national temperature (shown with dotted blue lines) and spatially varied heating demand based on multi-regional temperature (shown with solid orange lines) in four regions. Hourly electrical heating demand is shown for five days, including the peak heating demand day. Reproduced from Halloran et al. [58] under a CC BY 4.0 license.

Because occupancy patterns determine hourly heating patterns during the heating season, as discussed in the heating demand section of Section 3.2.1, the shape of the heating demand profiles are similar in all regions for the days shown in Figure 3.4. However, there are important daily differences in the magnitude of heating demand based on the regional temperature. At Bus 19, an inland region in northern Britain south of Glasgow, both morning and evening heating peaks and total heating demand are underestimated when using the national approach. In contrast, using a national temperature-based approach at Bus 12, a coastal region in northern Britain in southwestern Scotland, tends to overestimate morning and evening peaks but underestimates total heating demand. Bus 7 is an inland region in southern Britain (Greater London) where using the national approach heating demand underestimates morning and evening peaks and overestimates the annual total heating. Because Bus 7 has the highest population of any region in Britain, it has the smallest inconsistencies between multi-regional temperature-based heating demand and heating demand based on a national, population-weighted temperature profile. For Bus 17, a coastal region in southern Britain in the East of England, it was found that using a homogeneous heating profile overestimated both morning and evening peaks and total heating demand.

3.3.5 Limitations & uncertainty

This chapter demonstrates the heating demand models using a single historical weather-year of temperature data, but robust power system planning should consider multiple weather years of data. While the differences identified in heating demand are expected to persist between weather-years because they result from enduring north-south and coastal-inland temperature differences, the specific differences between regions may vary. The impact of climate change on heating demand is also not considered. For high-electrification scenarios in the UK, Eggimann et al. [163] found that mean peak electricity demand and weather-related variability in peak demand would increase under the high-emissions RCP8.5 global warming scenario. This finding suggests that using historical weather data increases the uncertainty of peak heating demand projections.

The models for heat pump demand introduced in this chapter is only based on outdoor temperature, the primary driver of heating demand and COP values. Other weather variables, such as wind speed, humidity, and solar irradiance, have been shown to have a secondary effect on heating demand [27] but are not included in this model. Excluding these weather variables increases the uncertainty of these spatial heating demand projections, so future models of heating demand should incorporate them when more data about their impact on aggregated heat pump load is available.

These models also do not capture regional differences in housing stock and behavior, such as occupancy patterns and indoor temperature, on heating demand. While the EDRP data used for daily heating demand is weighted to be nationally representative, it does not account for regional differences in building stock. The age and efficiency of homes in England and Wales varies by region: 22% of homes in London and 23% of homes in Wales were built before 1900, compared to just 10% in the East of England [31]. In addition, home size varies among regions: in England, average floor areas range from 84 m^2 in London to 102 m^2 in the South East, and homes in rural areas tend to be larger on average (123 m^2) than those in urban areas (80 m^2) [33]. As more data is available about the effect of

these regional characteristics on heat pump demand, it should be incorporated into future models to increase accuracy.

Because of their basis in the RHPP trials, the hourly heating profiles used in these models may not be representative of heat pump operation in the entire British housing stock. The hourly heating demand profiles used in these models are based on the RHPP dataset, which Love et al. [79] note disproportionately represents social housing and heat pumps with smaller thermal capacities than other heat pumps installed in Britain during the same time period. Moreover, the locations of heat pump installations in the RHPP trial are unknown, and thus it is uncertain if this dataset captures representative hourly heat pump use patterns for the whole of Britain. The ongoing Electrification of Heat trial investigates the operation of heat pumps in a more representative sample of British homes [34], so a model based on the results of this trial could be used in future work.

To assess long-term changes in power demand, this chapter focuses on a high-penetration end state for residential heat pumps. Furthermore, this chapter assumes uniform national heat pump adoption across all regions. Thus, spatial differences in demand due to regional variation in heat pump adoption are not included. Future work could incorporate regional heat pump adoption projections from the FES [23] to project regional heat pump demand between now and 2050.

3.4 Key insights

This chapter introduces a novel approach for modeling residential heat pump demand by scaling data from field trials with high spatiotemporal resolution temperature data to generate spatially varied heat demand profiles. The results are compared with a conventionally-used single national heating profile. Large regional differences in total and peak heat demand are identified between the two approaches. Based on the results, the following key insights can be gained:

Both the national and multi-regional approach project that switching all British households to heat pumps would drastically alter historical electricity demand. Heat pumps would nearly double peak electricity demand from 51.4 GW in 2019

to 91.0 GW for the national heating profile and 91.9 GW for the multi-regional heating profile. Both approaches project that a complete switch to heat pumps would increase annual electricity demand by about 25%, from 298.6 TWh in 2019 to 374.3 TWh for the spatially uniform projection and 376.3 TWh for the spatially varied projection.

The regional hourly heating demand modeling approach is validated by comparison with historical annual heating demand and other projections of peak electrical heating demand. Both the national and multi-regional approaches only deviate by -0.7% and +0.7%, respectively, from the historical annual heating demand on the national level. However, the multi-regional model regional annual heating demand is in closer agreement with other models of regional heating demand than the national model. The projected peak electric heating demands of 41.4 and 42.3 GW for 2019 from the national and multi-regional approaches, respectively, are in line with recent peak electric heating demand for a mild winter with high performance heat pumps.

Comparing the multi-regional model with the national model reveals regional differences in peak demand and total annual heating demand. The national temperature-based model overestimates total heating demand in southern regions by up to 26% and underestimates demand in northern regions by up to 21%. In the hour when peak system-wide heating demand occurs, using national temperature overestimates the electric heating demand in coastal areas by up to 51% and underestimates it inland by up to 20% compared to the multi-regional approach.

This chapter reveals significant spatiotemporal variation in heating demand in Britain. In Chapter 4, both national and multi-regional heating demand will be incorporated into bulk power system planning to assess the impact of this spatiotemporal variation.

4

Planning with heat pump demand

Contents

This chapter addresses the research question: *How will spatiotemporal differences in residential heat pump demand impact bulk power system planning?*

4.1 Introduction

The spatiotemporally varied multi-regional heat demand profiles developed in Chapter 3 are integrated into a generation, storage, and transmission expansion planning model. The results are compared to a system planned using the spatially

uniform national-level profile from Chapter 3 to understand the power system impact of spatiotemporal heating demand resolution under different policy scenarios.

The primary research contribution of this chapter is assessing the impact of spatiotemporal differences in heat pump demand on bulk power systems planning. This is accomplished by developing GeoHeat-GB, an open-source capacity expansion model with regional hourly heating demand in Britain [164]. By assessing the power system planning implications of spatiotemporal variation in heat pump demand within a grid, this chapter addresses research gap 2 identified in Section 2.4.

This chapter is structured as follows. First, the methods and data are described in Section 4.2. In Section 4.3, results are discussed, starting with the power systems planning results for the central policy scenario in Section 4.3.1 and then additional scenarios in Section 4.3.2. Finally, conclusions are presented in Section 4.4.

4.2 Methods and data

The methods and data used in this chapter are summarized in Figure 4.1. This chapter continues to focus on the British case study introduced in Chapter 3 using input data from ERA5, the PyPSA-Eur dataset, Chapter 3, and Elexon. The methods are divided into transmission network clustering, capacity expansion planning, and operational regret analysis. The power system model used in this chapter expands on the electricity-only version of the capacity expansion model PyPSA-Eur to incorporate exogenous heating demand into power systems planning. This modified version of the model and additional documentation are available on the GeoHeat-GB GitHub repository, which includes modules for power system planning with additional demand from heat pumps [164].

The case study data are further described in Section 4.2.1, and the methods are detailed in Sections 4.2.2 through 4.2.4.

4.2.1 Case study data

This section describes the data used in British case study in this chapter, as summarized in Figure 4.1.

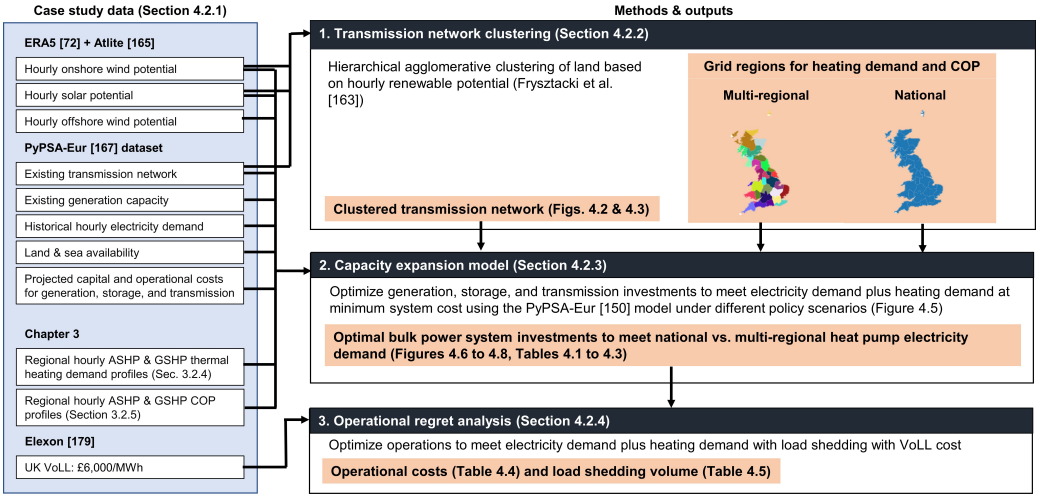

Figure 4.1: Summary of data sources, methods, and outputs for this chapter. Outputs for each step are highlighted in orange.

Reanalysis weather data

Weather data from the ERA5 dataset [72] are processed into hourly renewable onshore wind, offshore wind, solar photovoltaic, and hydropower generation potential at 0.3 degree spatial resolution using the Atlite toolkit [165]. Onshore and offshore wind generation potential are calculated using 100 m wind speed, the wind speed 100 m above the surface of the Earth, and forecast surface roughness, the aerodynamic roughness length. This parameter determines how wind speed changes with height above the surface of the Earth based on the roughness of the surface. The power curves for the Vestas V112 3-MW turbine were used for onshore wind, and the NREL 5-MW Reference Turbine was used for offshore wind. Hydropower potential is calculated using runoff, the depth of water from precipitation that drains over the surface or under the ground, and height, the surface elevation above sea level. Solar photovoltaic potential is calculated using top of atmosphere incident solar radiation, direct and diffuse influx, albedo, and air temperature at 2 m height to calculate panel efficiency. Because crystalline silicon solar panels have photovoltaic market share of at least 97% [166], they are the assumed technology for all PV.

Power system data

The PyPSA-Eur dataset was used as part of the electricity-only PyPSA-Eur capacity expansion model [167]. PyPSA-Eur uses Corine Land Cover data to calculate land availability for renewable expansion and excludes natural protection areas, such as protected habitats, based on Natura 2000 [168, 169]. Offshore wind locations for each country are limited to their exclusive economic zones [170], and bathymetric data from GEBCO 2014 is used to limit development where the seabed is too deep [171]. Information on the European power grid was obtained from the ENTSO-E interactive map [172] using GridKit [173]. This dataset includes existing buses, lines, links, generators, transformers, and converters. Hydroelectricity generation and storage capacities from [174, 175] are used along with hydroelectricity generation per country and year from the US Energy Information Administration for 2000-2014 [176]. Existing generation and transmission capacities are shown in Figure 4.3. Hourly demand data for each European country is compiled from electricity system operators [154]. Demand data for 2019 is used since it was the most recent representative period before the COVID-19 pandemic, which significantly altered demand patterns. This demand is spatially allocated across NUTS3 regions from Eurostat [177] within each country based on population and gross domestic product. Cost projections for 2030 from the PyPSA-Eur databundle, detailed in Appendix A, are used. Because these cost projections apply to all of Europe, not just Britain, costs are given in euros. In 2023, the average exchange rate was 1 EUR = 0.86979 GBP [178].

Value of lost load

The value of lost load (VoLL) of £6000 per MWh established in the UK [179] is used as the cost of load shedding.

4.2.2 Transmission network clustering

The British transmission system is modeled using 30 nodes and their corresponding regions, shown in Figure 4.2. Grid regions are determined based on hierarchical

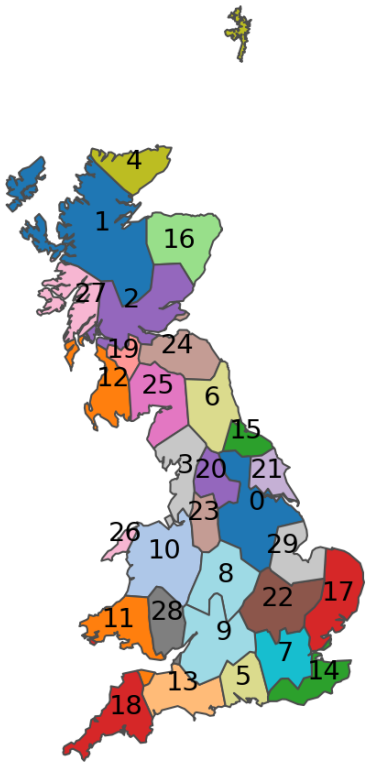

Figure 4.2: Map of clustered grid regions with corresponding electric bus number. Because the Shetland HVDC connection is under construction, Shetland is included in Bus 4. PyPSA-Eur excludes islands with areas less than approximately 800 km^2, so only Lewis and Harris, the Isle of Skye, mainland Shetland, and the Isle of Mull are included along with mainland Britain.

agglomerative clustering of the high-voltage transmission network. The approach developed by Frysztacki et al. [180], which groups buses in areas with similar hourly onshore wind and solar capacity factors, is used because it has been shown to improve the accuracy of capacity siting and power flows in models with high shares of renewable energy compared to other methods. The minimum number of regions that capture the transmission constraints of the British system, per the 2022 National Grid Electricity Ten Year Statement [181], is found to be 30.

This hierarchical agglomerative clustering algorithm results in disconnected parts of the same grid region, as can be observed in Figure 4.2. In particular, different parts of Buses 3, 11, 12, 14, 24, and 28 are separated by bodies of water

and not directly connected with transmission lines, even though they are modeled as such. The impact of these disconnected regions on total and peak regional heating demand as well as capacity expansion results is discussed in Appendix B. Because these differences are found to be small, the clustered regions with disconnected parts are used in the remaining analysis in this thesis.

Countries and regions with existing and planned HVDC connections with Britain are modeled with a single node per synchronous region in each country to approximate future electricity trade, as shown in Figure 4.3. Thus 9 additional nodes are included for France, Ireland, Northern Ireland, East and West Denmark, Germany, Belgium, Norway, and the Netherlands, with the size of each node indicating the total existing generation capacity in the country. Each of these additional nodes are characterized by their own hourly demand, generation, and renewable potential data to better simulate future trade patterns, particularly during times of low renewable potential in some areas when electricity from renewable generation in other areas could be used to help meet demand. This approach differs from that of Heuberger et al. [25], who modeled interconnectors as generators or storage units depending on historical trade patterns, because new connections have unknown trade behavior, and historical trade patterns across existing interconnections may change during the transition to low-carbon power systems across Europe. Because this chapter focuses on Britain, electricity trade between these interconnected countries and other European countries is not included in the model to limit computational requirements.

4.2.3 Capacity expansion model

The PyPSA-Eur electricity-only capacity expansion model v.0.6.1 [167, 182] is expanded to include exogenous heat pump demand. This model optimizes investment in and operation of generation, storage, and transmission to minimize cost while meeting inelastic electricity demand. Because power systems planners have little control over individual households' choice of heating system, heat pump adoption

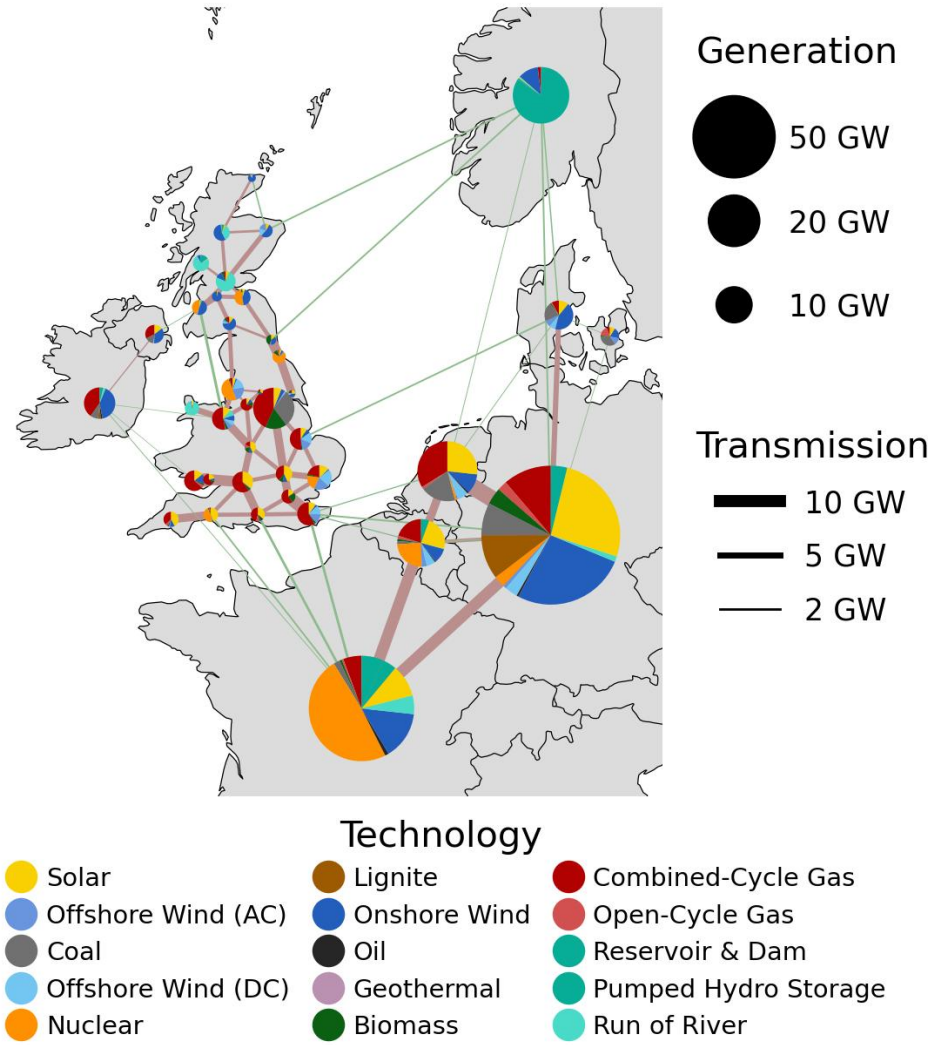

Figure 4.3: Map of clustered transmission network with AC transmission shown in pink and HVDC transmission shown in green. Line width is proportional to HVDC and AC transmission capacity. Existing generation and storage capacities for each bus are shown, with the bus size representing total capacity and the pie chart at each bus displaying the technology capacity shares.

is modeled exogenously in GeoHeat-GB. This approach contrasts with the sector-coupled PyPSA-Eur v.0.8.0 [183, 184] and higher, which endogenously determines the share of heat pumps by co-optimizing power systems planning and heating decarbonization. Despite this difference, the scripts in GeoHeat-GB that model additional demand from heat pumps are inspired by their analogs in PyPSA-Eur 0.8.0. The notation used to describe the model comes from the PyPSA [185] documentation.

The capacity expansion problem seeks to minimize the annualized capital costs c for all components and operational costs o for generators and storage units:

$$\min_{\substack{\bar{g}_{n,s},\bar{h}_{n,s},F_l,\\ g_{n,s,t},h_{n,s,t}}} \sum_{n,s} c_{n,s}\bar{g}_{n,s} + \sum_{n,s} c_{n,s}\bar{h}_{n,s} + \sum_{l} c_l F_l + \sum_{t} w_t \left(\sum_{n,s} o_{n,s,t} g_{n,s,t} + \sum_{n,s} o_{n,s,t} h_{n,s,t} \right) \tag{4.1}$$

The capacity of generator s at bus n is $\bar{g}_{n,s}$, and $\bar{h}_{n,s}$ is the nominal power of storage s at bus n. The capacity of branch l is F_l. The dispatch of generator s at bus n at time t is $g_{n,s,t}$, and $h_{n,s,t}$ is the dispatch of store or storage unit s at bus n at time t. The duration of time t in hours is w_t, which is 1 hour for all time steps in this optimization. The expandable components are generators, storage units, and lines.

The capacity of each generator $\bar{g}_{n,s}$ of technology s at bus n is limited based on the existing generation capacity $\tilde{g}_{n,s}$ at each bus n, as shown in Figure 4.3, and the maximum installable capacity $\hat{g}_{n,s}$:

$$\tilde{g}_{n,s} \leq \bar{g}_{n,s} \leq \hat{g}_{n,s} \; \forall \; n, s \tag{4.2}$$

For renewable generation, land availability determines the maximum installable capacity $\hat{g}_{n,s}$ in Equation 4.2; for non-renewable generators, the maximum installable capacity is modeled as infinite. The extendable generation technologies are solar, onshore wind, offshore wind, and open-cycle gas turbines. Other existing generation technologies cannot be expanded but can be operated, subject to the carbon budget in Equation 4.19.

The capacity of each storage unit $\bar{h}_{n,s}$ is limited based on existing capacity $\tilde{h}_{n,s}$ (for pumped hydro storage units), shown in Figure 4.3:

$$\tilde{h}_{n,s} \leq \bar{h}_{n,s} \leq \hat{h}_{n,s} \; \forall \; n, s \tag{4.3}$$

Battery storage is the only extendable storage unit included, and pumped hydro storage units are limited to their existing capacities.

The capacity of branches, including passive lines (such as AC lines) and controllable links (such as HVDC links), is limited based on the existing line capacity $\tilde{F}_l$, as shown in Figure 4.3, and installable potential $\hat{F}_l$, which is infinite for all AC and HVDC transmission:

$$\tilde{F}_l \leq F_l \leq \hat{F}_l \; \forall \; l \tag{4.4}$$

AC and HVDC transmission capacities can be expanded along existing corridors. Because the European power system is strongly meshed, changes in grid topology are not considered to maintain a linear optimization problem.

Generation dispatch $g_{n,s,t}$ is constrained based on each generator's nominal power $\bar{g}_{n,s}$ and time-dependent dispatch limit (per unit of nominal power) $\bar{g}_{n,s,t}$:

$$0 \leq g_{n,s,t} \leq \bar{g}_{n,s,t}\bar{g}_{n,s} \; \forall \; n, s, t \tag{4.5}$$

This time-dependent dispatch limit varies for weather-dependent renewable generators based on reanalysis weather data. For non-renewable generators, $\bar{g}_{n,s,t}$ is 1 because power plant de-rating is not considered.

Batteries and pumped hydro storage are modeled as storage units with a fixed ratio $r_{n,s}$ between the maximum state of charge and the nominal power $\bar{h}_{n,s}$. The state of charge $soc_{n,s,t}$ of storage is constrained as:

$$0 \leq soc_{n,s,t} \leq r_{n,s}\bar{h}_{n,s} \; \forall \; n, s, t \tag{4.6}$$

Storage unit discharge $h_{n,s,t}$ is limited by the unit's nominal power:

$$0 \leq h_{n,s,t} \leq \bar{h}_{n,s} \; \forall \; n, s, t \tag{4.7}$$

Storage unit charging $f_{n,s,t}$ is limited similarly:

$$0 \leq f_{n,s,t} \leq \bar{h}_{n,s} \; \forall \; n, s, t \tag{4.8}$$

The state of charge of storage units is related to charging and discharging by the following energy-balance constraint:

$$\begin{aligned} soc_{n,s,t} = \eta_{n,s}^{stand} soc_{n,s,t-1} + w_t \Big(\eta_{n,s}^{charge} f_{n,s,t} - \frac{1}{\eta_{n,s}^{discharge}} h_{n,s,t} \\ + inflow_{n,s,t} - spillage_{n,s,t} \Big) \; \forall \; n, s, t \end{aligned} \tag{4.9}$$

where $\eta_{n,s}^{stand}$ is the standing efficiency, $\eta_{n,s}^{charge}$ is the charging efficiency, and $\eta_{n,s}^{discharge}$ is the discharging efficiency of storage unit s at node n. Inflow $inflow_{n,s,t}$ for pumped hydro storage is calculated using the Atlite library [165] based on precipitation in each region, and spillage $spillage_{n,s,t}$ is a decision variable. Inflow and spillage are zero for battery storage.

All storage units have a cyclic state of charge constraint for the year-long time period considered:

$$soc_{n,s,-1} = soc_{n,s,T-1} \; \forall \; n, s \tag{4.10}$$

Linear optimal power flow is used to model power flow $f_{l,t}$ in AC lines based on the difference in voltage angles $\theta_{n,t}$ and $\theta_{m,t}$ at buses n and m and the series reactance x_l of the line:

$$f_{l,t} = \frac{\theta_{n,t} - \theta_{m,t}}{x_l} \; \forall \; t, \; \{l \mid l \text{ in AC lines}\} \tag{4.11}$$

For computational speed, Kirchhoff's Voltage Law is enforced for AC lines using the formulation introduced in Hörsch et al. [186] based on the independent cycles c in the transmission network graph. These independent cycles are each expressed as a linear combination of branches in the cycle incidence matrix C_{lc}:

$$C_{lc} = \begin{cases} 1 & \text{if branch } l \text{ is an element of cycle } c, \\ -1 & \text{if reversed branch } l \text{ is an element of cycle } c, \\ 0 & \text{otherwise.} \end{cases} \tag{4.12}$$

Thus, the sum of AC power flow around each independent cycle must be zero:

$$\sum_{l} C_{lc} x_l f_{l,t} = 0 \; \forall \; c, \; t, \; \{l \mid l \text{ in AC lines}\} \tag{4.13}$$

The power flow in AC lines is limited by the line capacity F_l:

$$|f_{l,t}| \leq \bar{f_l} \cdot F_l \; \forall \; t, \; \{l \mid l \text{ in AC lines}\} \tag{4.14}$$

where $\bar{f_l}$ is a per-unit security margin of 0.7.

While AC line reactance x_l depends on line capacity F_l, including this relationship in combination with Equations 4.11 and 4.14 would render the optimization problem nonlinear and thus increase its computational complexity. To maintain problem linearity while representing this dependence, the non-linear optimization problem of power flow with transmission capacity expansion is iteratively linearized by fixing the reactance and optimizing AC line capacity following the approach introduced by Hagspiel et al. [187]. The reactance of each line is then updated to reflect the optimized line capacity and the linear optimization is repeated until the maximum mean square difference in optimized line capacity F_l between iterations is lower than 0.05.

Power flow is limited on controllable branch flows such as HVDC links by their capacity without any security margin:

$$|f_{l,t}| \leq F_l \; \forall \; t, \; \{l \mid l \text{ in links}\} \tag{4.15}$$

Power flows are related by the nodal power balance, which enforces Kirchhoff's Current Law for electric components:

$$\sum_{s} g_{n,s,t} + \sum_{s} h_{n,s,t} - \sum_{s} f_{n,s,t} - \sum_{l} K_{nl} f_{l,t} = \sum_{s} d_{n,s,t} \; \forall \; n, t \tag{4.16}$$

where $d_{n,s,t}$ is the exogenous load at each node. The nodal incidence matrix K_{nl} is defined as follows:

$$K_{nl} = \begin{cases} 1 & \text{if branch } l \text{ starts at bus } n, \\ -1 & \text{if branch } l \text{ ends at bus } n, \\ 0 & \text{if branch } l \text{ is not connected to bus } n. \end{cases} \tag{4.17}$$

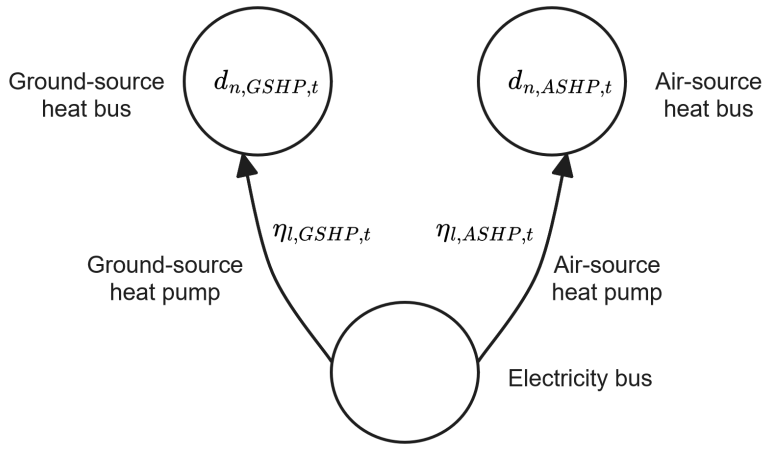

Figure 4.4: Diagram of heating nodes added to electricity network.

Heat demand

Heat pump demand is added to the capacity expansion model by creating ground-source and air-source heat buses corresponding to each electrical bus, as shown in Figure 4.4. The hourly thermal heating loads for ASHPs and GSHPs, $d_{n,ASHP,t}$ and $d_{n,GSHP,t}$, calculated in Section 3.2.4, including their respective hourly demand profiles shown in Figure 3.2 (a) and (b), are added to their respective heat buses for each region. Each heat node is connected to its corresponding electrical node with a unidirectional heat pump link with a time-varying efficiency $\eta_{l,s,t}$ reflecting the COP values for ASHPs and GSHPs calculated in Section 3.2.5. A cost for heat pump capacity is not included because they are likely to be household expenses, rather than power system expenses.

Transmission and carbon budget scenarios

To explore the impact of high spatiotemporal resolution heating demand on power system planning under a variety of policy futures, five different scenarios are analyzed. These scenarios were defined by the maximum allowable transmission expansion and the power sector carbon budget, as shown in Figure 4.5.

These two axes are chosen for their high impact on power systems planning and high uncertainty. Transmission expansion has faced policy and permitting hurdles

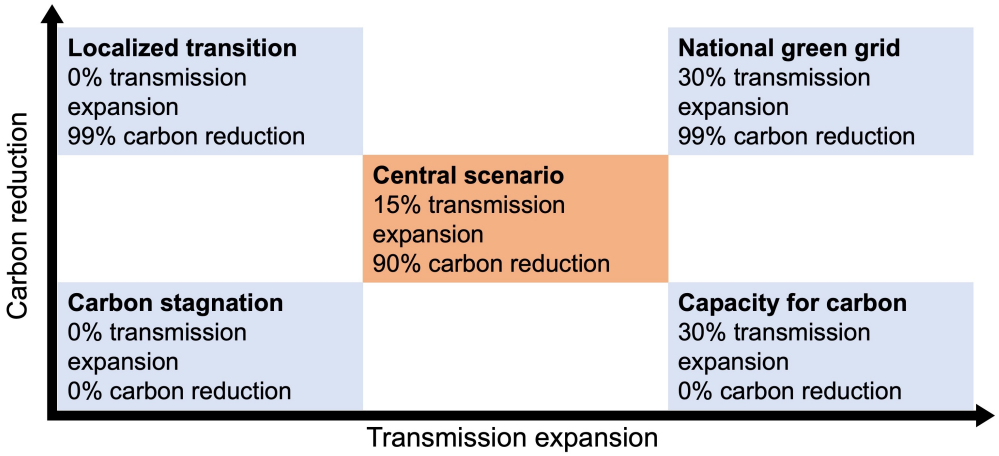

Figure 4.5: Matrix of policy scenarios developed in this chapter. Reproduced from Halloran et al. [58] under a CC BY 4.0 license.

and currently requires nearly a decade of permitting. Different carbon budgets in the power sector reflect the uncertainty about the availability of firm generation compared to the availability of gas generation today [188]. High-carbon scenarios represent a future in which the heating sector switches to electricity as its primary fuel, but the power system undergoes a less dramatic transition. In these scenarios, existing fossil fired capacity remains operational, but all new electricity demand from heat pumps is met with zero-carbon generation. Alternatively, policy could push the power sector to be more reliant on weather-dependent renewable generation and other zero-carbon generation sources, as reflected in the low-carbon scenarios.

Transmission expansion is limited by a volumetric increase V from the existing system line and link capacities $\tilde{F}_l$ and line and link lengths L_l:

$$\sum_{\substack{l \in \text{AC,} \\ \text{HVDC}}} F_l L_l \leq V \sum_{\substack{l \in \text{AC,} \\ \text{HVDC}}} \tilde{F}_l L_l \tag{4.18}$$

This sum is taken over all existing AC transmission lines and HVDC links. A maximum of 30% transmission expansion volume ($V = 1.3$) is estimated from National Grid Electricity Ten Year Statement 2022 power flow diagrams [181]. This figure represents a liberal expansion of transmission infrastructure. Conversely, low

transmission expansion scenarios are considered in which no additional capacity is added ($V = 1.0$). The central scenario includes 15% transmission expansion volume ($V = 1.15$).

A range of carbon reductions relative to 2019 power sector emissions are considered using different carbon budgets CAP_{CO2}. The carbon dioxide emissions constraint limits the total amount of carbon dioxide emissions from the power system:

$$\sum_{n,s,t} \frac{1}{\eta_{n,s}} w_t g_{n,s,t} E_s \leq CAP_{CO2} \tag{4.19}$$

Where E_s are the carbon dioxide emissions per MWh of each generation source and $\eta_{n,s}$ is the efficiency of generator source s at node n. For all modeled countries, 2019 carbon dioxide equivalent emissions from the public electricity and heat production sector [189] are used as the baseline. The central scenario value of a 90% carbon reduction is chosen in line with the UK CCC central scenario emissions for the power sector for 2035 [190]. For the low-carbon and high-carbon scenarios, 99% and 0% reductions are chosen, respectively. Because the adoption of 26.5 million residential heat pumps would increase total British electricity demand by 25%, as discussed in Section 3.3.1, while total power system emission remain constant, the 0% carbon reduction scenarios still represent an approximately 20% reduction in British per-MWh emissions. Thus, these scenarios represent futures in which low-carbon generation meets additional demand from heat pumps but does not grow quickly enough to decrease annual power system carbon dioxide emissions.

Self-sufficiency constraint

To avoid distorting the optimization by excluding any heating demand changes outside of Britain, each country is constrained to generate at least a self-sufficiency share S of their own historical electricity demand $d_{n,AC,t}$ plus 100% of their electric heat pump load $f_{l,t}^{elec}$ over the year-long time horizon considered:

$$\sum_{\substack{n\in\text{country},\\s,t}} g_{n,s,t} + \sum_{\substack{n\in\text{country},\\s,t}} inflow_{n,s,t} - \sum_{\substack{n\in\text{country},\\s,t}} spillage_{n,s,t} \geq S \sum_{\substack{n\in\text{country},\\t}} d_{n,AC,t} + \sum_{\substack{l\in\text{country HPs},\\t}} f^{elec}_{l,t} + \sum_{\substack{n\in\text{country},\\s,t}} (f_{n,s,t} - h_{n,s,t}) \tag{4.20}$$

These sums are over all nodes n within a country. Ninety-five percent self-sufficiency S was chosen because about 5% of British electricity consumption was met by net electricity imports from 2015 to 2021 [191]. This constraint on electricity trade also limits the distorting effect of assuming there is a single grid planner for all countries interconnected with Britain by, for instance, limiting the possibility of large solar capacity being built in southern France to meet the British winter heating demand peak.

To avoid unintended storage cycling of storage units, each country must generate 100% of its storage unit losses, as suggested by Kittel and Schill [192]. Because storage units are constrained to cyclic state of charge in Equation 4.10, storage losses can be calculated as the sum of storage charging power minus storage discharging power $\sum_{n\in\text{country},s,t}(f_{n,s,t} - h_{n,s,t})$ in each country.

4.2.4 Operational regret analysis

To assess the practical consequences of planning a power system with national heating demand data, an operational optimization with multi-regional heating demand is performed on the systems planned using both national and multi-regional heating demand in the capacity expansion model.

$$\min_{g_{n,s,t},h_{n,s,t}} \sum_t w_t \left(\sum_{n,s} o_{n,s,t} g_{n,s,t} + \sum_{n,s} o_{n,s,t} h_{n,s,t} \right) \tag{4.21}$$

The uniform national heating demand profiles and COP values are replaced with their multi-regional equivalents. Then, the hourly operation of the planned power system is optimized for the same weather-year for which it was planned. To maintain problem feasibility, load shedding is allowed at a cost of €6900 per MWh, in line with the VoLL established in the UK of £6000 per MWh [179] using the 2023 average

exchange rate [178]. The self-sufficiency constraint in Equation 4.20 is also removed to allow international electricity trade to balance local demand peaks as needed.

4.3 Results and discussion

In this section, the implications of spatiotemporal differences in heat pump demand for bulk power systems planning are discussed. The results of the capacity expansion model are discussed for the central scenario in Section 4.3.1 and for the additional scenarios in Section 4.3.2. Operational regret analysis results are discussed in Section 4.3.3, and limitations and uncertainty are discussed in Section 4.3.4.

4.3.1 Central scenario capacity expansion

This section discusses the results of capacity expansion for the central policy scenario (described in Section 4.2.3) using the national and multi-regional approaches.

Using spatially varied heating demand profiles leads to a 0.6% higher total system cost than using spatially uniform heating demand profiles, resulting in a net present system cost of €27.3 billion per year compared to €27.1 billion.

Despite similarity in total system costs, using spatially varied and uniform heating demand profiles leads to different spatial placement of power system infrastructure. Figure 4.6 displays the differences in generation, storage, and transmission capacity when planning with the national approach compared to multi-regional approach for modeling heating demand. Infrastructure with an oversized capacity when using a national temperature-based approach is shown in red, and infrastructure with an undersized capacity is shown in blue.

Compared to using the multi-regional temperatures, using heating demand based on the national temperature for capacity siting leads to widespread undersizing of generation and storage. The total absolute error (TAE) for generation and storage, which represents the amount of spatially misallocated capacity with respect to the multi-regional approach, is 2.6 GW, which corresponds to 0.32% of planned capacity in Britain. While this represents a low share of total capacity in Britain, misplacement of generation and storage is highly concentrated in a few regions,

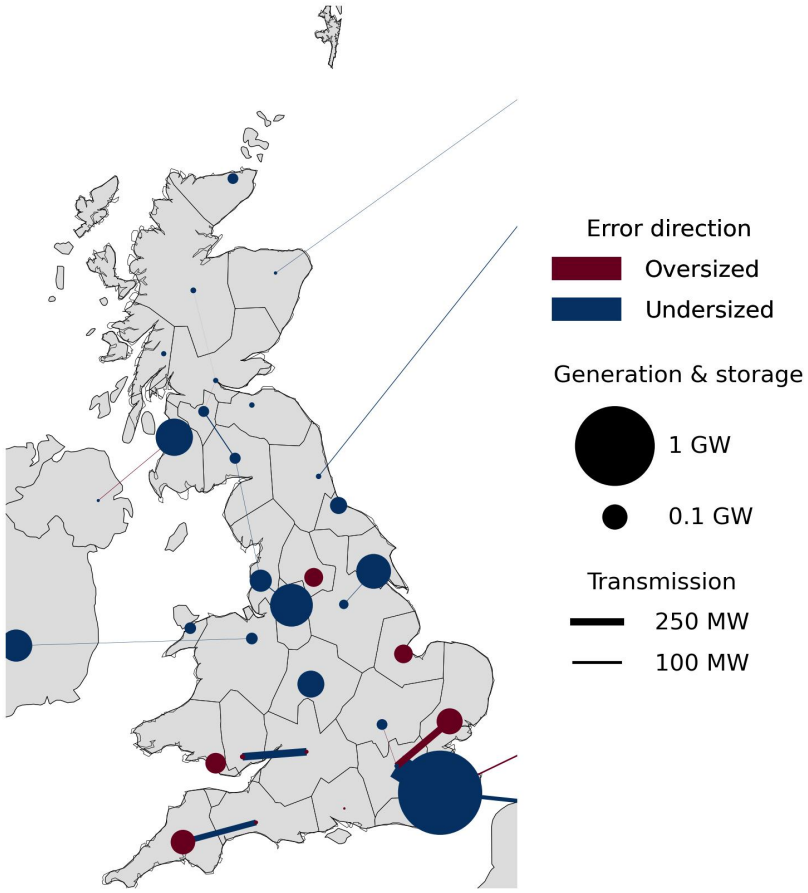

Figure 4.6: Generation, storage, and transmission planned capacity differences when using heating demand based on national temperature vs. multi-regional temperatures for the central scenario. Infrastructure with an oversized capacity when using uniform, national temperature-based heating demand is shown in red, and infrastructure with an undersized capacity is shown in blue. The legend displays transmission and generation and storage capacities for scale.

with errors ranging from 0.11 GW of oversizing at Bus 17 in the east of England to 1.11 GW of undersizing at Bus 14 on the southeast coast of England. Notably, this difference on the southeast coast is large relative to the current generation capacity at this bus shown in Figure 4.3: the southeast coast of England currently has 5.74 GW of generation capacity, so this error represent 19% of current capacity.

Using spatially uniform heating demand leads to spatial misallocation of transmission infrastructure as well: the TAE for transmission is 2.3 GW, and the total absolute percent error (TAPE) is 0.73%. These errors are concentrated at just a few lines, with line-specific errors ranging from 240 MW of oversizing for the line

between the east of England and London to 850 MW of undersizing for the line between the southeast coast of England and London.

Because of the complex interactions between heating demand, renewable availability, and transmission network topology, there is no clear relationship between spatial differences in heating demand, shown in Figure 3.4, and power system infrastructure misplacement, shown in Figure 4.6.

Generation and storage capacity oversizing occurs in some southern coastal areas where national temperature profiles overestimate heating demand, including southern Wales (Bus 11), the East of England (Bus 17), and Cornwall (Bus 18). Undersized transmission connections between southern Wales and Cornwall and the rest of the British electricity network suggest that more electricity generated at these buses is transmitted to inland areas with increased heating demand when using multi-regional heating demand. However, oversizing also occurs in the coastal region of the East of England & East Midlands (Bus 29), where national temperature profiles overestimate total heating demand but underestimate peak heating demand, and inland in central Britain in West Yorkshire (Bus 20), where national temperature underestimates both total and peak heating demand.

Undersizing of generation and storage capacity is widespread across Britain. The largest undersized capacity occurs on the southeast coast of England (Bus 14) despite national heating demand overestimating both total and peak heating demand there. The combination of this generation and storage undercapacity with undersized transmission capacity to London (Bus 7) suggests that this increased capacity is needed to meet increased multi-regional heating demand inland. The southeast coast of England is the optimal location for expanded generation capacity to meet increased multi-regional heating demand inland because it has HVDC connections to France, Belgium, Germany, and the Netherlands, as shown in Figure 4.3, that allow export of excess generation from expanded renewable capacity when demand is low in Britain. Generation and storage capacity is also undersized on the southwestern Scottish coast (Bus 12) where national heating demand underestimates total heating demand but overestimates peak demand. As expected, generation and

storage capacity is also undersized in many places where national heating demand underestimates total and peak heating demand: inland in England, including the greater Birmingham area (Bus 8) and greater Manchester area (Bus 23), and coastal areas in central Britain, including Buses 3 and 21.

The lack of a heuristic for predicting the power system impact of spatiotemporal differences in heating demand underlines the importance of using high resolution demand for spatial planning of power system infrastructure. Because of the complex interactions between heat pump demand, renewable generation potential, land availability, and transmission capacity, spatial bulk power system planning with high heat pump adoption will require considering spatial variation in each of these elements.

Figure 4.7 shows the breakdown of generation and storage capacity differences between capacity expansion planning using the national and multi-regional approach for modeling heating demand at each bus by technology type. Technologies with higher capacity when using the multi-regional approach are positive, and technologies with lower capacity when using the multi-regional approach are negative. This figure reveals technology changes at some buses that are not apparent from the capacity difference map in Figure 4.6.

When planning with multi-regional demand compared to uniform national demand, optimal battery capacity tends to be higher in regions with underestimated multi-regional heating demand. For instance, the greater Manchester (Bus 23) and greater Birmingham (Bus 8) regions see an increase in battery capacity to meet multi-regional heating demand. Similarly, Bus 3, a region in coastal central Britain with underestimated total national heating demand, also sees an increase in battery capacity. This increased battery capacity may be used to meet increased local demand peaks. Conversely, battery storage capacity decreases in Cornwall (Bus 18) where multi-regional heating demand is overestimated. This finding is consistent with the work of Heuberger et al. [25], who find that spatially granular modeling increases the value of energy storage when planning for EV adoption.

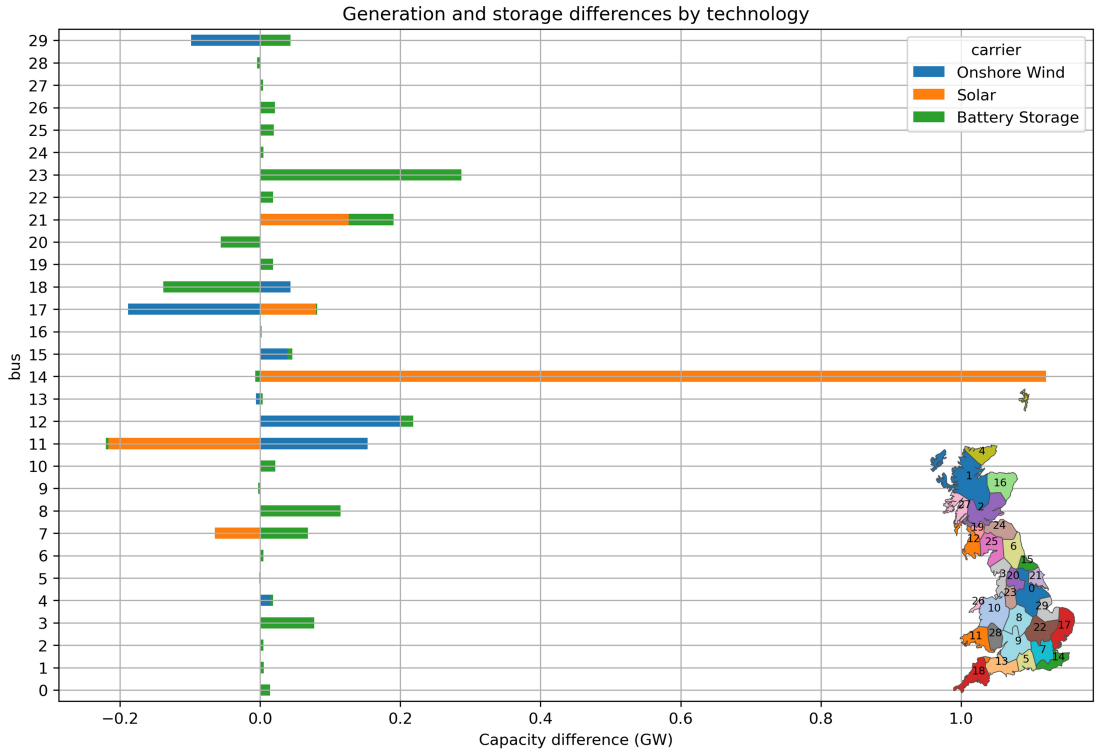

Figure 4.7: Breakdown of generation and storage differences at each bus between the national heating demand and multi-regional heating demand capacity expansion plans by technology. Undersized capacity in the national case is shown as positive, and oversized capacity is shown as negative. Regional map inset for reference.

Optimal solar capacity tends to be higher in regions with underestimated multi-regional demand and optimal onshore wind capacity tends to be higher in regions with overestimated multi-regional demand when planning with multi-regional demand compared to uniform national demand. For instance, Bus 21, a coastal region in central Britain, sees an increase in both solar and battery capacity to meet multi-regional demand. On the other hand, southern Wales (Bus 11), where multi-regional demand is overestimated, shifts from solar to onshore wind capacity. Onshore wind capacity also increases on the southwestern coast of Scotland (Bus 12), where multi-regional peak heating demand is overestimated. These differences may be because of the better seasonal match between heating demand and wind and decreased need for solar to meet diurnal peaks in heating demand. Conversely, at Bus 29, where national total demand is underestimated, onshore wind capacity decreases and battery capacity increases.

Table 4.1: National vs. multi-regional heating demand annualized system costs

Scenario	National system cost (B€)	Multi-regional system cost (B€)	System cost error (%)
Central	27.1	27.3	-0.6
Localized transition	56.7	57.2	-0.9
National green grid	48.5	48.9	-0.8
Capacity for carbon	19.2	19.3	-0.5
Carbon stagnation	19.6	19.7	-0.5

The exceptions to these trends in generation changes occur in southeastern Britain, which has some of the highest solar potential on the island. Multi-regional heating demand is overestimated in both the east of England (Bus 17) and the southeast coast of England (Bus 14). Bus 17 shifts from onshore wind to solar capacity to meet multi-regional heating demand, and the largest increase in capacity is for solar capacity at Bus 14. Because this increased solar capacity at Bus 14 is accompanied by increased transmission capacity to London (Bus 7), this extra generation capacity is probably used to meet increased multi-regional peak heating demand in greater London. At the same time, solar capacity decreases and battery capacity increases in greater London (Bus 7) to meet multi-regional heating demand. These differences illustrate how land-use constraints in an inland demand center shift the increased solar and battery capacity needed to meet local peaks to adjacent regions with higher land availability and good solar generation potential. These exceptions to the generation change trends underline the complexity of the interactions between renewable potential, heating demand, and network topology, which necessitates using high-resolution heating demand to plan power systems.

4.3.2 Capacity expansion for additional scenarios

This section discusses the results of capacity expansion planning for the remaining policy scenarios (described in Section 4.2.3) using the national and multi-regional approaches. Modeled system costs are discussed first, then generation and transmission siting differences between the national and multi-regional models.

System costs

Table 4.1 compares the annualized system costs for the two approaches in each scenario.

Table 4.2: National heating demand generation and storage capacity errors

Scenario	TAE (GW)	Max. bus error (GW)	Min. bus error (GW)	TAPE (%)
Central	2.6	0.11	-1.11	0.3
Localized transition	15.0	0.94	-6.59	1.1
National green grid	25.0	5.62	-4.88	2.1
Capacity for carbon	4.9	0.58	-1.18	0.8
Carbon stagnation	5.3	0.98	-1.20	0.9

In all of the scenarios considered, using the national model of heating demand underestimates total annualized systems costs by less than 1% with respect to the multi-regional model, as shown in Table 4.1. This result suggests that using high spatiotemporal resolution heating demand data is not necessary to estimate total systems costs within the range of policy scenarios considered.

The scenario systems costs shown in Table 4.1 also highlight the value of transmission expansion in low carbon budget scenarios. Increasing transmission expansion from 0% to 30% leads to approximately €8 billion of net present value savings for 99% carbon reduction but only about €0.4 billion in savings for 0% carbon reduction. Note that these costs are for the entire modeled system, including interconnected countries. Assuming that electricity demand is roughly proportional to power system costs, Britain accounts for about 22% of total system costs shown.

Generation and storage locations

Figure 4.8 illustrates the generation, storage, and transmission planned capacity differences between the national and multi-regional models. Table 4.2 compares error metrics for the spatial misallocation of storage and generation capacity using the national heating demand approach with respect to the multi-regional heating demand approach in each scenario for the regions within Britain.

Using spatially uniform heating demand leads to non-optimal siting of generation and storage capacity within Britain for meeting multi-regional heating demand in all scenarios, with larger differences in non-central scenarios. The largest TAE shown in Table 4.2 are 25.0 GW for the national green grid scenario and 15.0 GW for the localized transition scenario, which suggests that high spatiotemporal resolution heating demand is especially important when planning systems with low carbon budgets. The TAPE values for placement within Britain are greater than the central

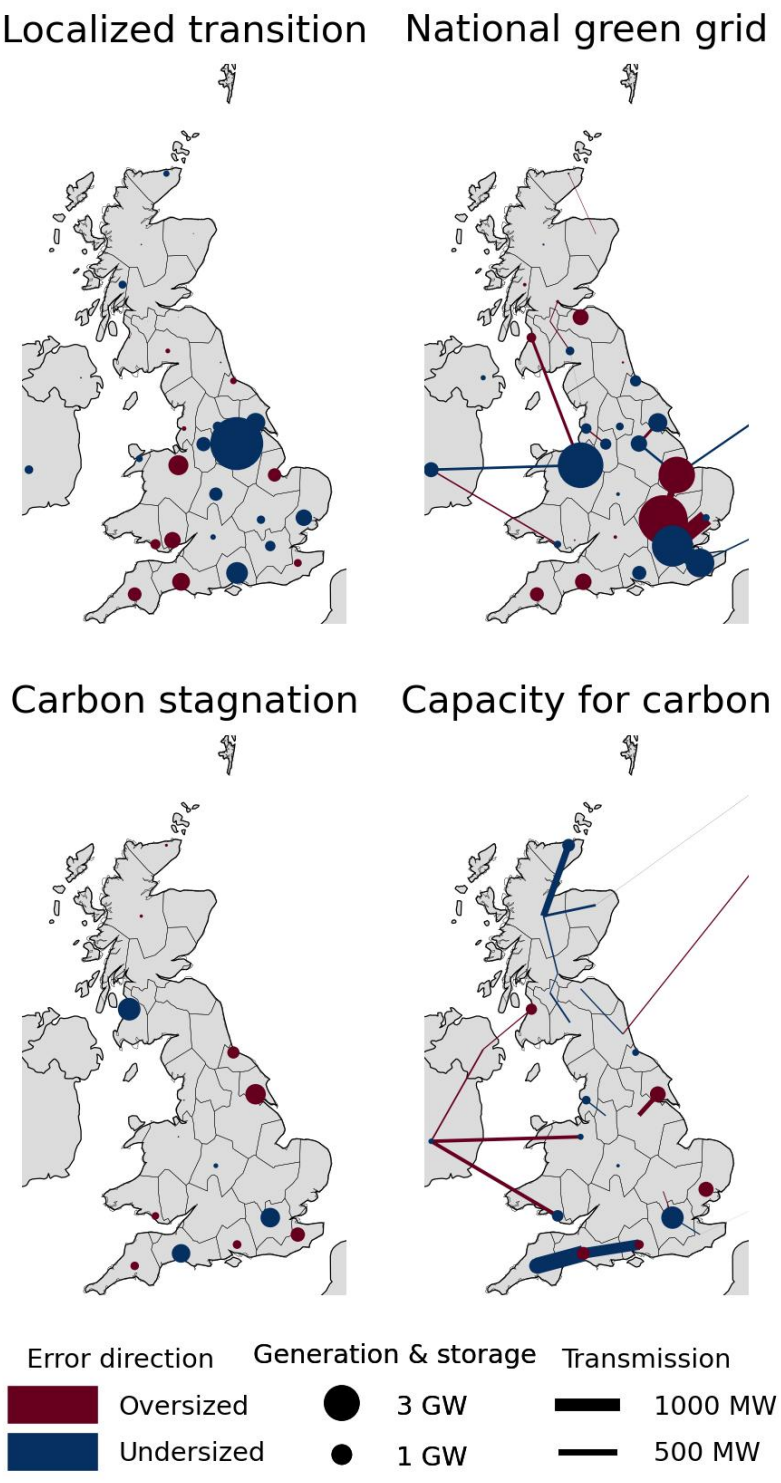

Figure 4.8: Generation and transmission planned capacity differences using heating demand based on national temperature vs. local temperature for four different transmission expansion and carbon budget scenarios. Infrastructure with an oversized capacity when using uniform, national temperature-based heating demand is shown in red, and infrastructure with an undersized capacity is shown in blue. The legend displays transmission and generation and storage capacities for scale.

scenario TAPE value, which indicates that these higher total misplacement values for low-carbon scenarios are not solely due to higher generation and storage capacity in Britain. These results suggest that high spatiotemporal resolution heating demand is crucial for spatial power system planning under a wide variety of policy futures.

The range of errors in generation and storage capacity with respect to the multi-regional approach shown in Table 4.2 demonstrates that spatial misallocation of storage and generation is highly concentrated at a few buses. The maximum bus error indicates the largest capacity oversizing at a bus, and the minimum bus error indicates the largest undersizing at a bus. This pattern can be observed in Figure 4.8 as well. Capacity misplacement is concentrated in a few regions for the high-carbon scenarios, carbon stagnation and capacity for carbon. In low-carbon scenarios, localized transition and national green grid, the spatial mis-sizing of generation and storage capacity is more widespread among the buses, though the largest errors are concentrated at a few buses. This difference arises due to the weather dependence of renewable generation: a high-renewable system relies on overcapacity and storage to meet demand, so planning with the incorrect demand profiles has a widespread impact on the spatial distribution of generation and storage.

As in the central scenario, no clear heuristic emerges in the additional scenarios for the differences in storage and generation capacity siting when using national heating demand in power system planning compared to multi-regional heating demand. As Figure 4.8 shows, the location of over- and undersized assets changes depending on the carbon budget, which reflects the influence of firm generation availability on storage and generation capacity needs. In the high-carbon scenarios, the largest differences are in coastal Britain. In the low-carbon scenarios, the capacity differences are spread across Britain with large differences near the coasts and significant differences inland. These results demonstrate that using high spatiotemporal resolution heating demand data changes the optimal generation and storage placement under a wide variety of transmission expansion and carbon budget constraints.

Table 4.3: Transmission capacity errors

Scenario	TAE (GW)	Max. line error (GW)	Min. line error (GW)	TAPE (%)
Central	2.3	0.24	-0.85	0.7
National green grid	6.1	1.27	-1.32	1.8
Capacity for carbon	4.9	0.37	-1.28	1.6

Transmission expansion locations

Table 4.3 shows the error metrics with respect to the multi-regional heating demand approach for the spatial allocation of transmission capacity when using spatially uniform heating demand in each of the scenarios considering transmission expansion. The maximum line error indicates the largest capacity oversizing of a line, and the minimum line error indicates the largest undersizing of a line.

Under all scenarios, planning with spatially uniform heating demand profiles leads to sub-optimal placement of transmission system upgrades to meet spatially varied heating demand. The TAE and TAPE for transmission capacity are slightly higher in the capacity for carbon scenario than in the central scenario. Both errors are even higher in the national green grid scenario: the TAE and TAPE are about 2.5 times higher than under the central scenario at 6.1 GW and 1.8%. Note that transmission TAPE is calculated based on total system capacity, in contrast to generation and storage TAPE which is only calculated based on British capacity. The long timeline for transmission expansion makes these spatial differences crucial because expanding transmission lines to the optimal capacity to meet multi-regional demand can take a decade or more.

This analysis of generation, storage, and transmission capacity differences underlines the importance of using high spatiotemporal resolution heating demand data in bulk power systems planning. In all carbon budget and transmission expansion scenarios, using the multi-regional model of heating demand leads to different spatial distributions of infrastructure than using the national model. Moreover, using spatially varied heating demand leads to higher differences in infrastructure placement under low carbon budget scenarios compared to the central scenario, which demonstrates that high spatiotemporal resolution heating

Table 4.4: Operational costs for meeting multi-regional heating demand

Scenario	National grid cost (€B)	Multi-regional grid cost (€B)	National additional cost (%)
Central	46.4	10.3	352
Localized transition	18.4	2.2	750
National green grid	18.7	2.5	636
Capacity for carbon	15.8	15.0	5
Carbon stagnation	15.3	16.0	5

demand is crucial for spatial planning to achieve power sector decarbonization goals at the lowest cost.

4.3.3 Operational regret analysis

Operating a power system planned based on a uniform national heating demand to meet multi-regional heating demand is more expensive than operating a system planned to meet multi-regional heating demand. Table 4.4 compares the operational costs to meet multi-regional heating demand for a power system planned based on national heating demand and a multi-regional heating demand.

Under the central scenario, planning with uniform national demand increases operational costs by €36.1 billion per year, which is 352% higher than the operating costs for the system planned with multi-regional demand. These additional costs primarily come from increased load shedding. The relative difference in operational costs is even higher under the low-carbon scenarios: the localized transition national system operational costs are 750% higher and the national green grid costs are 636% higher due to increased load shedding in both scenarios. These relative increases are so high due to the low operational costs for high renewable power systems in the absence of load shedding. For the high-carbon scenarios, the operational costs to meet multi-regional heating demand with a system planned to meet national demand are only 5% higher. For both the capacity for carbon and carbon stagnation scenarios, these cost increases come from load shedding as well as increased coal and combined-cycle gas generation dispatch.

Table 4.5 compares the volume of load shedding necessary , that is, the amount of unmet electricity demand, to meet multi-regional heating demand for a system planned to meet national demand versus a system planned to meet multi-regional demand.

Table 4.5: Load shedding to meet multi-regional heating demand

Scenario	National system load shed (TWh)	Multi-regional system load shed (TWh)
Central	5.18	0.00
Localized transition	2.34	0.00
National green grid	2.32	0.00
Capacity for carbon	0.05	0.00
Carbon stagnation	0.04	0.00

Power systems planned with uniform national heating demand require more load shedding to meet multi-regional heating load than the systems planned to meet multi-regional heating demand. Load shedding is highest for the central scenario and the low-carbon scenarios with TWhs of load shed. Load shedding is half as high in the low-carbon scenarios than in the central scenario because of the high renewable generation and storage overcapacity required to achieve a 99% carbon reduction. In contrast, there is less generation and storage capacity in the central scenario to achieve just a 90% carbon reduction. For the high-carbon scenarios, load shedding is two orders of magnitude lower than in the central and low-carbon scenarios. This difference suggests that planning with high spatiotemporal resolution heating demand data is particularly important for power systems reliability with high shares of renewable generation.

In the central and low-carbon scenarios, load shedding is concentrated in inland population centers in southern and central Britain. While less than half (2.20 TWh) of load shedding in the central scenario occurs in Britain, much of this load shedding occurs in population centers, including 0.92 GWh in greater London (Bus 7) and 0.49 GWh in greater Manchester (Bus 23). In the localized transition and national green grid scenarios, British load shedding makes up a much smaller share of the total, at just 0.40 and 0.31 TWh, respectively. In the localized transition scenario, the majority of British load shedding (0.31 TWh) occurs in greater London (Bus 7) due to limited land availability for renewable generation and limited transmission capacity to import electricity from other regions. The majority of British load shedding (0.21 GWh) occurs in greater Manchester (Bus 23) for the national green grid scenario.

Although no heating demand changes are modeled outside of Britain, the majority of load shedding in the central and low-carbon scenarios occurs outside of Britain. This indicates that operating a British power system planned using national demand to meet multi-regional heating demand increases the cost of British electricity exports above the VoLL, thus leading to load shedding in other countries. Load shedding outside of Britain also reflects the limitations of planning a high-renewable system without including the entire European grid. In the high-carbon scenarios, all load shedding occurs in Britain.

The load shedding volumes shown in Table 4.5 are for systems planned with perfect foresight of hourly demand and renewable generation potential. Uncertainty in forecasting these weather-dependent quantities could lead to higher load shedding. Nonetheless, these results demonstrate how ignoring spatiotemporal variation in planning leads to spatial misplacement of infrastructure that requires load shedding in population centers to meet demand.

4.3.4 Limitations & uncertainty

This chapter demonstrates the impact of regional differences in heating demand on bulk power systems planning using a single historical weather-year of temperature and renewable generation data. While the regional differences in heating demand identified in Chapter 3 are expected to persist between weather-years because of their geographic drivers, both regional heating demand and renewable potential will vary between weather-years. This variation between weather-years introduces uncertainty about the results presented in this chapter.

The capacity expansion model used in this chapter does not fully represent power system reliability constraints. While a heuristic is included for N-1 transmission security in Equation 4.14, no generation security constraints are included. Moreover, no capacity reserve requirements or representation of British capacity market are included. This incomplete representation of system contingencies may increase the generation capacity differences identified in Section 4.3.1 and Section 4.3.2 as well

as the load shedding discussed in Section 4.3.3. Future work could incorporate more power system reliability constraints to reduce this uncertainty.

An additional source of uncertainty in this chapter are the cost projections used in the capacity expansion model, which are shown in Appendix A. While relative differences in cost projections between technologies may shift the total generation and storage mix, the spatial distribution differences when planning with national versus multi-regional heating demand are expected to remain unchanged.

The capacity expansion optimization itself also includes sources of structural uncertainty. The linearized power flow assumed in Equation 4.11 is standard in capacity expansion models but only approximates non-linear power flow. The feasibility tolerance used to solve the optimization model is 1×10^{-6}, which corresponds to 1 W and 1 Wh at the model scaling used. This feasibility tolerance thus introduces very little uncertainty about the results.

4.4 Key insights

This chapter analyzes the implications of spatiotemporal differences in residential heat pump load for bulk power system planning. This question is addressed by comparing the results of capacity expansion planning using multi-regional heating demand profiles from Chapter 3 with those based on a single national heating profile in Britain. Large regional differences in total and peak heat demand are identified between the two approaches. These differences lead to moderate differences in the spatial planning of generation and storage capacity, especially in low-carbon scenarios. Based on the results, the following key insights can be gained:

Hourly regional heating demand projections are necessary to correctly site generation and storage capacity in bulk power system planning. Under a central scenario for carbon reduction and transmission capacity expansion in the British power system in 2035, using a spatially uniform heating demand profile leads to a total absolute error in the spatial allocation of generation and storage of 2.6 GW (0.3%) compared to a high-resolution demand pattern based on local temperatures. While this represents a low share of total capacity, these capacity differences are

spatially concentrated in a few locations and primarily reflect the need for more battery storage capacity to meet regional heating peaks when using multi-regional heating demand. For low carbon budget scenarios, the total absolute error increases to 25.0 GW (2.1%) with 30% transmission expansion and 15.0 GW (1.1%) with no transmission expansion. This trend suggests that high spatiotemporal resolution heating demand data is even more important for spatial planning of bulk power systems with very high shares of renewable generation. As countries transition from gas boilers to heat pumps for residential heating, high spatiotemporal resolution data about residential heat pump demand is crucial for power system planners striving for ambitious decarbonization targets.

Spatial misplacement of power system infrastructure due to low spatial resolution heating demand projections leads to load shedding and thus increases operational costs. Under the central scenario, operating a system planned with national heating demand to meet multi-regional heating demand requires 5.2 TWh of load shedding. Of this load shedding, 2.2 TWh occured in Britain, accounting for 0.6% of annual electricity demand. In the low-carbon scenarios, 2.3 TWh of load shedding is necessary for the systems planned with national heating demand to meet multi-regional heating load. In the central and low-carbon scenarios, this load shedding is concentrated in the population centers in the greater London and greater Manchester regions. Power outages in these urban areas during the coldest days of the year could undermine political support for the transition to heat pumps.

This chapter reveals the importance of battery storage capacity for meeting spatiotemporally varied heating demand, as using regional hourly demand data increased the need for battery storage capacity in many regions with underestimated multi-regional heating demand peaks. Heat pump flexibility has the potential to reduce these heating peaks. The next chapters explore the regional potential of heating flexibility (Chapter 5) and its role in power systems planning (Chapter 6).

5

Heating flexibility potential

Contents

This chapter addresses the research question: *What is the regional heating flexibility potential from residential building thermal inertia?* A data-driven method for quantifying this heating flexibility duration at high spatial resolution is introduced and validated using Britain as a case study.

5.1 Introduction

This chapter presents a novel heating consumption-based method for quantifying heating flexibility duration in the current building stock at high spatial resolution. The approach integrates high spatial resolution heating consumption data, temperature, and building size data to capture the geographic diversity of the national building stock. The method was tested in Britain and validated by comparing the results with the EPC-based method from Canet and Qadrdan [104] and a temperature-based method using heat pump trial data from 742 homes [193].

While this method can be applied to buildings in different sectors with different heating fuels, the scope of this case study only includes the residential sector. Because of the availability of high spatial resolution data on heating fuel consumption in Britain, this case study quantifies the flexibility duration potential of gas-heated homes. Therefore, the flexibility duration of homes in regions that are not on the gas grid is not quantified.

The primary research contribution of this chapter is introducing a method for quantifying national heating flexibility potential at high spatial resolution based on annual heating consumption data and historical temperature data. By representing the geographic diversity of a national building stock with sufficiently low computational requirements to be incorporated into complex power system models, this chapter addresses research gap 3 identified in Section 2.4. The software for this method is openly available in the GeoHeatFlex GitHub repository [194]. This method is applied to characterize the residential heating flexibility potential in Britain at high spatial resolution. This dataset is openly available on the Oxford Research Archive [195].

This chapter is structured as follows. First, the methods and case study data are described in Section 5.2. Second, the results are divided into Section 5.3.1 describing the spatial variation in heat capacity and heat loss rate, the two most important variables in the model; Section 5.3.2 discussing the model validation; and Section 5.3.3 presenting the results for the case study of gas-heated British homes. Finally, the key outcomes are discussed in Section 5.4.

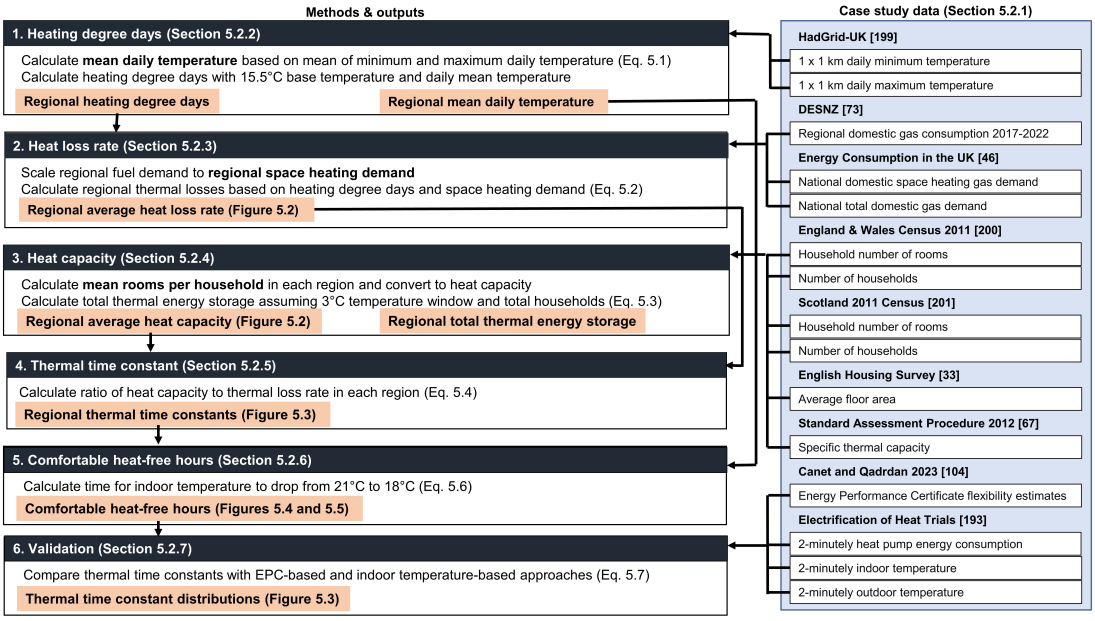

Figure 5.1: Summary of methods and case study data used in this chapter. Outputs for each step are shown in orange boxes, and intermediate outputs for each step are shown in bold.

5.2 Data and methods

Figure 5.1 summarizes the methods and data used in this chapter. Section 5.2.1 introduces the British case study and demonstration input data, and Sections 5.2.2 through 5.2.6 introduce the method. Section 5.2.7 discusses the validation of this heating consumption-based method.

5.2.1 Case study data

The heating consumption-based method for calculating heating flexibility duration introduced in Sections 5.2.2 through 5.2.6 is applied to a case study of gas-heated homes in Britain. For each step, values are calculated for each 2011 LSOA in England and Wales and each 2011 Data Zone (DZ) in Scotland. LSOAs are regions with an average of 1,500 residents and a minimum of 1,000 residents, while DZs are slightly smaller, with populations between 500 and 1,000 [196]. There are 34,753 LSOAs in England and Wales and 6,505 DZs in Scotland. The boundaries for these regions are available from Office for National Statistics [197] and Government of Scotland [198].

Historical minimum and maximum temperature observations at 1 x 1 km resolution from HadUK-Grid [199] are used to calculate HDDs and regional daily winter temperature percentiles. The HadUK-Grid dataset is used in this chapter instead of the ERA5 reanalysis dataset used in Chapter 3 because of its higher spatial resolution (1 x 1 km compared to approximately 30 x 30 km), which allows more accurate calculation of HDDs at the LSOA and DZ level. While the HadUK-Grid dataset provides higher spatial resolution than ERA5, it has lower temporal resolution, only providing minimum and maximum daily temperature; therefore, it would not be suitable for calculating hourly COP values in Chapter 3. Annual HDDs are calculated based on the gas heating season of the annual metered domestic gas demand data, which is typically from May of each year to the following May [196].

Heating demand for each region is based on annual metered domestic gas consumption from the Department for Energy Security and Net Zero (DESNZ) [73]. Because the gas data methodology changed in 2017, only data from 2017 to 2021 is used [196]. Total gas consumption is scaled to space heating demand in each region based on the national share of domestic gas consumption used for space heating for each year [46]. For instance, 76% of domestic gas consumption in Britain in 2017 was used for space heating demand, so 76% of annual domestic gas consumption in each LSOA and DZ is assumed to be used for space heating. Heat losses are based on 5-year averages of total space heating gas consumption and HDDs from 2017 to 2021.

The average number of rooms in homes in each region is obtained from the 2011 censuses [200, 201]. Based on the mean number of rooms in English homes and the mean floor area of 94 m^2 from the English Housing Survey [33], the average number of rooms is converted to floor space assuming 17.6 m^2 of floor area per room. The Standard Assessment Procedure medium heat capacity value of 250 $kJ/m^2°C$ is used to convert floor area to heat capacity [67].

5.2.2 Heating degree days

HDDs are calculated based on gridded historical minimum and maximum temperature observations. Following the approach used in the annual State of the UK

Climate report [202], the mean daily temperature for each point is calculated based on the maximum and minimum temperature observations:

$$T^{mean} = \frac{T^{max} + T^{min}}{2} \tag{5.1}$$

HDDs are calculated based on the resulting daily mean temperature T^{mean} assuming a base temperature of 15.5℃, in line with the annual State of the UK Climate report [202]. Gridded annual HDDs are assigned to each region based on the location of the representative point of each region. If the representative point is not within the gridded range, the mean number of HDDs among all neighboring regions is assigned.

5.2.3 Heat loss rate

The average heat loss rate for residential buildings in each region r is calculated using a top-down methodology from Chen et al. [99] based on annual heating consumption Q_r and HDDs HDD_r:

$$H_r = \frac{Q_r}{24 \sum HDD_r} \tag{5.2}$$

HDDs are multiplied by 24 hours to give heat loss rate H_r in kW/℃ .

5.2.4 Heat capacity

Because of inconsistent treatment of property types and incomplete residential property coverage of floor area measurements from other data sources[1], the average heat capacity C_r in each region is calculated based on the average number of rooms per household from the 2011 censuses [200, 201]. Based on data from the English Housing Survey [33], this value is converted to an estimated floor area assuming 17.6 m^2 of floor area per room and finally to heat capacity using the Standard Assessment Procedure medium heat capacity value of 250 kJ/m^2℃ [67].

[1]While the Valuation Office Agency collects data about residential property floor size, they use two different methods for houses and bungalows and for flats and maisonettes. EPCs use the same measure of floor area for all homes but are only available for 60% of residential buildings in England and Wales [203].

The average heat capacity and the number of households in each region A_r is used to calculate the total thermal energy storage in the building fabric for each region. For a flexibility window ΔT^{flex}, the total thermal energy storage capacity $\bar{e_r}$ in each region is:

$$\bar{e_r} = C_r A_r \Delta T^{flex} \tag{5.3}$$

5.2.5 Thermal time constant

Spatial variation in the duration of heating flexibility is accounted for using the average time constant τ_r for each region r. This lumped thermal parameter reflects how quickly heat is lost from residential buildings in each region, depending on the temperature difference between indoor and outdoor air. The time constant is the ratio of the total heat capacity C_r to the total heat losses H_r for each region:

$$\tau_r = \frac{C_r}{H_r} \tag{5.4}$$

5.2.6 Comfortable heat-free hours

Newton's law of cooling relates the time constant τ_r with the indoor air temperature at a given time t to the outdoor air temperature T_r^{air} (assumed constant in time) in each region r and initial indoor air temperature $T_{r,0}^{in}$:

$$T_{r,t}^{in} = T_r^{air} + (T_{r,0}^{in} - T_r^{air}) e^{-t/\tau_r} \tag{5.5}$$

Assuming that all houses are pre-heated to 21℃ and occupants are comfortable at temperatures as low as 18℃, the minimum indoor temperature that the World Health Organization recommends in cold and temperate climates [29], the number of comfortable heat-free hours t_r^c in each region r is calculated as:

$$t_r^c = -\tau_r \ln \frac{18 - T_r^{air}}{21 - T_r^{air}} \tag{5.6}$$

The number of heat-free hours in each region is calculated based on a variety of outdoor temperatures. To provide an even comparison of the residential building

stock across Britain, comfortable heat-free hours are calculated using a uniform outdoor air temperature T_r^{air} of 5°C in every region r. To account for regional variation in typical winter temperatures, the number of heat-free hours is also calculated for different percentiles of historical regional daily winter temperatures from 2010 to 2022. This time period was selected to capture both changing winter patterns under climate change as well as extreme cold periods in winter 2010/11.

5.2.7 Validation methodology

To validate this heating consumption-based method, the regional thermal time constants are compared with those obtained from 2 different data sources: the EPC-based method from Canet and Qadrdan [104] and an indoor temperature-based method using 2-minutely temperature and energy use data from a sample of 742 homes in the Electrification of Heat trial [193].

EPC-based method

Thermal building characteristics calculated based on the EPC-based method [104] are available for each dwelling category (flats, terraced, semi-detached, and detached) and heating system in each LSOA in England and Wales [204]. Considering only gas-heated households, the time constant for gas-heated homes in each dwelling category in each LSOA is calculated based on the thermal capacity and thermal losses using Equation 5.4. Since Canet and Qadrdan [104] present thermal losses for both the current building stock and potential retrofit, current and retrofit time constants are calculated.

Indoor temperature-based method

The Electrification of Heat trial includes 742 households in Southeast England, Northeast England, and Scotland with heat pumps. A cleaned interim dataset including 2-minutely internal temperature, external temperature, and heat pump energy output from November 2020 to August 2022 for 740 of these homes is available [193].

The time constants of the homes included in this trial were calculated using an indoor temperature-based method. This approach uses an exponential fit of the internal temperature decrease when the heat pump, as well as any boiler or backup heater, was off. The internal temperature drop was fitted using the following equation, based on Equation 5.5:

$$T_t^{in} = \bar{T}^{air} + (T_0^{in} - \bar{T}^{air})e^{-t/\tau} \tag{5.7}$$

Because Equation 5.5 assumes constant outdoor temperature, the time-averaged outdoor air temperature $\bar{T}^{air}$ is used to fit this equation.

Only data from time periods during the heating season (from October to April) and with both internal and external temperature data availability are considered to avoid data from warm days. Moreover, three data pre-processing steps were applied. First, periods were selected when the heating was off for at least 90 minutes, and second, time periods with sudden, large drops in temperature (more than 5℃ in 2 minutes) were excluded based on the assumption that an external door or window was opened. Third, because Equation 5.5 assumes constant outdoor temperature, only time periods with less than 2℃ variation in outdoor air temperature were considered. All homes have at least 1 time period that fits these criteria. For homes with multiple time periods that fit these criteria, the mean of the fitted τ values for each period is taken as the time constant for that house.

5.3 Results and discussion

This section discusses the results and their implications for heating flexibility in Britain. First, the regional variation in heat capacity and heat loss rates is presented in Section 5.3.1. Then, Section 5.3.2 presents the time constants calculated using the heating consumption-based approach and validates them with two other methods: the EPC-based method from Canet and Qadrdan [104] and a temperature-based method using heat pump trial data from 742 homes [193]. Section 5.3.3 explores heating flexibility duration in Britain using uniform and spatially varied outdoor temperatures, and Section 5.3.4 discusses the limitations of this chapter.

5.3.1 Heat capacity and heat loss rate

Regional time constants are the ratio of heat capacity to heat loss rate. Buildings with higher heat capacity (kWh/℃) can store more thermal energy in the building fabric and maintain the building temperature for longer while the heating is off. In this chapter, heat capacity is proportional to building size based on the mean number of rooms per household. Buildings with higher heat loss rates (kW/℃) are worse-insulated and lose more energy to their surroundings when the outdoor temperature is below the indoor temperature. In this chapter, higher heat loss rates reflect higher gas consumption per HDD. The regional values of heat capacity and heat loss rate are illustrated in Figure 5.2, which reveals significant geographic variation.

Figure 5.2a displays the mean heat capacity in each region. The median heat capacity in each region is 6.5 kWh/℃; however, heat capacity varies greatly among regions, ranging from 10 kWh/℃ in rural regions to 3 kWh/℃ in densely populated urban regions. These figures reflect the diversity in the size of dwellings in Britain. Assuming a 3℃ temperature flexibility window, the total thermal energy storage capacity in the British housing stock, including both gas- and non-gas-heated homes, is 500 GWh_{th}. This figure is not directly comparable to electricity storage because the amount of delayed electricity consumption depends on the temperature-dependent COP of the heat pumps. For a cold day COP value of 2.5, this thermal energy storage capacity is equivalent 200 GWh of electricity storage. Note that this figure is an order-of-magnitude estimate calculated assuming a uniform room size, 3 ℃ temperature window, and specific heat capacity across the housing stock. The impact of these assumptions on the results is discussed in Section 5.3.4.

Figure 5.2b displays the mean heat loss rate in gas-heated dwellings in each region. Regions with too few houses on the gas grid to be included in the metered demand data are in gray. Median heat losses per region are 0.21 kW/℃, but there is significant regional variation from 0.12 kW/℃ at the 1st percentile to 0.41 kW/℃ at the 99th percentile. High heat losses in the outer regions of Greater London stand out. Unlike heat capacity, there is not a clear spatial pattern in heat losses that

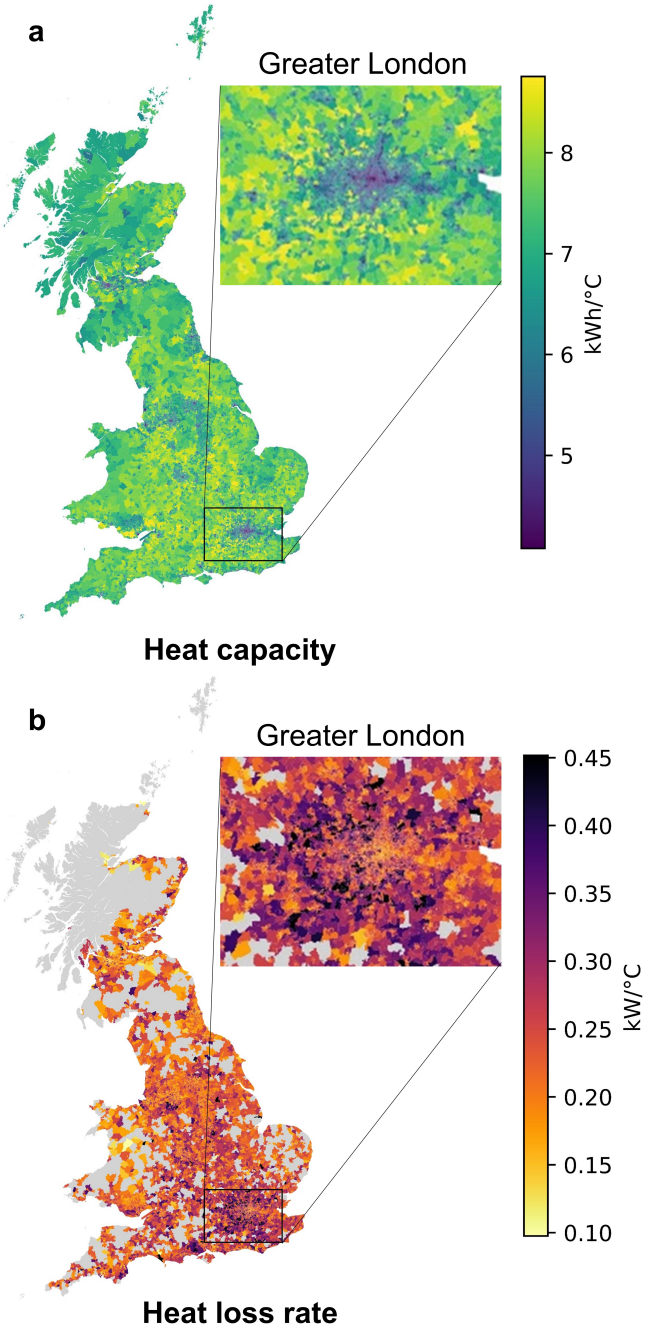

Figure 5.2: Maps of (a) mean heat capacity in each region and (b) mean heat loss rate in houses heated with gas in each region. Inset maps display details for the Greater London area. Domestic gas consumption data is unavailable for regions shown in gray. LSOA boundaries [197] and DZ boundaries [198] licensed under the Open Government Licence v.3.0. LSOA boundaries contains OS data © Crown copyright and database right 2023. DZ boundaries copyright Scottish Government, contains Ordnance Survey data © Crown copyright and database right 2021.

can be predicted from population density. This underlines the importance of using the method presented in this chapter to analyze regional heat losses.

5.3.2 Model validation

The heating consumption-based method introduced in this chapter calculates the thermal time constant (h) for each region on the ratio of thermal capacity to heat loss rate presented in Section 5.3.1. In this section, the heating consumption-based thermal time constants are compared with time constants obtained from the EPC-based approach and the indoor temperature-based method. Figure 5.3 illustrates the distribution of time constant value for each approach. The results demonstrate that time constants calculated based on the heating consumption-based method are consistent with those calculated for the British housing stock using other methods as follows.

The blue line shows the results from the heating consumption-based method using national data at high spatial resolution presented in this chapter. The median time constant value is 30.6 hours.

The orange and green lines illustrate the distribution of time constants from the EPC-based method for the current building stock in England and Wales as well as the retrofit potential of the building stock. The similar magnitude of time constants obtained from the heating consumption-based and EPC-based methods verifies the soundness of the heating consumption-based results. However, because EPCs overestimate heating losses [107, 108], the EPC-based method for the current building stock results in a lower median time constant of 22.8 hours than the heating consumption-based method. In contrast, the distribution of time constants from the EPC-based method for retrofit potential, with a median value of 33.8 hours, closely matches the distribution of heating consumption-based time constants. This agreement may reflect building retrofits that have taken place since the last EPC assessment, which is updated every 10 years, as well as energy-saving occupant behaviors that EPCs do not consider. Because the EPC-based method represents each dwelling category in each region separately, there are smaller peaks in the

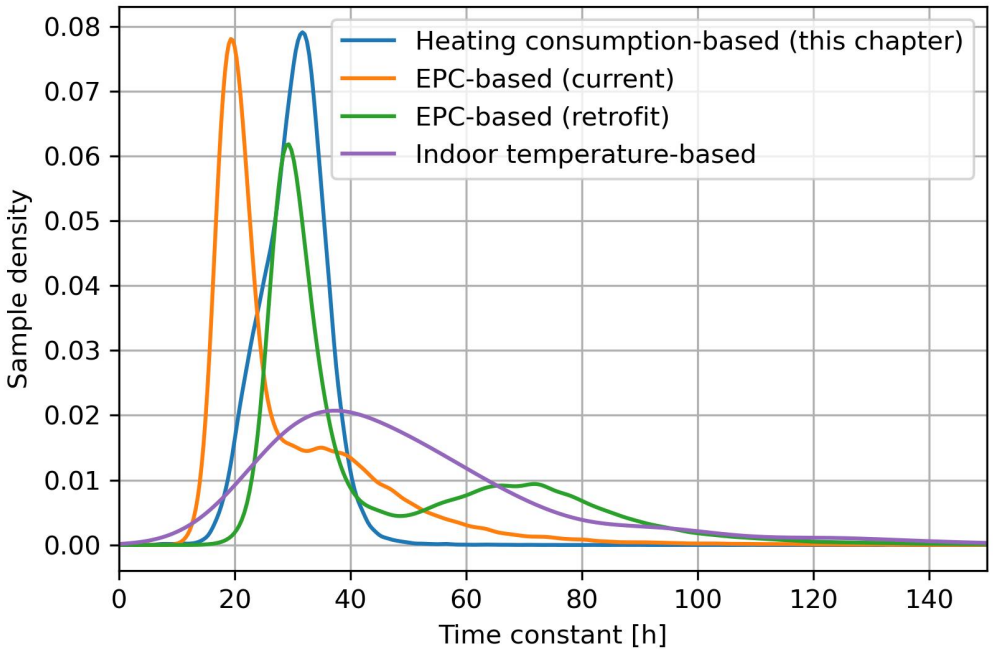

Figure 5.3: Comparison of thermal time constants for the British housing stock based on the heating consumption-based approach introduced in this chapter, the EPC-based method for current and retrofit housing stock, and an indoor temperature-based method using data from heat pump trials in 742 homes. Note that because this chapter calculates regional mean time constants, rather than time constants for individual homes, the very high time constant homes observed using other methods are not captured.

EPC-based time constant distributions at higher time constant values. These peaks represent high heat capacity detached dwellings with low heat loss rates. The uncertainty introduced in the results of this chapter because only one time constant value is calculated per region is discussed in Section 5.3.4.

Finally, the purple line shows the distribution of time constants obtained with the indoor temperature-based method using a sample of 742 homes in the Electrification of Heat trial. These results further support the validity of the consumption-based time constant values. The median time constant for these homes is 44.4 hours, which is 50% higher than the median heating consumption-based regional time constant value of 30.6 hours. This difference can be explained by the fact that compared to the national average, the Electrification of Heat trial includes a higher proportion of detached and semi-detached houses, which tend to have higher floor

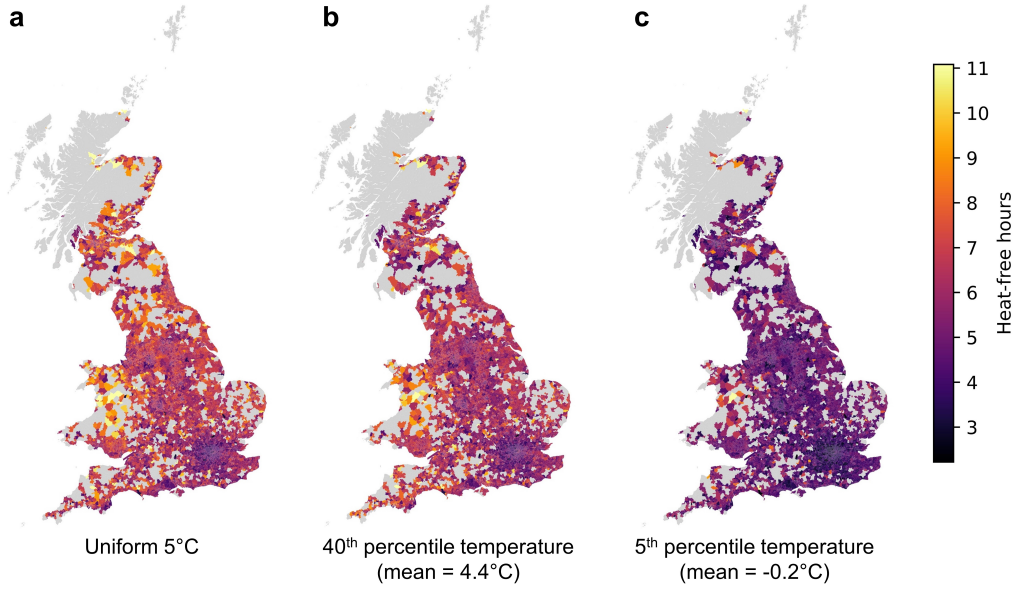

Figure 5.4: Maps of average comfortable heat-free hours per flexible event in each region, for an indoor window of 18℃ to 21℃ with (a) a uniform outdoor temperature of 5℃ and (b) 40thpercentile and (c) 5thpercentile regional daily winter temperature for 2010 to 2022. Map (a) displays the regional variation in flexibility duration due to building stock differences, while maps (b) and (c) demonstrate the effect of regional temperature differences on heat-free hours. Domestic gas consumption data is unavailable for regions shown in gray. LSOA boundaries [197] and DZ boundaries [198] licensed under the Open Government Licence v.3.0. LSOA boundaries contains OS data © Crown copyright and database right 2023. DZ boundaries copyright Scottish Government, contains Ordnance Survey data © Crown copyright and database right 2021.

areas and higher thermal capacities, and a lower proportion of flats, which have lower floor areas and lower thermal capacities [34]. In addition, properties were excluded from the trial if their heat demand was too high, so these data represent a well-insulated building stock with low heat losses.

5.3.3 Residential flexibility duration

Due to the geographical diversity in the current residential building stock and outdoor temperature, flexibility duration varies considerably among regions in Britain. Figure 5.4 displays the number of comfortable heat-free hours in each region for an indoor temperature window from 18℃ to 21℃ and various outdoor temperatures.

Figure 5.4(a) displays the number of comfortable heat-free hours in each region for an indoor temperature window from 18℃ to 21℃ with a uniform

outdoor temperature of 5℃. The median number of heat-free hours is 6.4, with an interquartile range of 5.5 to 7.0 hours. A few areas in central Wales, northern England, and Scotland stand out with higher-than-average heat-free hours. Despite regional differences in heat capacity and heat losses in Greater London (as shown in the inset maps in Figure 5.2), the region has uniformly low heat-free hours. Both small, well-insulated flats in central London, with low heat capacity and low heat losses and large, poorly-insulated detached houses with a high heat capacity and high heat losses in the surrounding areas result in similarly low heating flexibility duration. Notably, this chapter does not consider heating flexibility power, which determines the total amount of energy shifted along with flexibility duration. Regions with small, well-insulated flats are likely to have lower total heat pump capacity than regions with large, poorly insulated detached houses. Therefore, central London is expected to have lower flexibility power capacity than the surrounding regions despite having similar flexibility duration.

Figure 5.4(b) displays heat-free hours for the 40^{th} percentile daily winter temperature in each region. The regional mean value of the 40^{th} percentile daily winter temperature is 4.4℃. Comparing Figure 5.4b with Figure 5.4a, which has a uniform outdoor temperature close to the mean temperature in (b), demonstrates the effect of accounting for regional differences in outdoor temperature on heat-free hours. In many central and northern regions, heat-free hours decrease, and they increase heat-free hours in southern coastal regions. Figure 5.4(c) demonstrates that for 5^{th} percentile temperatures, flexible heat-free hours reduce to less than 5 hours in the vast majority of regions.

Accounting for daily variation in winter temperatures demonstrates the impact of outdoor temperature on heating flexibility duration. Figure 5.5 shows the distribution of comfortable heat-free hours for each region at different historical temperature percentiles during winters from 2010 to 2022.

At lower outdoor temperatures, the median number of heat-free hours in each region drops: for the 80^{th}percentile temperature, the median is 7.8 hours and for the 5th percentile temperature, the median is 4.7 hours. The range of regional heat-free

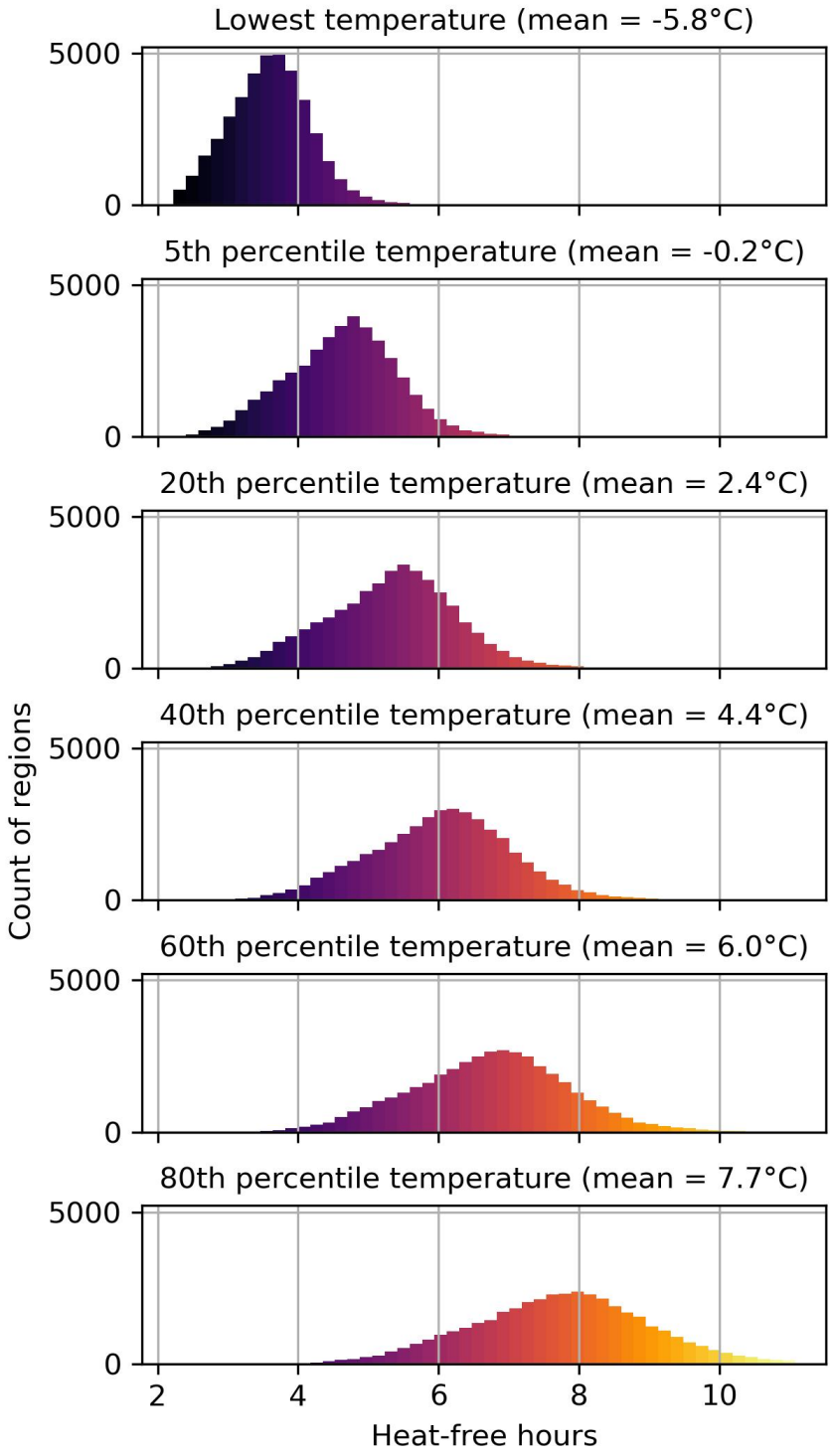

Figure 5.5: Histogram of average comfortable heat-free hours in each region for various outdoor temperature percentiles during winter 2010 to 2022 illustrating that cold weather decreases the duration of heating flexibility. Mean temperatures in each subfigure title are the mean regional temperature at each percentile. Note that the colormap matches Figure 5.4.

hours also decreases as the outdoor temperature drops. For the 80thpercentile temperature, the interquartile range is 6.9 to 8.6 hours, and for the 5thpercentile temperature, the interquartile range is 4.1 to 5.1 hours. This range decrease means that regions with higher-than-median thermal time constants will experience larger flexibility duration drops in cold weather than regions with lower-than-median thermal time constants. This increased sensitivity to outdoor temperature will limit the ability of heating flexibility from regions with high thermal time constants to support the power system during long cold snaps.

Although the current building stock offers significant flexibility duration during typical winter days, flexibility duration drops significantly during extreme cold events. For the lowest daily winter temperature from 2010 to 2022, with a mean value of -5.8℃, the median flexibility duration was just 3.6 hours with an interquartile range of 3.2 to 4.0 hours. This decreased duration will limit the ability of heating flexibility in the current building stock to ensure power system reliability during extreme cold events, which are predicted to be a major challenge for the electricity system in the future with electrified heating. This finding suggests that longer-duration forms of flexibility will be necessary to maintain power system reliability during extreme cold events.

5.3.4 Limitations & uncertainty

The heat capacity of homes used in the calculation of thermal time constants is a major source of uncertainty. Because of a lack of data availability, a constant value of floor space per room is assumed across all regions and heat capacity per floor area. These assumptions likely reduce the spread of thermal capacity values by overestimating floor area in densely populated areas and underestimating floor areas in sparsely populated areas. Because both the thermal time constant and, in turn, comfortable heat-free hours, are linearly proportional to thermal capacity, as shown in Equation 5.4 and Equation 5.6, these assumptions thus reduce the regional spread of time constant values and heat-free hours. Due to the availability of high spatial resolution measured data for gas consumption and outdoor air

temperature as well as the multi-year averaging of these values, regional heat losses are more certain than heat capacity values.

Because thermal time constants and heat capacities are calculated for each region without differentiating between different housing types or insulation levels, the method introduced in this chapter cannot capture the distribution of these values within each region, only mean values per region. Therefore, the underlying distribution of time constants and heat capacity within each region is unknown and extreme values are not captured. This analysis assumes that the mean regional values are adequately representative of the residential building stock in each region.

Because this method uses gas consumption data, the time constants calculated only represent homes with gas heating. Gas consumption data are only available for regions with 5 or more homes with gas meters, so time constants cannot be calculated for regions off the gas grid, which includes 971 of 34,753 LSOAs (2.8%) and 583 of 6,976 of DZs (8.4%). In addition, the time constants calculated for regions where gas consumption data are available do not necessarily represent the properties of homes in those regions that use non-gas heating. While no high-resolution data about the consumption of other heating fuels is currently available, future work may be able to capture the properties of non-gas heated homes at high spatial resolution.

The method presented in this chapter also does not account for regional variation in the internal temperatures of homes. When calculating HDDs, a uniform base temperature of 15.5℃ is used for all households. This assumption does not account for differences in set points due to energy poverty or behavioral norms. In addition, the calculation of comfortable heat-free hours assumes that all houses pre-heat to 21℃ and end at 18℃, but the range of comfortable temperature for households depends on the age and health of occupants, as well as personal and cultural preferences.

The method introduced in this chapter estimates the technical potential for residential heating flexibility in the existing building stock; however, the actual flexibility achieved will depend on its economic value relative to its cost and the willingness of residential customers to participate in flexible heating. Moreover,

this chapter assumes a simple pre-heating strategy wherein households increase the temperature of their homes to the maximum and then turn off their heating until their minimum indoor temperature is reached. More sophisticated control strategies may be required to implement residential heating flexibility.

5.4 Key insights

This chapter aims to quantify the energy capacity and duration of heating flexibility available from the existing building stock at high spatial resolution. While many existing methods model the interaction of heating flexibility with the power system, there is a need to represent the geospatial diversity of heating flexibility potential in complex power systems models. To this end, a method for assessing heating flexibility potential based on thermal time constants calculated from historical heating energy consumption, temperature, and building size is introduced. This method is applied to a case study of gas-heated homes in Britain and validated by comparing thermal time constants with those obtained from EPCs and a heat pump trial. The number of comfortable heat-free hours without heating was presented for a constant outdoor temperature of 5℃ as well as different percentiles of regional winter temperatures. Based on the results, the following key insights can be gained:

The proposed method produces high spatial resolution thermal time constant values that are broadly consistent with those found using EPC-based and indoor temperature-based methods. The heating consumption-based thermal time constant values are higher than those obtained using current EPC values (median value of 30.6 hours vs. 22.8 hours), which is expected because EPCs tend to overestimate heating demand. Compared to heat pump trial data with a median of 44.4 hours, the values obtained from this chapter's method are slightly lower. This difference is explained by the disproportionate representation of detached and semi-detached houses in the trial, as well as the exclusion of homes with high heating demand. Thus, the proposed consumption-based method produces more accurate thermal time constant estimates for the current housing than the EPC-based method and at higher spatial resolution than the indoor temperature-based method.

In the case study of Britain, significant heating flexibility energy capacity and duration are identified in the existing housing stock. For a 3℃ temperature flexibility window, the total thermal energy storage capacity in residential buildings of both gas and non-gas-heated homes is 500 GWh_{th}. For a cold day COP value of 2.5, this is equivalent to 200 GWh of electricity storage. This result demonstrates that thermal energy storage using building thermal inertia has the potential to be a flexibility resource of the same magnitude as battery storage: the total battery storage requirements for 2050 are between 35 and 63 GWh for the net zero scenarios in the 2023 FES [150]. The housing stock also has significant heating flexibility duration potential: assuming a uniform 5℃ outdoor temperature and indoor temperature range from 18 to 21℃, regions had a median of 6.4 comfortable heat-free hours and an interquartile range of 5.5 to 7.0 heat-free hours. However, heating flexibility duration varies significantly among regions. Due to low thermal capacity in central London and high heating losses in the surrounding home counties, there is relatively low flexibility duration in Greater London and the Southeast. High flexibility duration is identified in some rural areas due to higher heat capacity and lower heat losses.

Accounting for the impact of historical outdoor temperatures demonstrates that extreme cold events can drastically decrease flexibility duration compared to typical winter temperatures. For the 20^{th}percentile of daily winter temperatures, the median regional heat-free hours is 5.9, with an interquartile range from 5.2 to 6.5 hours. At these temperatures, heating flexibility can compete with the typical 4-hour duration of lithium-ion batteries during the heating season. However, for the lowest daily winter temperatures in each region from 2010 to 2022, this heating flexibility duration nearly halved to a median of 3.6 hours with an interquartile range of 3.2 to 4.0 hours. This temperature-driven decrease in flexibility duration will limit the ability of heating flexibility to contribute to power system reliability during extreme cold events.

The results of this chapter demonstrate how this novel consumption-based method can characterize the heating flexibility potential of the current building stock at high spatial resolution. This approach provides building stock data

that can be incorporated into complex power system planning models. The next chapter (Chapter 6) evaluates the role of heating flexibility in generation, storage, and transmission expansion planning for bulk power systems with high shares of renewable generation. While the high spatial resolution flexibility potential data produced in this chapter are aggregated for use in bulk power system planning, the original resolution data may be useful for distribution system planning and other applications outside of the scope of this thesis.

6

Planning with heating flexibility

Contents

This chapter addresses the question: *Where will residential heat pump flexibility offer the most value to the bulk power system?* High spatial resolution heating flexibility data is incorporated into bulk power system planning to identify the cost-optimal heating flexibility locations for a variety of power systems.

6.1 Introduction

The regional heating flexibility potential estimates developed in Chapter 5 are integrated into a generation, storage, and transmission expansion planning model to understand the impact of heating flexibility on the bulk power system under different policy scenarios.

The first research contribution of this chapter is assessing where residential heating flexibility offers the most value in optimal power system planning by incorporating high spatial resolution flexibility potential into bulk power systems planning. By analyzing where demand-side flexibility is most valuable within a bulk power system with high residential heating electrification, this chapter addresses research gap 4 identified in Section 2.4.

While modeling provides insights about the cost-optimal locations of flexibility from the point of view of the bulk power system, there is a large amount of structural uncertainty about the willingness and ability of households in different regions to heat flexibly. To address this uncertainty, this chapter also examines near-optimal regional flexibility participation and provides insight into alternative regional flexibility participation patterns, which is its second research contribution. By including structural uncertainty in demand-side flexibility participation in near-optimal spatial planning, this chapter addresses research gap 5 identified in Section 2.4.

The remainder of this chapter is structured as follows. Section 6.2 introduces the methods and case study data. Section 6.3 discusses the results, and Section 6.4 presents the key outcomes from the chapter.

6.2 Methods and data

The methods and data for this chapter are summarized in Figure 6.1. All input data have been introduced in previous chapters. The methods are split into spatial aggregation of flexibility potential, separating space and hot water heating demand, heating flexibility in capacity expansion planning, and near-optimal alternatives.

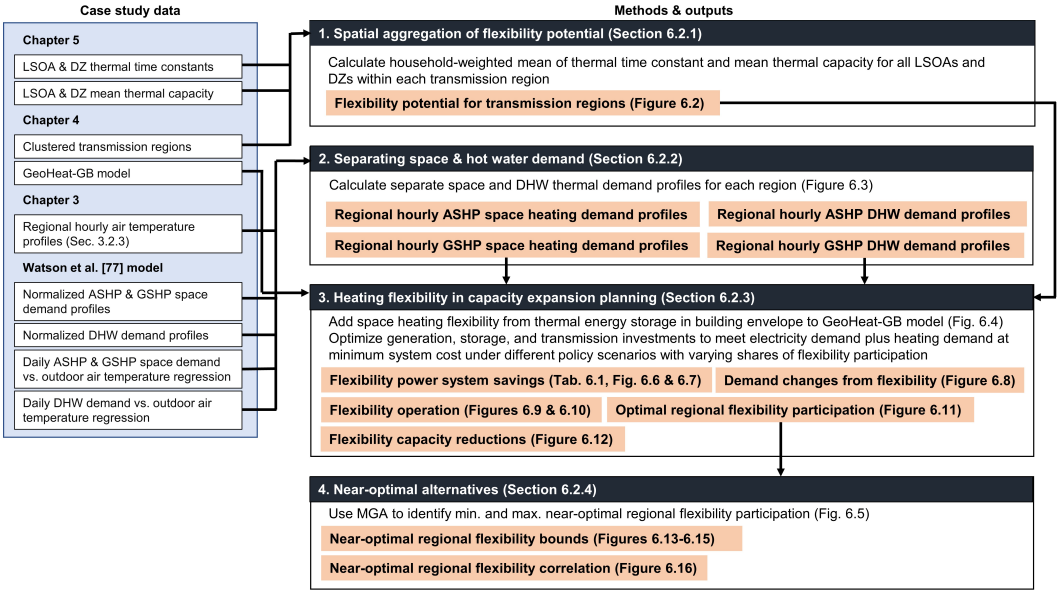

Figure 6.1: Summary of methods and data for this chapter. Outputs for each step are highlighted in orange.

6.2.1 Spatial aggregation of flexibility potential

The residential heating flexibility potential calculated in Chapter 5 is aggregated to the grid regions developed in Section 4.2.2 to be incorporated into bulk power system planning, as shown in Figure 6.2. The thermal time constant for each grid region τ_i is calculated based on the household-weighted mean thermal time constant for all LSOAs and DZs r within a grid region i:

$$\tau_i = \frac{\sum_r A_r \tau_r}{\sum_r A_r} \tag{6.1}$$

To avoid underestimating the mean time constant in grid regions with high shares of homes off the gas grid, LSOAs and DZs for which a thermal time constant τ_r cannot be estimated due to a lack of gas demand data are excluded from both the thermal time constant values τ_r and the total number of households A_r used in this calculation. Thermal capacity for each grid region C_i is calculated based on the household-weighted mean thermal capacity for all LSOAs and DZs within a grid region:

$$C_i = \frac{\sum_r A_r C_r}{\sum_r A_r} \tag{6.2}$$

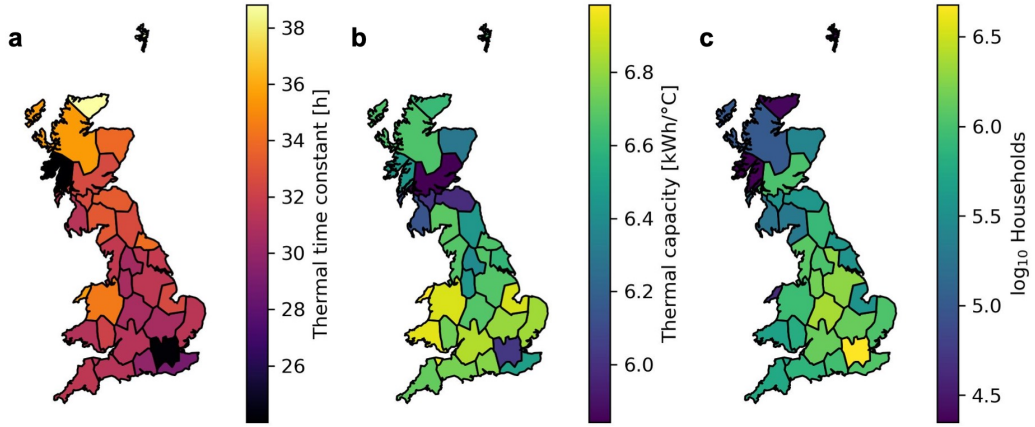

Figure 6.2: Map of aggregated (a) time constants and (b) thermal capacity and (c) total households on a log scale for the 30 grid regions in Britain.

Because thermal capacities for LSOAs and DZs C_r are calculated based on census data about the average number of rooms in each household in Section 5.2.4, no LSOAs or DZs need to be excluded from this calculation due to a lack of data.

6.2.2 Separating space and hot water demand

Because thermal energy storage in the building envelope can only be used for space heating demand flexibility, heating demand is separated into space heating demand and domestic hot water (DHW) demand. Watson et al. [77] calculate half-hourly DHW demand based on the EDRP dataset and assume that the rest of heat pump demand in the RHPP trials is for space heating. These normalized profiles are shown in Figure 6.3.

The daily ASHP space heating demand per household regression is:

$$Q_{r,d}^{ASHP,space} = \begin{cases} 83.8 - 5.53 \cdot T_{r,d}^{air} \text{ kWh} & T_{r,d}^{air} < 14.3℃ \\ 15.8 - 0.77 \cdot T_{r,d}^{air} \text{ kWh} & 14.3℃ \leq T_{r,d}^{air} < 20.5℃ \\ 0 \text{ kWh} & T_{r,d}^{air} \geq 20.5℃ \end{cases} \tag{6.3}$$

The daily GSHP space heating demand per household regression is:

$$Q_{r,d}^{GSHP,space} = \begin{cases} 85.8 - 5.64 \cdot T_{r,d}^{air} \text{ kWh} & T_{r,d}^{air} < 14.3℃ \\ 16.9 - 0.82 \cdot T_{r,d}^{air} \text{ kWh} & 14.3℃ \leq T_{r,d}^{air} < 20.6℃ \\ 0 \text{ kWh} & T_{r,d}^{air} \geq 20.6℃ \end{cases} \tag{6.4}$$

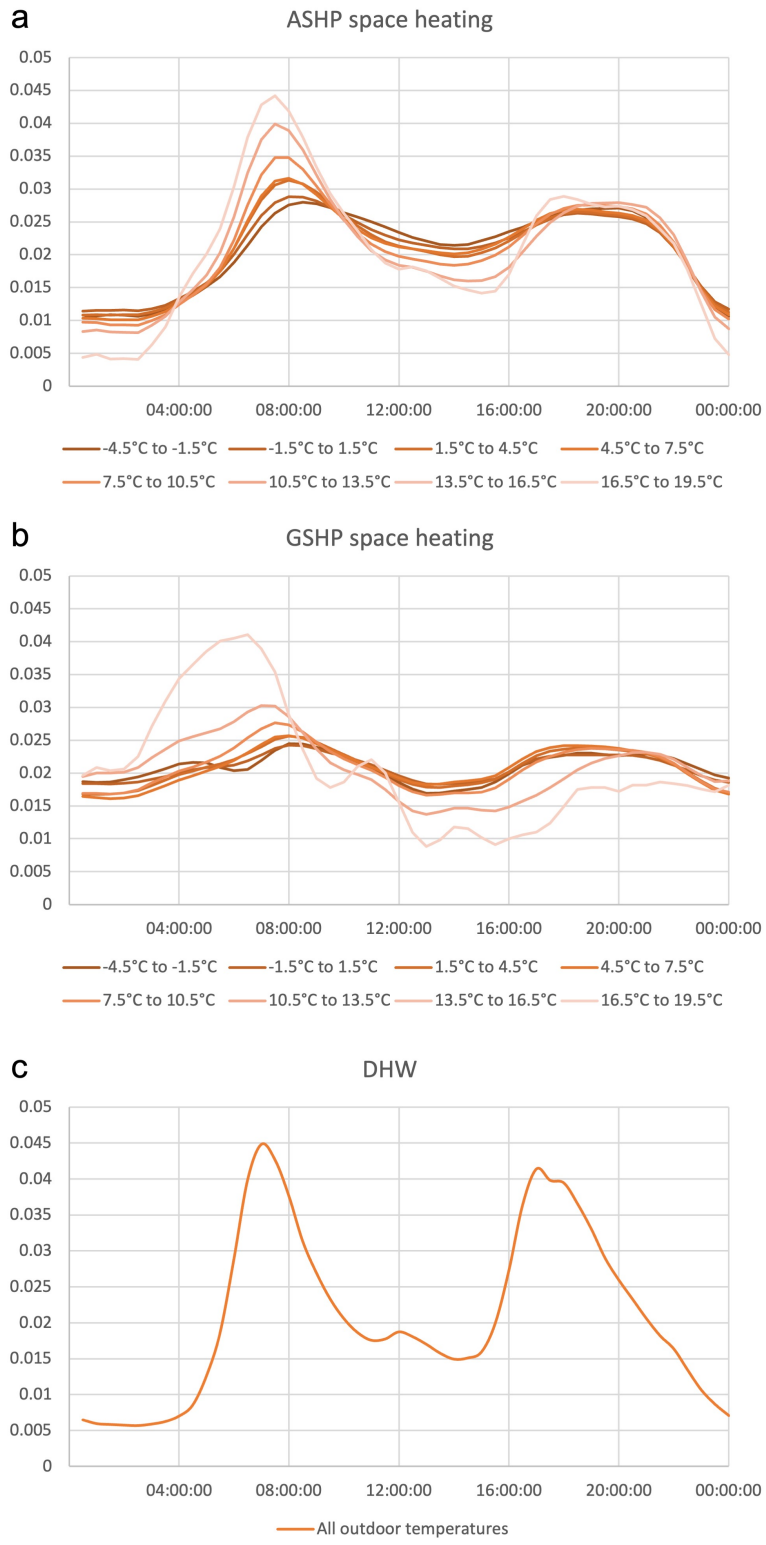

Figure 6.3: Demand profiles for (a) ASHP space heating, (b) GSHP space heating, and (c) DHW, normalized to 1 unit-day from Watson et al. [77].

The regression for DHW is the same for both ASHPs and GSHPs:

$$Q_{r,d}^{DHW} = 12.9 - 0.324 \cdot T_{r,d}^{air} \text{ kWh} \tag{6.5}$$

These regressions are combined with hourly heating demand profiles and scaled based on the number of households in each region as described in Section 3.2.4.

Thus, the total heat demand at each node remains the approximately the same [1]:

$$\begin{gathered} d_{n,s,t} = d_{n,s,t}^{DHW} + d_{n,s,t}^{space} \\ \forall \{n \mid n \text{ heat buses}\},\ s \in \{\text{ASHP, GSHP}\},\ t \end{gathered} \tag{6.6}$$

COP values for ASHP and GSHP are calculated based on Equations 3.4 through 3.7 as described in Section 3.2.5.

6.2.3 Flexibility in capacity expansion planning

The GeoHeat-GB capacity expansion planning model introduced in Chapter 4 is expanded to include residential heating flexibility in the capacity expansion optimization for Britain and interconnected regions. To assess the value of heating flexibility to the power system, no cost is considered for heating flexibility; however, the share of total households participating in heating flexibility is constrained. The capacity expansion problem is solved multiple times for each scenario to assess the value of heating flexibility with increasing flexibility participation rates. For each investment problem, a global limit P is set on the share of British households participation in flexibility. The regional distribution of heating flexibility participation is optimized from the bulk power system system point of view alongside generation, storage, and transmission expansion. This approach allows the creation of a demand curve for residential heating flexibility, which shows the value of heating flexibility to the bulk power system at different flexibility participation levels.

[1] Using separate space and DHW heat demand regressions and profiles from Watson et al. [77] for ASHPs and GSHPs leads to a total annual space and DHW demand of 337.7 TWh. Due to rounding of regression coefficients, this figure is 0.8% lower than the multi-regional annual heating demand calculated in Section 3.2.4 using a total heating demand regression of 340.4 TWh. Separating space and DHW demand reduces the multi-regional heating demand error compared to the ECUK historical consumption from +0.7% (as calculated in Section 3.3.2) to -0.05%.

Assessing the cost of residential heating flexibility and the optimal participation level is left to future work.

A decision variable $a_{n,s}$ is defined for the number of households heating flexibly at each bus n with either ASHPs or GSHPs s. This variable can be between 0 and the total number of households in each region $A_{n,s}$ using ASHPs or GSHPs.

$$\begin{aligned} 0 \leq a_{n,s} \leq A_{n,s} \\ \forall \{n \mid n \text{ heating flexibility buses}\},\ s \in \{\text{ASHP, GSHP}\} \end{aligned} \tag{6.7}$$

Because heat pump adoption is not considered outside of Britain, $A_{n,s}$ is 0 for buses not in Britain. As in Chapter 4, 100% heat pump adoption is assumed within Britain, with 25% of households in each region using GSHPs and 75% using ASHPs.

The total number of flexible households at all buses n is constrained by the flexibility participation constant times the total number of potentially flexible households with ASHPs or GSHPs:

$$\begin{aligned} \sum_n a_{n,s} = P \sum_n A_{n,s} \\ \forall \{n \mid n \text{ heating flexibility buses}\},\ s \in \{\text{ASHP, GSHP}\} \end{aligned} \tag{6.8}$$

Following the approach used in the sector-coupled PyPSA-Eur model [183, 184], heating flexibility is modeled by adding a flexibility charging/discharging link between each bus' heat bus and a thermal energy storage bus, summarized in Figure 6.4. In this case, thermal energy storage in the building envelope is considered rather than thermal energy storage in the hot water tank. A single flexibility charging and discharging link is used for each node to avoid unintentional storage cycling [192].

Total heat pump capacity at each bus is constrained assuming an average thermal heat pump capacity κ of 10 kW:

$$\begin{aligned} F_{l,s} = \kappa A_{n,s} \\ \forall \{l \mid l \text{ heat pumps}\}\ s \in \{\text{ASHP, GSHP}\} \end{aligned} \tag{6.9}$$

By convention, flexibility charging/discharging link power is positive when charging (i.e. consuming additional electricity to store energy in thermal energy storage) and negative when discharging (i.e. reducing heat pump demand using

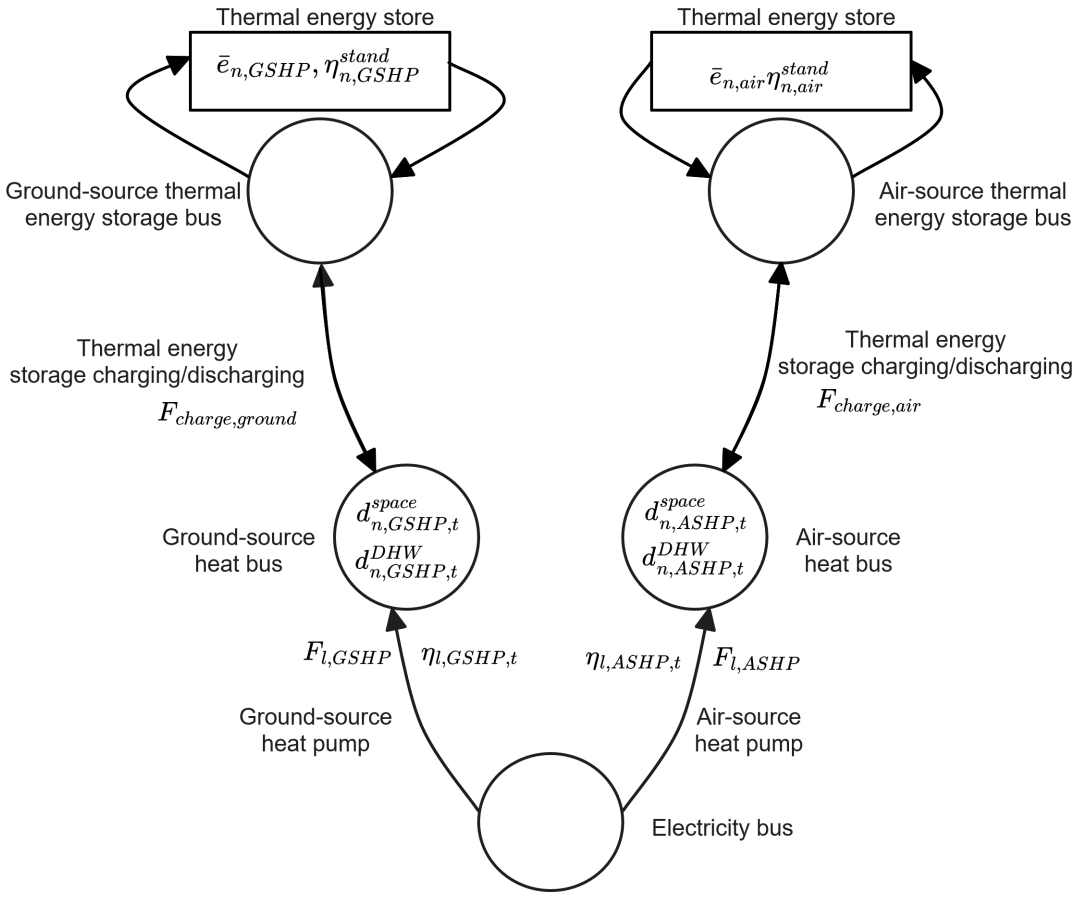

Figure 6.4: Diagram of thermal energy storage nodes added to electricity and heat network.

heat from thermal energy storage). The power capacity of the flexibility charging link is constrained by the share of flexible households at each bus times the average thermal heat pump capacity:

$$F_{l,s} = \kappa a_{n,s} \qquad (6.10)$$
$$\forall\{l \mid l \text{ thermal energy storage charge links}\},\ s \in \{\text{ASHP, GSHP}\}$$

Because of the nodal balance constraint at each heat bus, the combination of constraint 6.10 and the set parameter value in Equation 6.9 reflect the decreased ability of heat pumps to charge heating flexibility at peak heat demand times due to the limited capacity of heat pumps.

Because this chapter considers only heating flexibility from building envelope thermal storage, heating flexibility can only be used to meet space heating demand.

Therefore, the minimum heating flexibility discharge power flow is limited to the regional space heat times the share of flexible households at each bus n and each time step t:

$$\begin{aligned} f_{l,s,t} &\geq -\frac{a_{n,s}}{A_{n,s}} d_{n,s,t}^{space} \\ \forall\{l \mid l \text{ thermal energy storage charge/discharge links}\}, \\ s \in \{\text{ASHP, GSHP}\},\ t \end{aligned} \tag{6.11}$$

Thermal energy storage in the building envelope is modeled using store components in PyPSA [185], which have time-dependent dispatch $h_{n,s,t}$ and energy $e_{n,s,t}$. Store dispatch is unconstrained:

$$\begin{aligned} -\infty \leq h_{n,s,t} \leq +\infty \\ \forall\{n \mid n \text{ thermal energy storage buses}\},\ s \in \{\text{ASHP, GSHP}\},\ t \end{aligned} \tag{6.12}$$

For this reason, power flow to the thermal energy storage buses via the charging/discharging links is constrained in Equations 6.10 and 6.11.

Store energy is constrained by the energy capacity $\bar{e}_{n,s}$:

$$\begin{aligned} 0 \leq e_{n,s,t} \leq \bar{e}_{n,s} \\ \forall\{n \mid n \text{ thermal energy storage buses}\},\ s \in \{\text{ASHP, GSHP}\},\ t \end{aligned} \tag{6.13}$$

Store dispatch and energy are related by the store energy balance:

$$\begin{aligned} e_{n,s,t} = (\eta_{n,s}^{stand})^{w_t} e_{n,s,t-1} - w_t h_{n,s,t} \\ \forall\{n \mid n \text{ thermal energy storage buses}\},\ s \in \{\text{ASHP, GSHP}\},\ t \end{aligned} \tag{6.14}$$

where $\eta_{n,s}^{stand}$ is the standing losses for the store.

The thermal energy storage energy capacity at each bus is constrained based on the number of flexible households $a_{n,s}$, the flexibility temperature window ΔT^{flex} (3℃ in this thesis), and the average thermal capacity C_n of houses in that bus region:

$$\begin{aligned} \bar{e}_{n,s} = C_n a_{n,s} \Delta T^{flex} \\ \forall\{n \mid n \text{ heating flexibility buses}\},\ s \in \{\text{ASHP, GSHP}\} \end{aligned} \tag{6.15}$$

The impact of assuming a uniform flexibility temperature window is discussed in Section 6.3.9.

Thermal energy storage hourly standing losses set according to thermal time constant:

$$\eta_{n,s}^{stand} = 1 - e^{1/\tau_n} \quad \forall\{n \mid n \text{ heating flexibility buses}\},\ s \in \{\text{ASHP, GSHP}\} \tag{6.16}$$

A periodicity constraint is set on thermal energy storage:

$$e_{n,s,0} = e_{n,s,T} \quad \forall\{n \mid n \text{ heating flexibility buses}\},\ s \in \{\text{ASHP, GSHP}\} \tag{6.17}$$

The requirement that each country meets 100% of its heat pump electricity consumption in the self-sufficiency constraint in Equation 4.20 avoids unintended storage cycling of heating flexibility to artificially increase self-sufficiency, as Kittel and Schill [192] warn.

6.2.4 Near-optimal alternatives

To address the structural uncertainty in heating flexibility participation, MGA is applied to assess near-optimal regional distributions of flexibility participation. The one at a time (OAT) search algorithm [143][2] is used to establish the limits on near-optimal flexibility participation in each region.

Figure 6.5 compares the cost-minimizing optimization described in Section 6.2.3 with MGA using the OAT algorithm. The axes are power system costs C and a decision variable, in this case $\bar{e}_{n,s}$, the energy capacity of thermal energy storage of type s at bus n.

The image on the left shows an illustrative slice of the cost minimization used in Section 6.2.3 for the total system cost C versus the maximum capacity of the store $\bar{e}_{n,s}$ of type s at node n. The edges of the feasible space, shown in green, are

[2]This name for the search algorithm that Neumann and Brown [143] introduced was coined by Pedersen et al. [144].

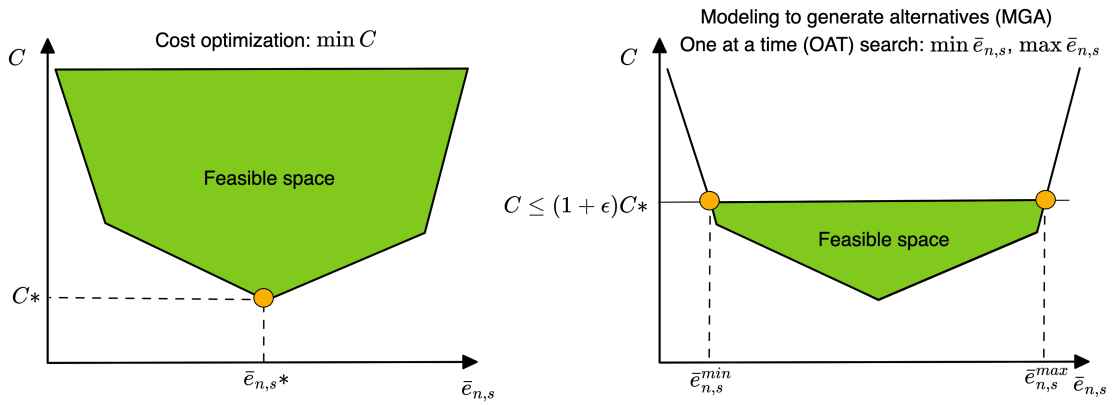

Figure 6.5: Diagram comparing cost-minimizing optimization and MGA with the OAT search algorithm.

determined by the linear constraints. For traditional capacity expansion modeling, the optimization seeks the minimum cost $C*$ subject to these constraints, shown with an orange dot. This solution includes the cost-optimal store capacity $\bar{e}_{n,s}*$.

The same illustrative slice for the MGA approach is shown on the right. Rather than seeking the optimal cost, a new budget constraint is introduced that requires system cost to be within a given slack value ϵ of the optimal system cost. The portion of the feasible space within this budget is known as the near-optimal space. This chapter uses the OAT method to search the near-optimal space, so the optimization seeks the minimum and maximum values (in this case, $\bar{e}_{n,s}^{min}$ and $\bar{e}_{n,s}^{max}$) of a decision variable (or set of decision variables) within the near-optimal space, shown with orange dots. By arguments of convexity, Neumann and Brown [143] show that near-optimal solutions exist for all values between the minimum and maximum values, so the OAT search algorithm can be used to establish the boundary values of the near-optimal space. In this chapter, this algorithm is used to search for the minimum and maximum regional values of thermal energy storage that are within ϵ of the system costs for the optimal spatial layout of thermal energy storage.

Following the simplified notation introduced by Neumann and Brown [146], $c^T x$ represents the linear objective function in Equation 4.1 and $Ax \leq b$ and $Dx = f$ represent the set of linear constraints for the power system in Equations

4.2 to 4.19 and the heating flexibility constraints in Equations 6.7 to 6.17. The minimized system cost $C*$ is thus:

$$C* = \min\{c^T x \mid Ax \leq b, Dx = f\} \tag{6.18}$$

To explore near-optimal spatial distributions of heating flexibility participation, the budget constraint is added to limit solutions to those that are within ϵ percent of the minimum cost $C*$. The minimum and maximum capacities of thermal energy storage at each bus n that are at most ϵ more expensive than the optimum are thus:

$$\begin{aligned} \bar{e}_{n,s}^{min} = \min\{\bar{e}_{n,s} \mid Ax \leq b, Dx = f, c^T x \leq (1+\epsilon)C*\} \\ \forall\, n,\ s \in \{\text{air-source, ground-source}\} \end{aligned} \tag{6.19}$$

$$\begin{aligned} \bar{e}_{n,s}^{max} = \max\{\bar{e}_{n,s} \mid Ax \leq b, Dx = f, c^T x \leq (1+\epsilon)C\} \\ \forall\, n,\ s \in \{\text{air-source, ground-source}\} \end{aligned} \tag{6.20}$$

The near-optimal regional flexibility capacities are explored for the most valuable 5% of flexible households. For each scenario, a slack value ϵ is chosen so that the power system savings from flexibility are at least 95% of those achieved with optimal regional flexibility participation.

6.3 Results and discussion

This section discusses the results of incorporating thermal energy storage into bulk power system planning. Section 6.3.1 assesses the marginal power systems savings for each flexible household under different policy scenarios, and Section 6.3.2 examines the components of these system savings. Changes in demand due to heating flexibility are explored in Section 6.3.3, and flexibility operation is examined in detail in Section 6.3.4. Section 6.3.5 discusses the optimal heating flexibility participation in different regions from the perspective of the bulk power system, and Section 6.3.6 examines the spatial changes in storage and generation capacity due to heating flexibility. Section 6.3.7 examines the minimum and maximum near-optimal

Table 6.1: Bulk power system savings from heating flexibility.

Scenario	System cost (€B) 0% flexibility	System cost (€B) 100% flexibility	System savings (%) 100% flexibility
Central	27.36	26.42	3.4
National green grid	48.89	47.32	3.2
Localized transition	57.23	55.55	2.9
Capacity for carbon	19.43	18.70	3.8
Carbon stagnation	19.77	18.77	5.0

regional flexibility participation, and Section 6.3.8 discusses the correlations in flexibility participation at different buses for the near-optimal solutions. Finally, Section 6.3.9 discusses the limitations of this chapter.

6.3.1 Power system savings from heating flexibility

Power system savings from flexibility depend on the carbon budget and transmission expansion capacity of the power system. Table 6.1 displays the bulk power system savings for 100% flexibility participation in each scenario.

In the central scenario, total savings from 100% flexibility participation are €0.94 billion. Total power system savings from 100% heating flexibility participation range from €0.73 billion in the capacity for carbon scenario to €1.68 billion in the localized transition scenario. These savings amount to total cost reductions of 2.9% to 5.0%, with smaller percent changes in the low-carbon scenarios due to their higher total system costs. These total system savings are consistent with the 3% savings that Zeyen et al. [76] find for optimal deployment of hot water tank thermal energy storage for both individual building and district heating systems in the residential and commercial sectors in the European grid. Because this chapter only considers thermal energy storage in individual residential buildings, the benefits of thermal energy storage in Britain are slightly higher than a Europe-wide average that Zeyen et al. [76] consider.

Figure 6.6 displays the power system demand curve for heating flexibility with the marginal power system savings per flexible household for varying levels of flexibility participation for all scenarios. These marginal savings are based on the difference in the annualized net present value cost of all electricity system components, assuming a 7% discount rate. This analysis produces bulk power system demand curves for

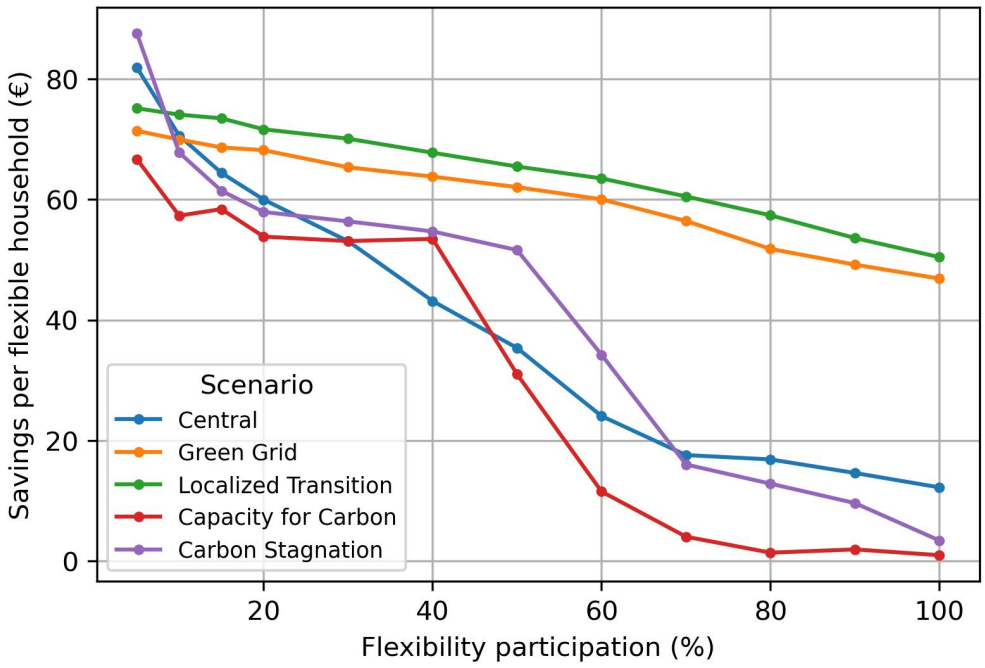

Figure 6.6: Marginal annual savings for the bulk power system per flexible household at different levels of flexibility participation for all scenarios.

heating flexibility. Because of uncertainty about the cost of residential heating flexibility, this analysis does not create supply costs curves for flexibility nor attempt to find the optimal flexibility participation rate. Further research is needed to assess the cost of residential heating flexibility at different participation levels to identify the optimal flexibility participation rate for the bulk power system.

For all scenarios, the first 5% of households heating flexibly offer significant savings for the bulk power system, ranging from €67 to €88 annually per household[3]. In the low-carbon scenarios, the marginal value of flexibility remains high across flexibility participation rates: annual system savings decrease roughly linearly from 5 to 100% flexibility participation to €47 per household in the national green grid scenario and €50 per household in the localized transition scenario. In contrast, system savings drop precipitously in the central and high-carbon scenarios between 5 and 10% flexibility participation. In the central scenario, diminishing returns on increasing flexibility participation continue until the marginal systems savings

[3]Note that these figures represent the bulk power system savings, not the actual payment that these households would receive for flexibility.

per household reach €12 per household at 100% participation[4]. In the high-carbon scenarios, system savings per household remain relatively constant from 15 to 50% participation in the carbon stagnation scenario and from 10 to 40% in the capacity for carbon scenario. The marginal value of flexibility then drops precipitously at 60 and 50% flexibility participation, respectively, before falling to less than €5 per household at 100% flexibility participation. For all scenarios, the marginal system savings per household are lower than the average savings of €120 per household that Hedegaard and Münster [115] find for optimal investment in building structure heat storage in 34% of houses. This difference could be due to longer flexibility duration and higher energy capacity because of the higher heat capacity of the Danish housing stock (9 to 24 kWh/°C) that they consider compared to the British housing stock considered in this thesis (3 to 10 kWh/°C, as shown in Figure 5.2).

The marginal value of heating flexibility depends primarily on the carbon budget and, to a lesser extent, the transmission expansion allowed in each scenario. Above 5% flexibility participation, the marginal value of flexibility is higher in the low-carbon scenarios than the high-carbon scenarios, and the difference becomes larger at higher flexibility shares. For the same carbon budget, flexibility has a higher marginal value when transmission expansion is restricted: in the low-carbon scenarios, the difference is about €4 per flexible household. The difference in flexibility value per household among the high-carbon scenarios varies with participation rate. At low participation rates, the difference in marginal value of flexibility is over €10. This difference narrow to less than €5 per household from 15 to 40% participation and is above €10 per household from 50 to 80% participation. As the value of flexibility decreases at above 80% participation, this gap narrows to less than €10 per household.

[4]This figure represents the bulk power system savings from all households with heat pumps heating flexibly. If all households heat flexibly, households may not necessarily be compensated for flexibility by other domestic ratepayers, but less flexible non-domestic customers may compensate them for the power system savings.

6.3.2 Power system savings components

Figure 6.7 displays the composition of marginal power system savings per flexible household for each scenario.

In the central and low-carbon scenarios, the vast majority of power system savings from heating flexibility is due to reduced battery investment costs. Battery investment reductions dominate flexible heating savings in the central scenario up to 60% participation, and above this participation level, savings come from both battery and onshore wind capex reductions. Below 50% flexibility participation, each flexible household replaces €50 to €92 of battery investments. Above 50% flexibility participation, each flexible household reduces battery investments by €11 to €23 and onshore wind investments by €6 to €11. Battery investment reductions make up the most of the power systems savings from heating flexibility across all participation levels in the low-carbon scenarios. In the national green grid scenario, each flexible household replaces between €39 and €65 of battery investment, and in the localized transition scenario, each flexible household replaces €46 to €77 of battery investment. These findings are consistent with those of Li and Pye [122] and Brown et al. [123], who find that flexibility reduces the need for electricity storage.

In the high-carbon scenarios, heating flexibility savings are primarily due to reduced generation investment costs. In the carbon stagnation scenario, heating flexibility reduces investment in open-cycle gas generation capacity across participation levels, as well as onshore wind capacity up to 10% flexibility participation. At 60% flexibility participation, heating flexibility also reduces onshore wind investment and increases solar investment[5]. In the capacity for carbon scenario, each flexible household up to 40% participation reduces investment in open-cycle gas generation by €40 to €56. At 50% flexibility participation, flexibility reduces onshore wind as well as AC and HVDC transmission capacity. At 60% participation and above, flexibility primarily reduces operational expenses.

[5]Note that while solar generation potential is lower in the winter, it is still available during the heating season, as shown in Figure 6.9.

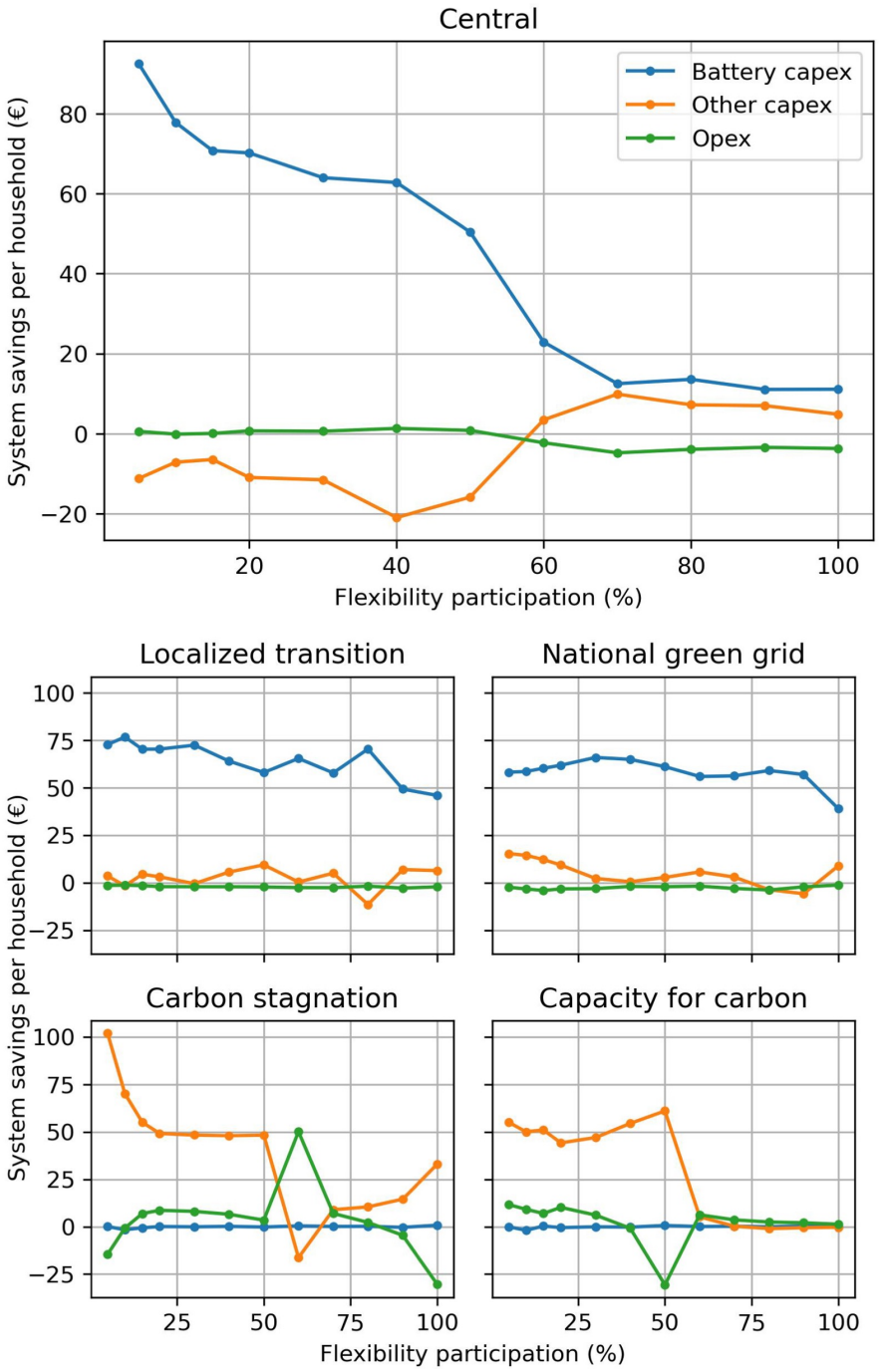

Figure 6.7: Breakdown of marginal annual power system savings per flexible household into battery capex (capital expenditures), other capex, and opex (operational expenditures) at different levels of flexibility participation for each scenario.

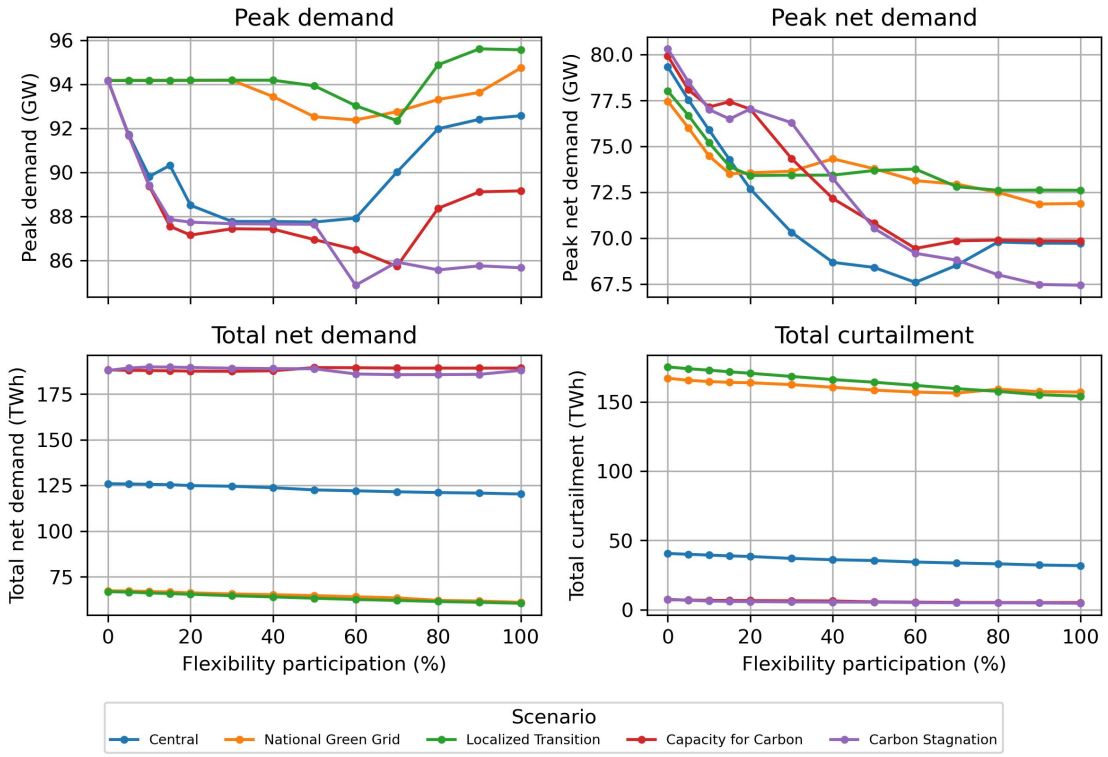

Figure 6.8: Changes in peak demand, peak net demand, total net demand, and total curtailment with flexibility participation for the 2019 weather-year for all scenarios.

In all scenarios, most of the power system savings from heating flexibility comes from reducing dispatchable capacity requirements. In the high-carbon scenarios, this dispatchable capacity is primarily open-cycle gas generation, and in the central and low-carbon scenarios, this dispatchable capacity is mostly battery storage. In the next sections, heating flexibility operation will be assessed to understand how flexibility reduces the need for dispatchable capacity.

6.3.3 Demand changes

To understand the investment changes discussed in the previous section, Figure 6.8 compares the changes in peak demand and net demand, which is demand minus wind and solar generation potential in Britain, for each scenario. Total net demand is the sum of net demand when demand exceeds wind and solar generation potential, and total curtailment is the sum of net demand when wind and solar generation potential exceed demand.

The upper left panel of Figure 6.8 displays the difference in how increasing flexibility participation changes peak demand in the central and high-carbon scenarios versus the low-carbon scenarios. In the high-carbon scenarios, the first 15% of flexibility participation rapidly reduces peak demand by about 6 GW. In the central scenario, the reduction in peak demand for the first 15% of flexibility participation is less dramatic, dropping just 4 GW. In contrast, in the low-carbon scenarios, the first 30% of flexible households do not reduce peak demand at all. From 40 to 60% flexibility participation, flexibility slightly reduces peak demand in the low-carbon scenarios. Above about 60% flexibility participation, peak demand increases or stagnates in all scenarios. This trend suggests that for widespread flexibility participation, bulk power system savings are achieved by another mechanism than reducing peak demand.

The upper right panel of Figure 6.8 displays changes in peak net demand with flexibility participation. In the high-carbon scenarios, the first 10% of households slightly reduce peak net demand by about 3 GW. From 20 to 60% participation, flexibility further reduces peak net demand by a further 8 GW in the high-carbon scenarios. Similarly, in the central scenario, the first 60% of flexible households reduce peak demand by 12 GW. In contrast, in the low-carbon scenarios, peak net demand decreases by just 4 GW from 0 to 15% flexibility participation and decreases very little with higher flexibility participation.

For the central and low-carbon scenarios, the decreases in peak net demand below 60% flexibility participation explain the reduced need for investment in dispatchable resources shown in Figure 6.7. In the central scenario, battery investment savings are inversely correlated with peak net demand: battery investment savings increase as peak net demand falls up to 50% participation, above which peak net demand stagnates and battery savings are much lower. This decrease in net demand reduces battery storage capacity by 10 GW at 60% flexibility participation. Similarly, open-cycle gas generation investment savings in the high-carbon scenarios are inversely correlated with peak net demand. These decreases in net peak demand reduce open-cycle gas peaking capacity at 60% flexibility participation by 11 GW in the

capacity for carbon scenario and 18 GW in the carbon stagnation scenario. These patterns suggest that heating flexibility reduces the need for dispatchable resources by shifting heating load to reduce peak net demand.

The low-carbon scenarios do not exhibit the same inverse correlation between peak net demand and dispatchable resource investment. In these scenarios, flexibility reduces peak net demand very little beyond the first 15% of flexible households, but battery investment savings remain high from 15% to 100% flexibility participation. This suggests that heating flexibility reduces the need for battery capacity by another mechanism in the low-carbon scenarios.

The lower panels of Figure 6.8 provides insight into the differing roles of flexibility in the low-carbon and high-carbon scenarios. The lower left panel of Figure 6.8 displays the differences in total net demand between scenarios, and the lower right panel displays total curtailment. In the central and high-carbon scenarios, total net demand is higher than total curtailment, which indicates that demand typically exceeds renewable potential. In contrast, in both low-carbon scenarios, total net demand is lower than total curtailment, which indicates that renewable potential typically exceeds electricity demand.

The lower left panel of Figure 6.8 shows how heating flexibility participation changes total net demand in each scenario. Heating flexibility reduces total net demand in the central and low-carbon scenarios but not in the high-carbon scenarios. In the central scenario, flexibility reduces total net demand by 6.4 TWh from 126.0 TWh at 0% participation to 120.3 TWh at 100% participation. While total net demand in the low-carbon scenarios is about half of total net demand in the central scenarios, flexibility also reduces total net demand by 6.4 TWh in the low-carbon scenarios. In the national green grid scenario, total net demand drops from 67.4 TWh with no flexibility to 61.0 TWh with 100% flexibility participation. In the localized transition scenario, total net demand drops from 66.9 TWh without flexibility to 60.5 TWh at 100% flexibility participation. In contrast, in the carbon stagnation scenario, total net demand remains at 188.0 TWh at 0% and 100% flexibility. In the capacity for carbon scenario, heating flexibility slightly increases total net demand from 188.2

TWh at 0% flexibility participation to 189.3 TWh at 100% flexibility participation because dispatchable gas generators and expanded transmission capacity allow total net demand to be met at low cost compared to lower carbon scenarios, which require increased battery energy storage capacity to meet total net demand..

The lower right panel of Figure 6.8 shows how heating flexibility participation changes total curtailment in each scenario. Heating flexibility reduces curtailment in all scenarios, with larger decreases in the central and low-carbon scenarios. In the central scenario, heating flexibility reduces curtailment by 8.8 TWh from 40.6 TWh at 0% flexibility participation to 31.8 TWh at 100% flexibility participation. In the national green grid scenario, heating flexibility reduces curtailment by 10.0 TWh from 167.1 TWh with no flexibility participation to 157.1 TWh with 100% flexibility participation. In the localized transition scenario, heating flexibility reduces curtailment by 21.1 TWh from 175.3 TWh without flexibility to 154.2 TWh with 100% flexibility participation. These decreases in curtailment along with net demand reduce the need for battery capacity by 16 GW/96 GWh in the green grid scenario and 17 GW/102 GWh in the localized transition scenario. In the high-carbon scenarios, there is much less curtailment: just 7.3 TWh in the capacity for carbon scenario and 7.6 TWh in the carbon stagnation. Heating flexibility reduces curtailment in these scenarios to 5.1 TWh and 4.7 TWh, respectively, at 100% flexibility participation.

6.3.4 Flexibility operation

This section further assesses the role of flexibility in different scenarios by examining hourly patterns in heating flexibility operation. Figure 6.9 shows hourly space heating demand, heating flexibility use, and British wind and solar potential in the central scenario with 5% flexibility participation.

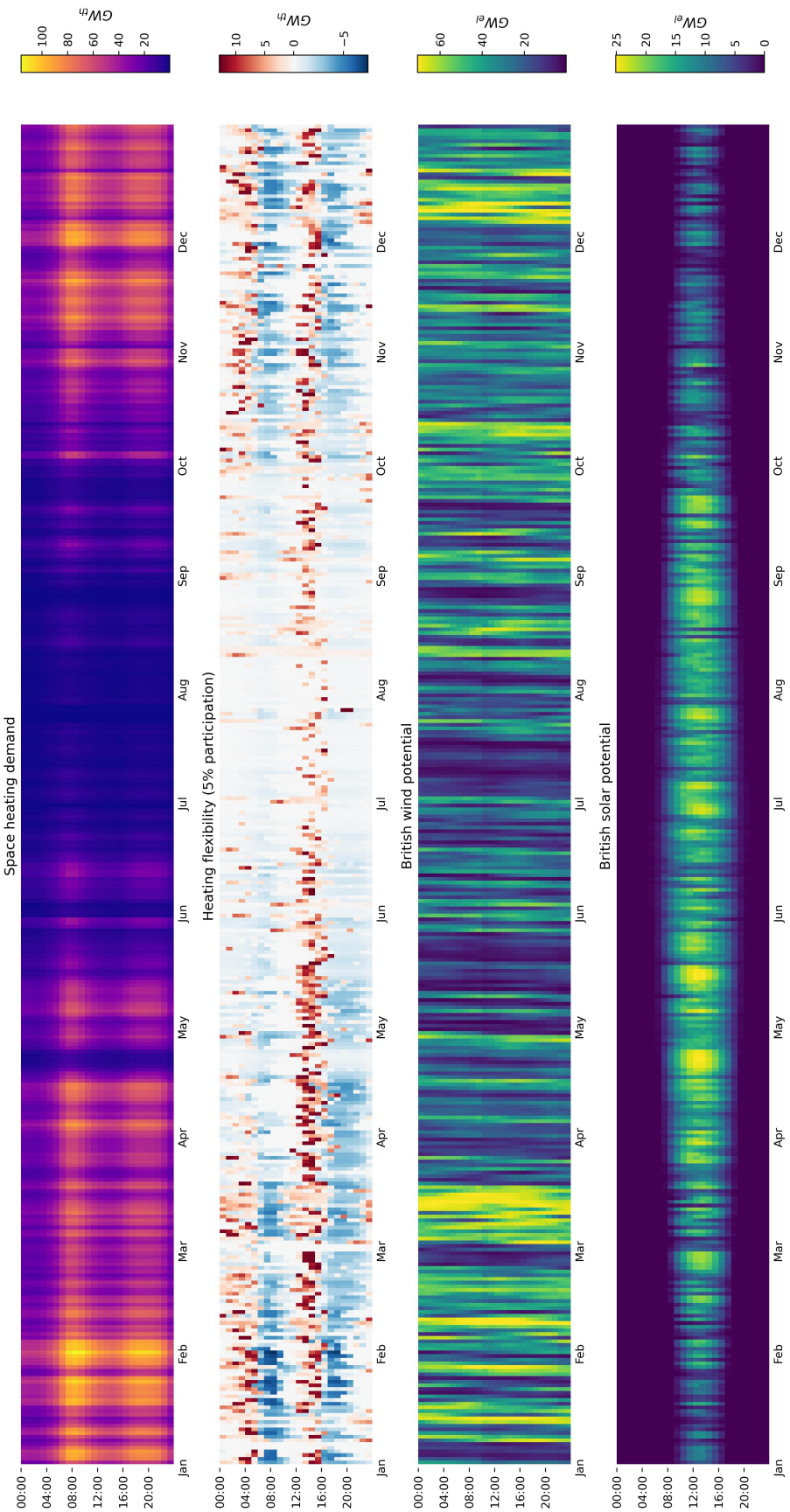

Figure 6.9: Heat map of hourly space heating demand, heating flexibility, British wind potential, and British solar potential under for the 2019 weather-year. Space heating demand displays the baseline demand without flexibility, and flexibility charging (shown in red) and discharging (shown in blue) are for 5% flexibility participation in the central scenario. Both quantities are shown in thermal GW. British wind and solar potential are shown including curtailed generation in electrical GW with capacities optimized for 5% flexibility participation in the central scenario.

The top panel of Figure 6.9 shows that residential space heating demand exhibits daily peaks in the morning from 06:00 to 10:00 as well as in the evening from 17:00 to 22:00. This daily pattern is driven by occupant behavior as people prepare for work or school in the morning and return home in the evening. As discussed in Section 3.3.1, peak heating demand occurs on 31 January, and space heating demand is much lower during warmer weather from mid-May to early October.

The second panel of Figure 6.9 illustrates that heating flexibility typically reduces peak heating demand by shifting heating load from peak demand times a few hours earlier. During the heating season, flexibility is used nearly every day to pre-heat homes between 00:00 and 06:00 and reduce heating demand during the morning peak. In some cases, heating flexibility pre-heats homes rapidly just before the morning peak, and sometimes heating flexibility pre-heats homes slowly from 22:00 to 06:00, probably depending on the overnight wind generation patterns. Heating flexibility also pre-heats homes between 12:00 and 16:00 to reduce heating load during the evening peak.

The frequent use of heating flexibility underlines the importance of flexibility automation. At 5% flexibility participation in the central scenario, each flexible household on average saves the bulk power system €82 annually and downshifts 1.2 MWh of electric heating demand throughout the year, so power system savings are €68/MWh of downshifted demand. For an example flexible event in which a household reduces electricity demand by 1 kW for an hour, they would earn just €0.068. These savings are much lower than the average price for live flexibility event payments of £4,559/MWh paid through the Demand Flexibility Service in winter 2022/23 [37], when many households manually adjusted their electricity demand. While these payments were high because this was a trial, they provide a sense of the payments that may be required to incentivize manual adjustment of electricity demand. Moreover, the timing of flexibility use overnight and in the middle of the workday are likely to make manual adjustment of heating schedules inconvenient for most residential consumers.

Comparing heating flexibility in the second panel of Figure 6.9 with British wind and solar potential in the third and fourth panels, respectively, reveals that overnight pre-heating is correlated with high wind potential periods, and afternoon pre-heating is correlated with high solar potential periods. For instance, in the last week of February when wind potential is low and solar potential is high, almost no overnight pre-heating is observed, and daytime pre-heating is concentrated in a few hours between 13:00 and 16:00. In contrast, when wind potential is high and solar potential is low from early to mid-March, flexibility shifts heating demand overnight. During the day, thermal energy storage charges at lower power for longer duration (between 10:00 and 16:00) since there is relatively little solar potential at midday.

Notably, there is still some space heating demand and heating flexibility in July and August, as the regressions in Equations 6.3 and 6.4 predict 0 kWh of space heating demand at 20.6 ℃. This mid-summer space heating is likely concentrated at a few households in colder areas of Britain with elderly or disabled people who maintain a higher home temperature. However, because this chapter models all heating demand and heating flexibility in each region in a combined manner, flexibility charging is limited by the capacity of all heat pumps at flexible households in the region. This modeling assumption explains why flexibility charging is so high at some times during the summer despite relatively low heating demand. The impact of this assumption is dicussed in Section 6.3.9.

Figure 6.10 displays the hourly heating flexibility use for the non-central scenarios. Comparing the top two panels of this figure for the low-carbon scenarios with the bottom two panels for the high-carbon scenarios reveals a stark difference in the use of heating flexibility under different carbon budgets. In the high-carbon scenarios, heating flexibility follows a strict twice-daily charging and discharging pattern throughout the heating season to reduce heating load at peak demand times. Heating flexibility often charges in 2 to 3 hours at higher power and discharges at higher power immediately afterwards. In contrast, heating flexibility charges and discharges over longer time periods at lower power in the low-carbon scenarios. In these scenarios, heating flexibility shifts away from twice-daily charging and

sometimes shifts demand between days. For instance, in the high-wind period in early to mid-March (shown in Figure 6.9), low-power flexibility charging can be observed during peak heating demand times from 16:00 to 20:00 and overnight. This difference suggests that heating flexibility shifts from peak-shaving in the high-carbon scenarios to longer-term shifting to balance lulls in wind and solar generation in the low-carbon scenarios. In low-carbon scenarios, renewable generation overcapacity reduces peak net demand at 0% flexibility participation (as shown in Figure 3.4), but total curtailment is much higher. Thus, heating flexibility is used to shift demand over longer time periods to better match renewable generation, rather than peak-shaving.

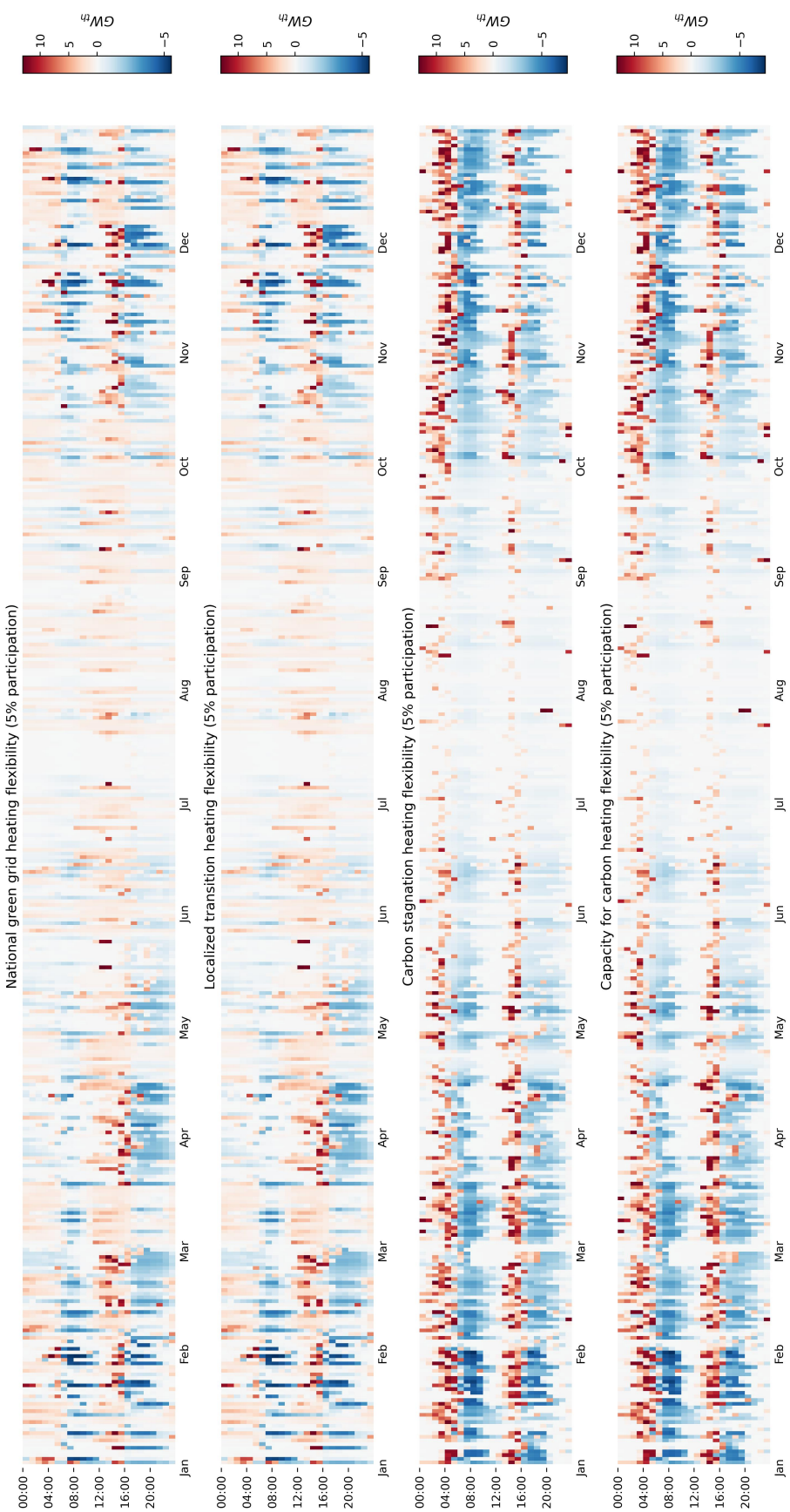

Figure 6.10: Heat map of hourly heating flexibility for the 2019 weather-year for the national green grid, localized transition, carbon stagnation, and capacity for carbon scenarios. Flexibility charging (shown in red) and discharging (shown in blue) are for 5% flexibility participation in all scenarios and are shown in thermal GW.

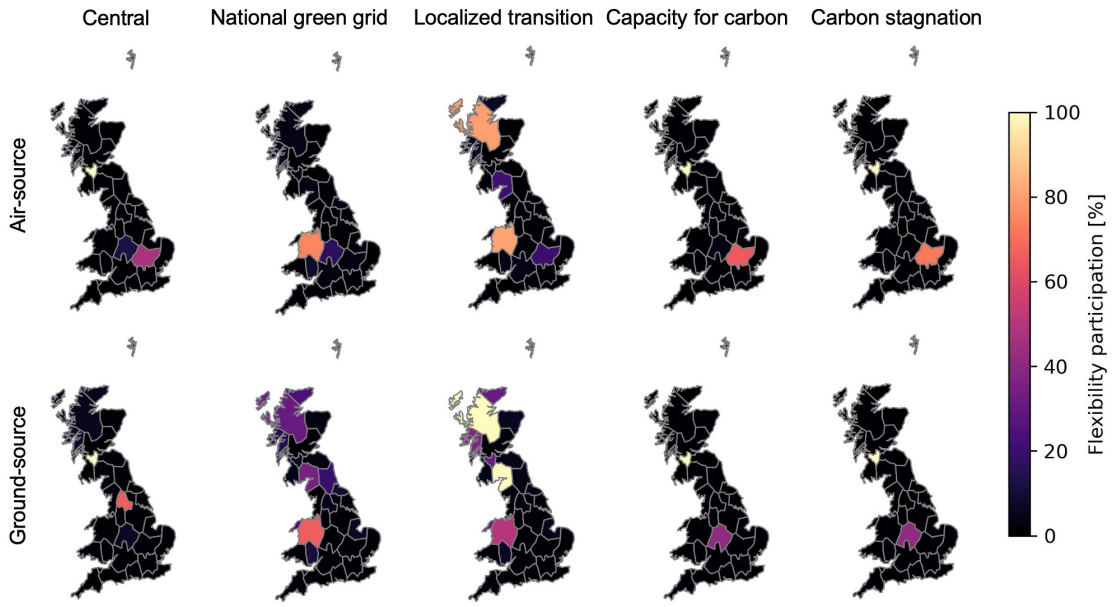

Figure 6.11: Cost-optimal regional flexibility participation at 5% flexibility participation.

6.3.5 Cost-optimal flexibility locations

Figure 6.11 shows the optimal regional participation in heating flexibility at 5% flexibility participation for each scenario. Note that in all scenarios, optimal flexibility is split between northern and southern Britain.

For the central scenario, the highest flexibility participation is in regions with moderate time constants that are adjacent to population centers, as shown in Figure 6.2. In the central scenario, flexibility participation is concentrated in the region south of Glasgow (Bus 19), the population center of Scotland and fifth most populous urban area in Britain, with 100% of households there participating in flexibility. GSHP heating flexibility participation is also high inland in central Britain in West Yorkshire (Bus 20). Because the greater London region (Bus 7) has one of the lowest heating flexibility time constants, there is significant ASHP flexibility participation in the region north of London (Bus 22), where the time constant is much higher, with 47% of households with ASHPs there heating flexibly.

As in the central scenario, flexibility participation is concentrated in a few areas near regional population centers with moderate time constants in the high-carbon

scenarios. One hundred percent of households with ASHPs and GSHPs in the region south of Glasgow (Bus 19) heat flexibly in both high-carbon scenarios. The majority of households with ASHPs are also flexible in region north of London (Bus 22): 65% of households there are flexible in the capacity for carbon scenario and 72% in the carbon stagnation scenario. Households with GSHPs have high flexibility participation in the West Midlands region (Bus 8), which has the third-largest urban area in Britain, with 41% of households there participating in flexibility in both high-carbon scenarios. Both Bus 22 and Bus 8 have higher thermal time constants than greater London (Bus 7), as shown in Figure 6.2, which explains why it is optimal to allocate flexibility to these regions rather than to London itself.

For low-carbon scenarios, optimal flexibility participation shifts to areas with highest thermal time constants and thus the lowest thermal storage losses.

In the national green grid scenario, flexibility participation is concentrated in northern Wales, the region with the highest thermal time constant in southern Britain, where the majority of the population and electricity load are located. Seventy-five percent of households with ASHPs and 66% of households with GSHPs heat flexibly in northern Wales (Bus 10). In the adjacent region of northwestern Wales (Bus 26), 23% of households with GSHPs also heat flexibly. The remaining flexibility participation from households with GSHPs is primarily in regions with the highest thermal time constants in northern and central Britain: 31% of households in northwestern Scotland (Bus 1) and 24% in northern Scotland (Bus 4) heat flexibly, along with 35% in the North West England and southwestern Scotland (Bus 25) and 19% in North East England (Bus 6).

In the localized transition scenario, regional flexibility participation is more widespread among regions with high thermal time constants due to transmission constraints. As in the national green grid scenario, flexibility participation is high in northern Wales (Bus 10), with 81% of households with ASHPs and 50% of those with GSHPs heating flexibly. There is also high flexibility participation on the northwestern coast of Scotland (Bus 1), with 80% of households with ASHPs and 100% of households with GSHPs heating flexibly. Heating flexibility participation is

high throughout Scotland for households with GSHPs: 100% of households in North West England & southwestern Scotland (Bus 25), 37% of households in western Scotland (Bus 27), 32% of households in the region south of Glasgow (Bus 19), and 31% of households in northern Scotland (Bus 4) heat flexibly. Households with ASHPs participate in heating flexibility in regions with relatively high time constants, with 34% of households in northwestern Wales (Bus 26) and 20% inNorth West England & southwestern Scotland (Bus 25) heating flexibly. Despite its moderate time constant value, 20% of households with ASHPs heated flexibly in the region north of London (Bus 22) because of its proximity to the demand center.

6.3.6 Spatial generation & storage capacity changes

To elucidate the relationship between optimal flexibility participation locations and regional changes in capacity investments, this section discusses the spatial changes in generation and storage capacity from 0% to 5% flexibility participation. Figure 6.12 displays the change in battery capacity for the central and low-carbon scenarios and open-cycle gas turbine capacity for the high-carbon scenarios. As discussed in Section 6.3.2, these technologies account for the largest cost reduction in their respective scenarios.

Across the central and low-carbon scenarios, battery capacity reductions due to flexibility tend to be in populous regions in southern and central Britain that are adjacent to regions with high flexibility participation.

In the central scenario, reductions in battery capacity are spatially concentrated in southern Britain in greater London (Bus 7), the West Midlands (Bus 8), and the region north of London (Bus 22). When comparing with the optimal regional flexibility locations in Figure 6.11, the largest battery capacity decreases occur in an area with high flexibility participation at Bus 22 or in adjacent regions, which suggests that flexibility reduces the need for local battery capacity. However, there is very little change in battery capacity in the region south of Glasgow (Bus 19) and only slight decreases in battery capacity in regions adjacent to West Yorkshire (Bus 20). This suggests that flexibility in these regions reduces the need for batteries in

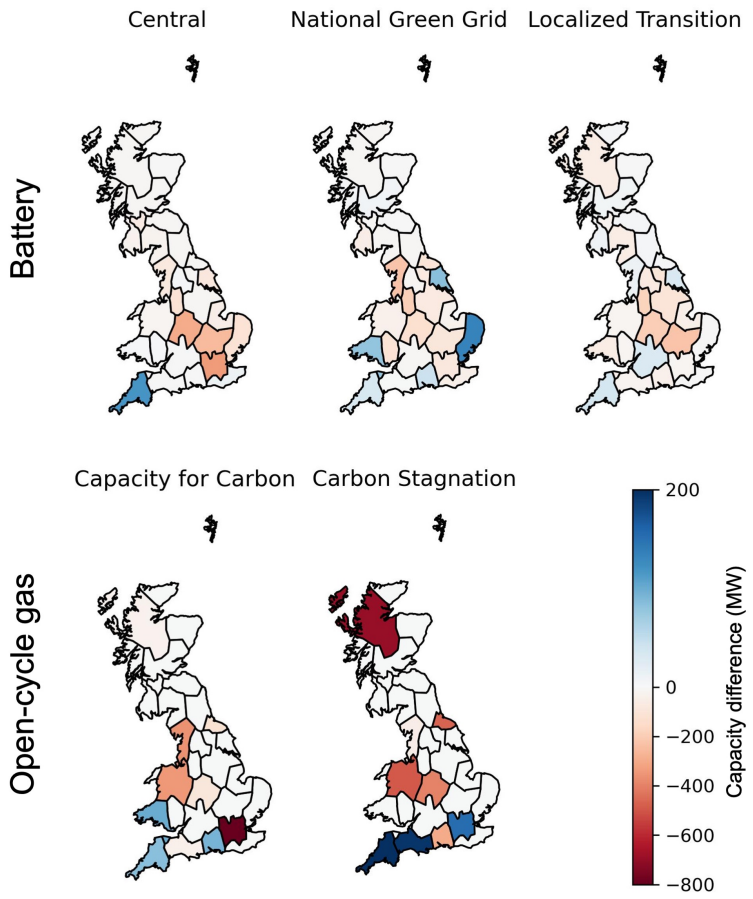

Figure 6.12: The largest technology differences for each scenario between 0% and 5% flexibility participation. The top row displays the regional changes in battery capacity for the central, national green grid, and localized transition scenarios. The bottom row displays the change in open-cycle gas capacity for the capacity for carbon and carbon stagnation scenarios.

southern Britain by relieving the transmission congestion between wind-rich regions in the north and the national demand center in the south.

In the national green grid scenario, battery capacity reductions are widespread across southern and central Britain, particularly in regions that are adjacent to regions with high flexibility participation. The largest battery capacity reductions are in the southern part of North West England (Bus 3) and greater Manchester region (Bus 23). Both regions are moderately populous and adjacent to regions with high flexibility participation, northern Wales (Bus 10) and North West England & southwestern Scotland (Bus 25). Indeed, almost every region adjacent to northern

Wales (Bus 10) has reduced battery capacity due to high flexibility participation there. There is also reduced battery capacity in the West Midlands (Bus 8), which had moderate flexibility participation, and adjacent regions, as well as greater London (Bus 7). These reductions suggest that heating flexibility in regions with high thermal time constants reduces the need for battery capacity in neighboring, more populous regions in the national green grid scenario.

In the localized transition scenario, battery capacity reductions are concentrated in populous regions in southern Britain that are adjacent to regions with high flexibility participation. The largest battery capacity reductions are in greater Manchester (Bus 23), the West Midlands (Bus 8), and the region north of London (Bus 22). Greater Manchester and the West Midlands are adjacent to northern Wales, which has high flexibility participation. The region north of London also has moderate flexibility participation. There are also smaller local reductions in battery capacity in regions in northern Britain with high flexibility participation, including northwestern Scotland (Bus 1), the region south of Glasgow (Bus 19), and North West England & southwestern Scotland (Bus 25). The concentrated nature of these battery capacity reductions suggests that flexibility can only reduce the need for battery capacity in adjacent regions due to flexibility constraints compared to the national green grid scenario.

In general, capacity changes in open-cycle gas generation in the high-carbon scenarios are concentrated at fewer buses than changes in battery capacity in the central and low-carbon scenarios. In the capacity for carbon scenario, the reduction in open-cycle gas capacity is concentrated in the load center in greater London (Bus 7). In contrast, heating flexibility reduces open-cycle gas capacity in a larger number of regions, excluding greater London, in the carbon stagnation scenario. This difference suggests that transmission constraints make open-cycle gas capacity reductions more widespread, as was observed with batteries in the localized transition scenario. Notably, the West Midlands (Bus 8) is the only region with high flexibility participation with a local reduction in open-cycle gas turbine capacity.

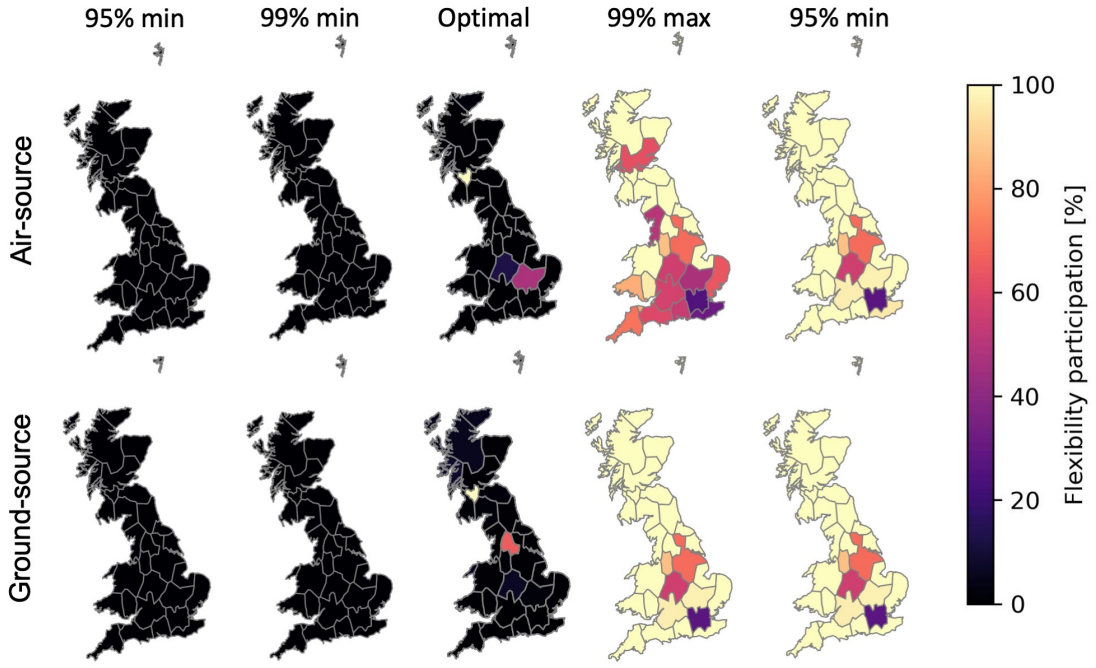

Figure 6.13: Minimum and maximum regional ASHP and GSHP flexibility participation for near-optimal flexibility allocation for the first 5% of flexibility participation in the central scenario. Note that the maps do not represent a single near-optimal spatial distribution of flexibility participation but instead show the minimum and maximum flexibility participation for each region where savings are at least 95% or 99% of the optimal flexibility savings. Optimal regional participation maps are included for reference.

This finding reveals the complex system effects of incorporating heating flexibility into the bulk power system, which leads to non-local changes in generation capacity.

6.3.7 Near-optimal regional flexibility participation bounds

In this section, the minimum and maximum near-optimal flexibility participation in each region are discussed. Figure 6.13 displays the minimum and maximum near-optimal ASHP and GSHP flexibility participation for the central scenario. Note that these maps do not represent a single near-optimal spatial distribution of flexibility participation but instead show the minimum and maximum flexibility participation for each region where savings are within 5% and 1% of the optimum.

In the central scenario, a wide range of regional flexibility participation achieves at least 95% of optimal flexibility savings. For both households with ASHPs and

GSHPs, the minimum flexibility participation is 0% across all regions. This means that at least 95% of optimal flexibility savings can be achieved without requiring that households with ASHPs or GSHPs in any particular region participate in heating flexibility. The maximum near-optimal participation for both households with ASHPs and GSHPs in all regions is either 100% or, in regions with more than 5% of British households, the share of households that makes up 5% of British households. For instance, the maximum flexibility participation in greater London (Bus 7) is 28% of households, which corresponds to 5% of British households. This result indicates that at least 95% of optimal flexibility savings can be achieved at 5% flexibility participation with high levels of participation from households with ASHPs or GSHPs in any region.

For households with ASHPs, a more limited range of regional flexibility participation can achieve at least 99% of optimal savings in the central scenario. The maximum flexibility participation is below 100% for many regions in southern Britain, as well as in central Scotland (Bus 2) and the southern part of North West England (Bus 3). Because of the relatively low thermal time constants in southern Britain and the southern part of North West England and low thermal capacity in central Scotland, achieving 99% of optimal savings with the first 5% of flexible households in these regions would require households in other regions to be flexible. In contrast, the minimum flexibility participation for households with ASHPs is 0% across all regions, so households from any particular region are not required to participate in heating flexibility to achieve 99% of optimal savings.

For households with GSHPs, the first 5% of flexible households can be located in any region to achieve 99% of optimal flexibility savings. As for 95% of optimal savings, the minimum flexibility participation is 0% across all regions, and the maximum in all regions is 100% or the share of households that makes up 5% of British households. This wider range of near-optimal regional flexibility participation for households with GSHPs compared to those with ASHPs is due to the flatter demand profile of GSHPs, shown in Figure 6.3. This demand profile of GSHPs limits the ability of households with GSHPs to pre-heat overnight to minimize

morning heating peaks, so households with GSHPs contribute less value from heating flexibility.

Figure 6.14 displays the minimum and maximum near-optimal ASHP flexibility participation for the non-central policy scenarios.

For households with ASHPs, regional participation to achieve at least 95% of optimal savings ranges from 0% to 100% or the share of households that makes up 5% of British ASHP households in all non-central scenarios. However, options for achieving at least 99% of optimal flexibility savings are more limited in all scenarios except the national green grid scenario. In the localized transition scenario, maximum regional flexibility participation is limited in greater London (Bus 7) and central Scotland (Bus 2), where thermal capacity values are low. These limits are explained by the need for longer flexibility duration in low-carbon scenarios, as shown in Figure 6.10, which require higher thermal capacity. In both high-carbon scenarios, flexibility participation is limited in regions in southern Britain due to lower thermal time constants and in central Scotland (Bus 2) due to lower thermal capacity. In the both high transmission expansion scenarios, increased transmission capacity reduces regional participation limits by allowing spatial balancing to substitute for temporal flexibility.

Figure 6.15 displays the minimum and maximum near-optimal GSHP flexibility participation for the non-central policy scenarios.

In all non-central scenarios, as in the central scenario, there is a wide range of near-optimal regional flexibility participation for GSHP households. For all non-central scenarios, the minimum near-optimal regional participation is 0% in all regions for both 95% and 99% of optimal flexibility savings. The maximum near-optimal regional flexibility participation is either 100% or the share of households that makes up 5% of British GSHP households. Across all scenarios, at least 99% of optimal flexibility savings can be achieved without requiring that any households with GSHPs in any region participate or if all households with GSHPs (up to 5% of British households) participate. This result reveals that structural uncertainty

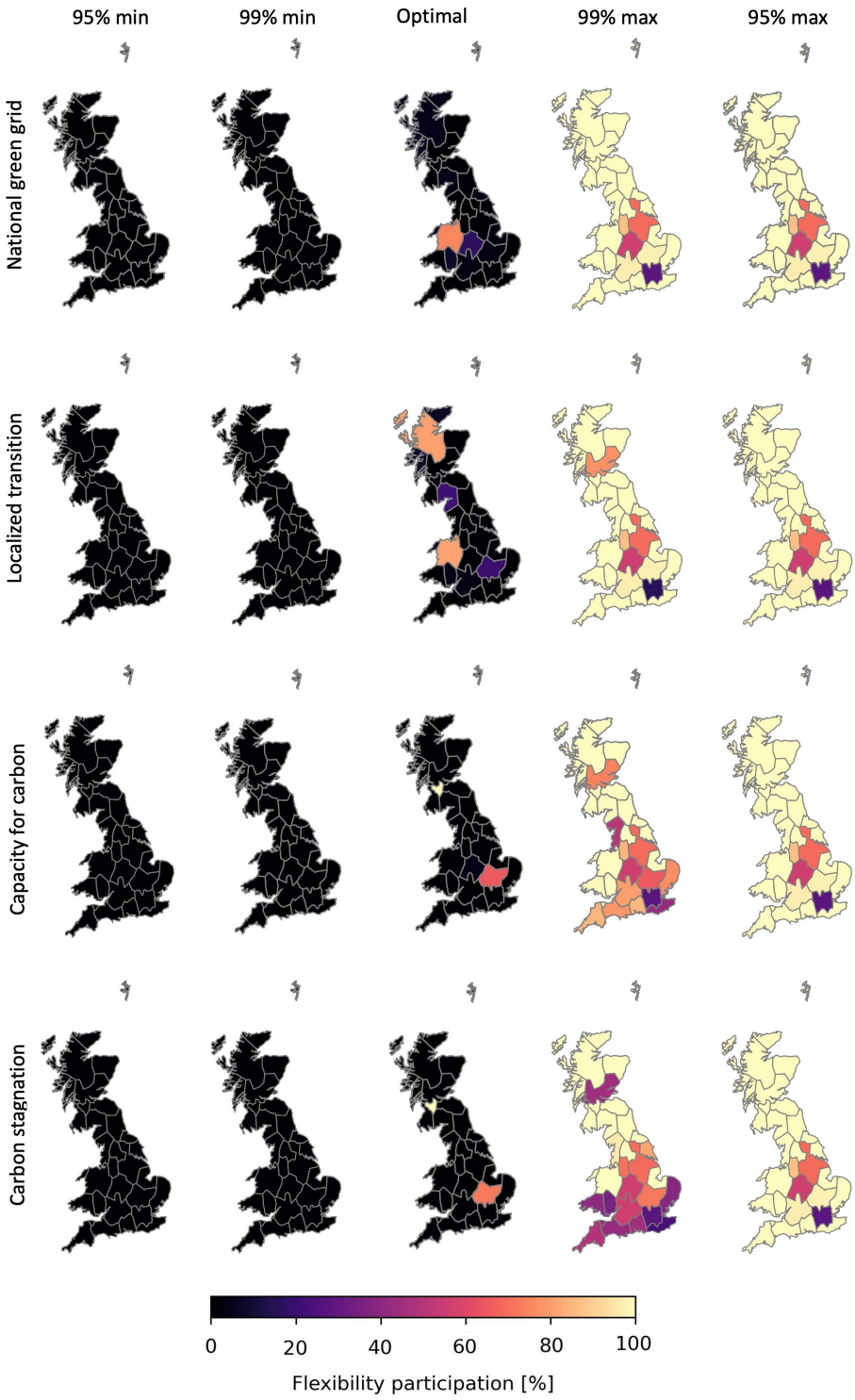

Figure 6.14: Minimum and maximum regional ASHP flexibility participation for near-optimal flexibility allocation for the first 5% of flexibility participation in the non-central scenarios. Note that the maps do not represent a single near-optimal spatial distribution of flexibility participation but instead show the minimum and maximum flexibility participation for each region where savings are at least 95% or 99% of the optimal flexibility savings. Optimal regional participation maps are included for reference.

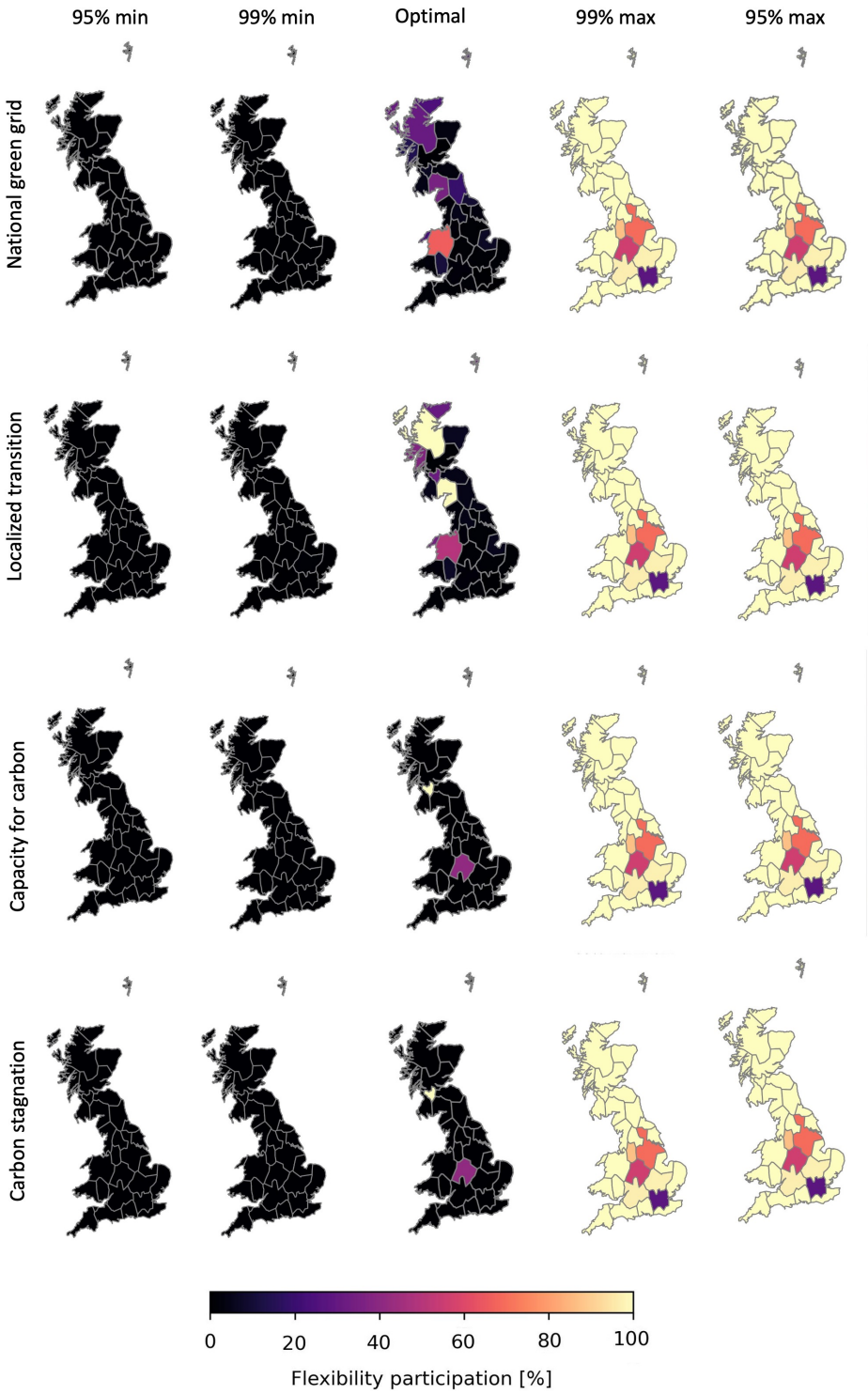

Figure 6.15: Minimum and maximum regional GSHP flexibility participation for near-optimal flexibility allocation for the first 5% of flexibility participation in the non-central scenarios. Note that the maps do not represent a single near-optimal spatial distribution of flexibility participation but instead show the minimum and maximum flexibility participation for each region where savings are at least 95% or 99% of the optimal flexibility savings. Optimal regional participation maps are included for reference.

about regional heating flexibility participation will not significantly impact bulk power system savings from GSHP flexibility.

Overall, the near-optimal flexibility results show that 95% of optimal flexibility savings can be achieved in all scenarios with regional flexibility participation ranging from 0% to 100% of households (or the share of households that makes up 5% of British households) for households with both ASHPs and GSHPs. For households with ASHPs, regional participation to achieve at least 99% of optimal savings is limited in regions with low thermal time constants and low thermal capacity. Thus, a broad range of regional flexibility participation can achieve near-optimal bulk power system savings.

6.3.8 Correlation between regional flexibility participation

While the previous section identifies a broad range of near-optimal flexibility participation rate, the flexibility capacity in different regions in the near-optimal solutions is interdependent. To capture this interdependence, Figure 6.16 shows the correlation between ASHP flexibility in each region and GSHP flexibility in each region for the near-optimal system designs in the central scenario. Note that buses are sorted by the latitude of the representative point for each region.

For ASHP flexibility, there are widespread slight negative correlations between near-optimal flexibility capacity at different buses because total flexibility participation is constrained. There is a positive correlation between flexibility at Bus 22 (north of London), which had high optimal ASHP flexibility participation, and many northern regions with relatively low population, including Bus 4 (northern Scotland), Bus 1 (northwestern Scotland), Bus 27 (western Scotland), Bus 19 (the region south of Glasgow), Bus 12 (southwestern Scotland), Bus 25 (North West England & southwestern Scotland), and Bus 26 (northwestern Wales). Flexibility capacity at Bus 22 is also negatively correlated with flexibility capacity in many other southern regions. This result indicates that flexibility in northern Britain complements flexibility in the region north of London in southern Britain. There are positive correlations between ASHP capacity in many northern regions with

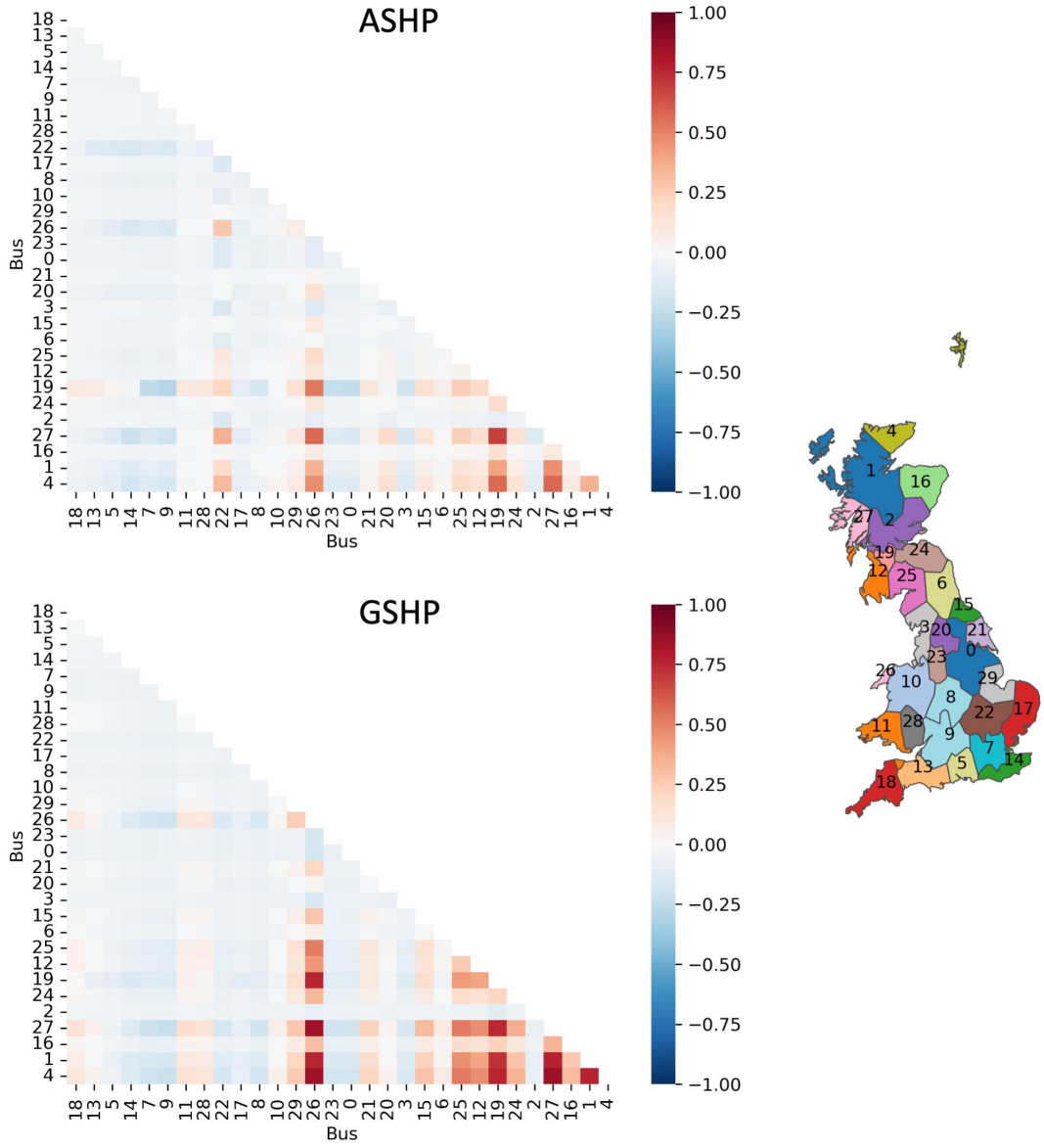

Figure 6.16: Correlation between ASHP flexibility capacity in each region and ASHP flexibility capacity in all other regions (top) and GSHP flexibility capacity in each region and GSHP flexibility capacity in all other regions (bottom) across all the near-optimal solutions for the central scenario. Buses are sorted by the latitude of the representative point for each region with southern buses on the top and left, and the regional map is inset on the right for reference.

low populations, as shown in the lower right corner of the correlation matrix. The clear exception to this is Bus 2 (central Scotland), which is the most populated region in northern Britain. Flexibility capacity in central Scotland substitutes for flexibility in other parts of northern Britain.

For GSHP flexibility, there are also widespread small, negative correlations between near-optimal flexibility in different regions because total flexibility participation is constrained. In contrast, there is much less complementarity between flexibility in the north and south of Britain as there was for ASHPs. Flexibility in the region south of Glasgow, which had very high optimal flexibility participation, is positively correlated with capacity at Bus 26 (northwest Wales), as well as many low-population regions in northern Scotland. West Yorkshire (Bus 20), the other region with high optimal flexibility participation, has a small positive correlation with flexibility in northwest Wales and no strong correlation with flexibility in other regions. As for ASHP flexibility, there are strong positive correlations among most low-population regions in northern Britain, with the exception of Bus 2 (central Scotland).

6.3.9 Limitations & uncertainty

The model introduced in this chapter assumes that the population-weighted average of building thermal time constants and thermal capacity are representative of the participants in heating flexibility in each region. In reality, flexibility participation within a region could be skewed towards fuel-poor households with inefficient homes or high-income households with large, efficient homes. This assumption introduces uncertainty about the value of heating flexibility to the bulk power system in different regions.

This model also assumes that all flexible households in a region have the same indoor air temperature at the same time. In reality, each region will have a distribution of household temperatures and thermal time constants. These distributions will create more variation in the operation of heating flexibility. Future

work could incorporate these distributions to understand how this variation will affect the results.

A uniform 3℃ temperature window is assumed for all households heating flexibly in this chapter. Households' temperature windows may vary based on the occupants' age, health, and personal preferences. Households with larger temperature windows would provide higher-value heating flexibility to the bulk power system, and households with smaller temperature windows would provide lower-value flexibility. This effect is expected to be particularly pronounced in low-carbon scenarios where flexibility is used for long-duration shifting.

Although Zeyen et al. [76] show that building retrofit provided larger energy systems savings than heating flexibility for a European energy system with 100% low-carbon heating, this chapter does not consider the impact of retrofit on reducing heating demand and increasing flexibility duration. This option was excluded because British retrofit programs have been extremely limited in the past decade and the CCC found that there are no clear policy plans to increase retrofit to level needed for net zero [205]. If retrofit policy significantly changes, future work could investigate the impact of heating flexibility in more efficient homes.

The capacity expansion model in this chapter does not include long-duration storage technologies. Therefore, the need for lithium-ion battery capacity to cover multi-week lulls in renewable potential is overestimated and thus total system costs are likely overestimated, particularly in the high-renewable scenarios. However, this modeling choice is unlikely to result in overestimated savings from building envelope flexibility because the competition between heating flexibility and lithium-ion batteries, flexible resources that operate on similar time scales, is captured.

This chapter demonstrates the value from heating flexibility in a typical year using a single weather-year of data. Heating flexibility value may be greater in years with extreme cold weather and may be lower in years with fewer cold periods. Future work could investigate the variable value of heating flexibility in different weather-years.

6.4 Key insights

This chapter investigates where residential heating flexibility offers the most value to future bulk power systems. Residential thermal energy storage potential is incorporated into a bulk power system planning model for varying heating flexibility participation rates. Both cost-optimal and near-optimal spatial distributions are explored for a range of policy scenarios. Based on the results of this modeling, the following insights can be gained:

Residential space heating flexibility can reduce power system costs to accommodate high heat pump adoption, especially under a low carbon budget. If all British households heat flexibly, the electricity system saves between €0.7 and €1.7 billion per year, with higher savings for power systems with a lower carbon budget. These savings amount to total cost reductions of 2.7% to 5.0%, with smaller percent changes in the low-carbon scenarios due to their higher total system costs. At 5% flexibility participation, the power system saves €67 to €88 annually per flexibly heated household in a typical weather-year. While systems savings exhibit diminishing returns for higher carbon budget scenarios, marginal per-household savings remain above €50 with all households heating flexibility for scenarios with a 99% carbon reduction from a 2019 baseline.

Heating flexibility reduces investment in dispatchable capacity by shifting heating load away from electricity demand peaks and improving the temporal match between renewable supply and electricity demand. In the high-carbon scenarios, flexibility reduces the need for open-cycle gas peaking generators by reducing the peak net demand, the difference between demand and renewable supply. In the central scenario, flexibility reduces the need for battery storage by reducing the peak net demand. Flexible heating is used to pre-heat the building envelope of homes overnight during high wind potential periods and in the afternoon during high solar potential periods. In the low-carbon scenarios, when renewable supply usually exceeds electricity demand in Britain, heating flexibility reduces the need for battery storage by decreasing peak net demand as well as temporally matching renewable supply and electricity demand.

From the bulk power system perspective, the most valuable locations for heating flexibility depend on the power system carbon budget. In the central and high-carbon scenarios, heating flexibility is most valuable in regions near load centers with moderate thermal energy storage losses, including the region north of London, the region south of Glasgow, West Yorkshire, and the West Midlands. As the role of heating flexibility shifts from peak shaving in high-carbon power systems to longer-term storage in low-carbon systems, thermal storage losses become more important than proximity to demand centers. This shift reflects how increasing the capacity of low marginal cost generation changes the dynamics of power systems from meeting demand peaks to matching supply and demand in time. In the low-carbon scenarios, the most valuable flexibility is widespread among the regions with the lowest thermal energy storage losses, such as northern and northwestern Wales and many regions in northern Britain.

The locations of dispatchable capacity reductions due to flexibility depend on the transmission expansion constraints that the power system faces. Across all scenarios, dispatchable capacity reductions tend to be concentrated in the national load center in southern Britain. In both low- and high-carbon scenarios with no transmission expansion, dispatchable capacity reductions are more widespread and primarily occur in regions with high flexibility participation or neighboring regions. In scenarios with liberal transmission expansion, dispatchable capacity reductions are concentrated in a few populous regions.

The near-optimal spatial distribution of heating flexibility reveal that a broad range of regional flexibility participation configurations can achieve at least 95% of the savings of cost-optimal regional flexibility participation. Across all scenarios, at least 95% of optimal flexibility savings can be achieved without requiring that any households with ASHPs or GSHPs in any region participate or if all households with ASHPs or GSHPs (up to 5% of British households) participate. For households with ASHPs, achieving at least 99% of optimal savings with 5% flexibility participation requires limiting participation in regions with low thermal time constants and low thermal capacity. Nonetheless, a broad range of regional flexibility participation can

achieve near-optimal flexibility savings. This finding reveals that residential heating flexibility programs can pursue other policy priorities, such as regional equity or rural participation, without forgoing significant bulk power system savings.

7 Conclusions

Contents

This thesis addresses the research question:

How will widespread residential heat pump adoption impact spatial planning of bulk power systems?

This research question is divided into two parts: the impact of heat pump demand and the impact of heating flexibility on bulk power systems planning.

7.1 Research conclusions

To understand the effect of residential heat pump demand on spatial planning of bulk power systems, two research sub-questions are considered. First, how will residential heat pump demand vary in space and time? Second, how will spatiotemporal differences in residential heat pump demand impact bulk power system planning?

To analyze the impact of residential heating flexibility on spatial planning of bulk power systems, a further two research sub-questions were considered. Third, what is the regional heating flexibility potential from residential building thermal inertia? Fourth, where will residential heat pump flexibility be most valuable to the bulk power system?

Due to the availability of high spatial resolution data, Britain was selected as a case study for this research. To explore a variety of policy futures, five policy scenarios are considered with different carbon budgets and transmission expansion limits. The **central** scenario includes a 90% carbon reduction from 2019 and a 15% transmission expansion limit. The low-carbon scenarios include 99% carbon reduction, with no transmission expansion in the **localized transition** scenario and 30% transmission expansion in the **national green grid** scenario. The high-carbon scenarios include 0% carbon reduction from 2019, with with no transmission expansion in the **carbon stagnation** scenario and 30% transmission expansion in the **capacity for carbon** scenario.

7.1.1 Heat pump demand

To analyze spatiotemporal variation in residential heat pump demand (*research sub-question 1*), a method for generating regional hourly heat pump demand profiles is introduced. Existing models of heat pump load that are computationally lightweight enough to be incorporated into power systems planning either do not accurately capture hourly heat pump usage patterns or do not represent sub-national heating demand variation. This model combines hourly heat pump demand profiles from field trials with local temperature data to produce regional hourly heating demand projections. The multi-regional demand projections were compared with a uniform national heating projection, which other projections commonly provide.

Both the multi-regional and uniform national projections agree that switching all British households to heat pumps will drastically change national electricity demand. For the warmer than average 2019 weather-year, heat pumps would nearly double

peak electricity demand from circa 50 GW (2019) to circa 90 GW[1]. Total electricity demand would also increase by 25% from 299 TWh to circa 375 TWh[2]. As the residential sector currently accounts for 30% of electricity demand in Britain, this increase would nearly double residential electricity demand. These large demand changes in a mild weather-year suggest that widespread heat pump adoption can create significant challenges for the power system.

While the multi-regional and national projections are in agreement about national-scale demand changes, using the multi-regional model reveals regional differences in heating demand. The uniform national heating projection overestimates annual heating demand in southern regions by up to 26% and underestimates in northern regions by up to 21%. At the time of peak national heating demand, the national demand projection overestimates electric heating demand in coastal areas by up to 51% and underestimates it inland by up to 20% compared to the multi-regional projections. These regional differences in heating demand will impact spatial infrastructure investment needs to accommodate widespread heat electrification.

To assess the impacts of these spatiotemporal differences in residential heat pump demand on bulk power systems planning (*research sub-question 2*), the multi-regional heat demand profiles are incorporated into a capacity expansion planning model. Existing bulk power systems planning studies have not explored the implications of spatiotemporal variation within a grid. The results of planning with multi-regional heating demand are compared to a system planned with uniform national demand to understand the effect of spatiotemporal demand variation on infrastructure requirements.

Spatiotemporal differences in residential heat pump demand changed the cost-optimal spatial distribution of storage and generation capacity. In the central scenario, the total absolute error in the spatial allocation of generation and storage when using uniform national heat pump demand is 2.6 GW (0.3% of British capacity). For the two low-carbon scenarios, these capacity differences increased to 15.0 GW

[1] 91 GW for the uniform national model, and 92 GW for the multi-regional model.
[2] 374 TWh for the uniform national model, and 376 TWh for the multi-regional model.

(1.1% of British capacity) in the localized transition scenario and 25.0 GW (2.1% of British capacity) in the national green grid scenario.

Some general trends in the spatial misallocation of storage and generation capacity can be identified for the central scenario. When planning with multi-regional demand compared to uniform national demand, optimal battery and solar capacity tend to be higher in regions with underestimated multi-regional heating demand to meet higher daily peaks. Optimal onshore wind capacity tends to be higher in regions with overestimated multi-regional heating demand to better match the seasonal pattern of heating demand.

Exceptions to these trends occur in southwestern Britain, which has some of the highest solar potential on the island. Although multi-regional heating demand is overestimated for the southeast coast of England, solar capacity increases there when planning with multi-regional demand. This generation capacity increase is accompanied by increased transmission capacity to London, which suggests that this extra generation capacity is used to meet increased peak heating demand in London due to higher land availability and better solar potential on the southeast coast. This exception underlines the importance of using high spatiotemporal resolution data for power system planning to account for these complex system interactions.

To evaluate the practical implications of these differences in the optimal spatial distribution of generation, storage, and transmission capacity, operational optimizations are performed to meet multi-regional heating demand for both the systems planned using multi-regional demand as well as uniform national demand. For all policy scenarios considered, bulk power systems planned to meet uniform national demand have insufficient transmission and generation capacity to meet multi-regional heating demand and thus require load shedding.

In the central scenario, meeting multi-regional demand requires 2.2 TWh of load shedding in Britain, which is 0.6% of annual electricity demand. In the central and low-carbon scenarios, British load shedding is concentrated in the greater London and greater Manchester areas, two inland population centers in southern Britain. These results suggest that planning a bulk power system using

uniform national heating demand projections would reduce reliability, particularly in some population centers.

7.1.2 Heating flexibility

To assess the potential energy capacity and duration of heating flexibility from building thermal inertia (*research sub-question 3*), a data-driven method to quantify heating flexibility potential at high spatial resolution using thermal time constants calculated from historical heating energy consumption, temperature, and building size is introduced. Existing methods for quantifying heating flexibility potential do not represent the geographic diversity of a national building stock with sufficiently low computational requirements to be incorporated into complex power system models. This novel approach is used to measure heating flexibility duration as the average number of heat-free hours in different regions at various outdoor temperatures. Due to data availability, flexibility duration can only be quantified for British households heated with gas, which account for 74% of households in England and Scotland and 72% of households in Wales [47, 48].

Thermal energy storage using building thermal inertia in the British housing stock can make a significant contribution to the flexibility requirements of the bulk power system. For a 3℃ temperature flexibility window, the total thermal energy storage in British homes is 500 GWh_{th}. Assuming a cold day COP value of 2.5, this thermal capacity is equivalent to 200 GWh of electricity storage. This result demonstrates that thermal energy storage using building thermal inertia has the potential to be a flexibility resource of the same magnitude as battery storage: the total battery storage requirements for 2050 are between 35 and 63 GWh for the net zero scenarios in the 2023 FES [150].

Several hours of heating flexibility potential were identified in the British housing stock, depending on the outdoor temperature. For 20^{th} percentile daily winter temperature from 2010 to 2022, the median regional comfortable heat-free hours is 5.9, with an interquartile range of 5.2 to 6.5 hours. However, for the lowest daily temperatures in this time period, heating flexibility duration nearly halved

to a median of 3.6 hours with an interquartile range of 3.2 to 4.0 hours. These flexibility durations would allow thermal energy storage to compete with typical 4-hour lithium-ion batteries.

Regional differences in flexibility capacity and duration reveal potential challenges for the heating transition. Due to smaller dwelling sizes in urban areas, heating flexibility energy capacity was lower in demand centers than in suburban and rural areas. In the greater London area, the combination of low energy capacity in central London and high heating losses in the surrounding areas resulted in low flexibility duration throughout the region. This low flexibility duration could pose a challenge for large-scale heat electrification, as this area also has limited land availability for renewable generation and will increasingly rely on electricity imports from surrounding regions.

To examine where residential heat pump flexibility will be most valuable to the bulk power system (*research sub-question 4*), high resolution flexibility potential estimates are incorporated into a capacity expansion planning model with varying shares of flexibility participation. Existing literature does not assess where demand-side flexibility will be most valuable within a bulk power system with high residential heating electrification. To account for the structural uncertainty about regional heating flexibility participation, spatial distributions of the first 5% of flexibility participation that achieve at least 95% of flexibility savings from optimal flexibility locations are also explored. Existing studies assessing near-optimal spatial planning of bulk power systems do not include structural uncertainty in demand-side flexibility participation.

Residential space heating flexibility can reduce bulk power systems costs from widespread heat pump adoption. Across all scenarios, if all British households heat flexibly, the bulk power system saves between €0.7 and €1.7 billion per year in total expenditures. Total savings across all scenarios range from 2.9% to 5.0% of total system expenditures. In scenarios with lower carbon budgets, the bulk power system saves more in absolute terms from flexibility but less in relative terms due

to higher total systems costs. At 5% flexibility participation, annual bulk power system savings per household range from €67 to €88 across scenarios.

Heating flexibility can reduce bulk power system investments required to meet heat pump demand. In the central and high-carbon scenarios, the first 60% of households heating flexibility reduce net peak demand by 11 to 12 GW. In the central scenario, this decrease reduces the need for battery storage investment by 10 GW at 60% flexibility participation. In the high-carbon scenarios, this decrease in net peak demand reduces open-cycle gas peaking capacity at 60% flexibility participation by 11 GW in the capacity for carbon scenario and 18 GW in the carbon stagnation scenario. In the low-carbon scenarios, renewable supply typically exceeds electricity demand, so heating flexibility reduces the need for battery storage by matching renewable supply and heating demand temporally. At 100% flexibility participation, heating flexibility reduces total net demand by 6 TWh as well as curtailment by 10 TWh in the national green grid scenario and by 21 TWh in the localized transition scenario. These decreases in net demand and curtailment reduce the need for battery capacity by 16 GW/96 GWh in the green grid scenario and 17 GW/102 GWh in the localized transition scenario.

The cost-optimal locations for heating flexibility from the bulk power system perspective depend on the power system carbon budget. In the high-carbon and central scenarios, heating flexibility is most valuable in regions near load centers with moderate thermal energy storage losses, including the region north of London, the region south of Glasgow, West Yorkshire, and the West Midlands. In low-carbon power systems, the role of flexibility shifts to longer-term storage, so thermal storage losses are more important than proximity to demand centers. The most valuable flexibility in low-carbon power systems is widespread among the regions with the lowest thermal energy storage losses, such as northern and northwestern Wales and many regions in northern Britain.

Transmission expansion limits determine where heating flexibility reduces dispatchable capacity. Across all scenarios, dispatchable capacity reductions tend to be concentrated in southern Britain, where most load is located. In both the

localized transition and carbon stagnation scenarios with no transmission expansion, dispatchable capacity reductions are widespread and primarily occur in regions with high flexibility participation or neighboring regions. In scenarios with liberal transmission expansion, dispatchable capacity reductions are concentrated in a few populous regions.

The near-optimal locations of heating flexibility reveal that a broad range of regional flexibility participation configurations can achieve at least 95% of the savings of cost-optimal regional flexibility participation. Across all scenarios, at least 95% of optimal flexibility savings can be achieved without requiring that any households with ASHPs or GSHPs in any region participate or if all households with ASHPs or GSHPs (up to 5% of British households) participate. For households with ASHPs, achieving at least 99% of optimal savings with 5% flexibility participation requires limiting participation in regions with low thermal time constants and low thermal capacity. Nonetheless, a broad range of regional flexibility participation can achieve near-optimal flexibility savings.

7.1.3 Concluding insights

Based on the British case study in this thesis, the following general conclusions about the impact of widespread residential heat pump adoption on spatial planning of bulk power systems can be drawn:

Residential heat pump demand and flexibility potential will vary spatially within an electricity grid. Using regional hourly heating demand projections reveals significant regional differences in total and peak heating demand due to local temperature differences in Britain, a medium-sized country with a temperate climate. These differences can be even more substantial in larger regions with more extreme climates. Heating flexibility potential varies based on regional housing stock. Lower heating flexibility duration in urban areas can pose a challenge for heat electrification as these regions have limited land available for renewable generation.

Spatial variation in demand and flexibility potential will impact the bulk power system planning for residential heat electrification. Notably, the effect of these

spatial differences depends on other parts of the power system. Local heating demand peaks in population centers can increase the need for generation capacity in adjacent regions with more land available for renewable expansion. In scenarios with liberal transmission expansion, heating flexibility reduces capacity investments near the demand center. In scenarios without transmission expansion, heating flexibility reduces capacity investments locally and in neighboring regions. These results demonstrate the importance of including these spatial heating differences in planning models that account for other sources of complexity.

This thesis reveals a data gap in understanding regional variation in heat pump demand and heating flexibility potential. Future heat pump trials should explore regional differences in heat pump operation to capture regional differences in occupancy patterns. High spatial resolution heating demand data for households off the gas grid is needed to provide a more complete picture of heating flexibility potential, especially in rural areas. These regionally-specific data will enhance bulk power system planning for heating electrification.

Understanding regional differences will allow power system planners to ensure that they can meet growing heating demand and strategically procure heating flexibility to maintain a cost-effective, reliable power system. While this thesis focused on the case study of Britain, the methods introduced can be applied across cold and temperate countries transitioning from fossil fuel-based heating systems to electric heat pumps.

7.2 Research contributions

The overall research contribution of this thesis is incorporating high spatial resolution heating data into bulk power system planning. The contributions of each research chapter are:

1. **Chapter 3: Hourly regional heat pump demand projections.** Introducing a high spatiotemporal resolution model of residential heat pump demand that combines a statistical model based on field trial data with high

spatiotemporal resolution weather data. This method represents heat pump demand profiles more accurately than existing degree-day models at higher spatial resolution than existing statistical models. The data requirements are limited to heat pump trial data and globally available reanalysis weather data.

2. **Chapter 4: Grid impact of spatiotemporal variation in heat pump demand.** Assessing the implications of spatiotemporal differences in heat pump demand on bulk power systems planning through the open-source model GeoHeat-GB [164].

3. **Chapter 5: High spatial resolution heating flexibility potential.** Introducing a method for quantifying national heating flexibility potential at high spatial resolution based on annual heating consumption data and historical temperature data. The software for this method is openly available as GeoHeatFlex [194]. This method is applied to characterize residential heating flexibility potential in Britain at high spatial resolution. This dataset is openly available on the Oxford Research Archive [195].

4. **Chapter 6: Optimal heating flexibility locations.** Assessing where residential heating flexibility offers the most value in optimal power system planning by incorporating high spatial resolution flexibility potential into bulk power systems planning.

5. **Chapter 6: Near-optimal heating flexibility locations.** Examining near-optimal system designs to accommodate residential heat pump demand to understand the impact of spatial participation in heating flexibility on system savings.

7.3 Future work

This thesis is subject to several limitations. The following areas are identified for future research to address these limitations:

1. **Increasing heating flexibility duration.** This thesis identified that heating flexibility would be most valuable in regions with the longest-duration flexibility for low-carbon power systems. Future work should investigate options to increase the duration of heating flexibility in individual homes through retrofit, incorporating phase-change materials into the building envelope, or other technologies. Future work should also address the impact of heating flexibility technologies with longer duration than building envelope thermal energy storage, such as district heating networks, on the bulk power system.

2. **Long-duration storage technologies.** This thesis considered only the proven storage technologies of lithium-ion batteries and pumped storage hydroelectricity. Future work should consider long-duration energy storage technologies such as hydrogen and zero carbon fuels, which have been identified as a critical part of low-carbon power systems [206, 207].

3. **Distribution network impact.** While this thesis focused on the bulk power system, the high spatial resolution data developed in this thesis can be applied to assess the impact of heating electrification on the distribution system.

4. **The effect of climate change on heating demand.** To demonstrate the impact of high spatial resolution data, this thesis considered only a single historical weather-year. Climate change is likely to decrease total heating demand in the UK [208], but changes in extreme cold events should also be considered as well as the impact of climate change on renewable generation.

5. **Commercial and industrial heat electrification.** Due to data availability, this thesis focused on heat electrification in the residential sector. Future work should include more detailed consideration of heat pump use in the commercial and industrial sectors.

6. **Simultaneous electrification of other sectors.** Residential heat electrification will interact with electrification of other sectors, including transport,

industrial, and commercial sectors. Bulk power systems planning should consider how these demand-side changes may interact.

Appendices

A

PyPSA-Eur Cost Projections

Capital costs are calculated based on investment costs and fixed operations and maintenance (FOM) costs. Investment costs are annualized using a 7% discount rate, with the exception of rooftop solar, for which a 4% discount rate is used [167], and the lifetime of the component, as shown in Tables A.1 and A.2. FOM costs are multiplied by the non-annualized investment cost to give annual costs. Total solar capital costs are calculated assuming 14% of solar is rooftop solar and the rest is utility-scale. For offshore wind, the investment cost of connection stations and connection to land shown in Tables A.2 and A.3 are added to the turbine investment costs. DC connections are assumed for wind turbines 30 km or more from the shore, and AC connections are assumed for wind turbines less and 30 km from shore. For HVDC links, capital cost is calculated using HVDC overhead costs shown in Table A.2 for the portion of the link on land and HVDC submarine costs for the portion of the link underwater.

Marginal costs are calculated as sum of variable operations and maintenance (VOM) costs plus fuel costs divided by thermal efficiency. These values are shown in Table A.4.

Table A.1: Generation and storage capital costs.

Technology	Investment (€/kW)	Source	FOM (%/a)	Source	Lifetime (a)	Source
Onshore wind	1035.56	[209]	1.22	[209]	30	[209]
Offshore wind	1523.55	[209]	2.32	[209]	30	[209]
Utility-scale solar	347.56	[209]	2.48	[209]	40	[209]
Rooftop solar	636.66	[209]	1.42	[209]	40	[209]
Pumped hydro storage	2208.16	[210]	1.00	[210]	80	[211]
Reservoir & dam	2208.16	[210]	1.00	[210]	80	[211]
Run-of-river hydro	3312.24	[210]	2.00	[210]	80	[211]
Open-cycle gas turbine	435.24	[209]	1.78	[209]	25	[209]
Nuclear	7940.45	[212]	1.40	[212]	40	[212]
Combined-cycle gas turbine	830.00	[209]	3.35	[209]	25	[209]
Coal	3845.51	[212]	1.60	[212]	40	[212]
Lignite	3845.51	[212]	1.60	[212]	40	[212]
Biomass	2209.00	[210]	4.53	[210]	30	[213]
Oil	343.00	[209]	2.46	[209]	25	[209]
Battery storage	142.00	[214]	-	-	25	[214]
Battery inverter	160.00	[214]	0.34	[214]	10	[214]

Table A.2: Transmission line costs.

Technology	Investment (€/MW/km)	FOM (%/a)	Lifetime (a)	Source
HVAC overhead	432.97	2.00	40	[187]
HVDC overhead	432.97	2.00	40	[187]
HVDC submarine	471.16	0.35	40	[215]
Offshore wind submarine AC connection	2685.00	-	-	[216]
Offshore wind underground AC connection	1342.00	-	-	[216]
Offshore wind submarine DC connection	2000.00	-	-	[217]
Offshore wind underground DC connection	1000.00	-	-	[218]

Table A.3: Transmission station costs.

Technology	Investment (€/MW/pair)	FOM (%/a)	Lifetime (a)	Source
HVDC inverter pair	162,364.8	2.00	40	[187]
Offshore wind DC station	400,000.0	0.00	25	[218]
Offshore wind AC station	250,000.0	0.00	25	[216]

Table A.4: Generation variable costs, efficiency, and emissions. A = assumption.

Technology	VOM (€/MWh)	Source	Fuel cost (€/MWh$_{th}$)	Source	Efficiency (p.u.)	Source	CO_2 intensity (tCO2/MWth)	Source
Onshore wind	1.35	[209]	-	-	1	A	0.00	A
Offshore wind	3.89	[209]	-	-	1	A	0.00	A
Solar	0.01	A	-	-	1	A	0.00	A
Pumped hydro storage	0.00	A	-	-	0.75	[210]	0.00	A
Reservoir & dam	0.00	A	-	-	0.90	[210]	0.00	A
Run-of-river hydro	0.00	A	-	-	0.90	[210]	0.00	A
Open-cycle gas turbine	4.5	[209]	20.1	[219]	0.41	[209]	0.20	[220]
Nuclear	3.5	[212]	2.6	[212]	0.33	[212]	0.00	A
Combined-cycle gas turbine	4.2	[209]	20.1	[219]	0.58	[209]	0.20	[220]
Coal	3.5	[212]	8.15	[219]	0.33	[212]	0.34	[220]
Lignite	3.5	[212]	2.9	[210]	0.33	[212]	0.41	[220]
Biomass	0.00	A	7	[221]	0.47	[210]	0.00	A
Oil	6.00	[209]	50	[222]	0.35	[209]	0.27	[220]

B

Disconnected grid regions

The hierarchical agglomerative clustering algorithm discussed in Section 4.2.2 based on hourly wind and solar potential results in disconnected parts of the same grid region. Figure B.1 shows that parts of Buses 2, 3, 11, 12, 14, 21, 24, and 28 are separated by bodies of water and not directly connected with transmission lines, even though they are modeled as such in Chapters 4 and 6.

To assess the impact of these disconnected regions on the results of this thesis, these clustered regions are manually re-connected. Small parts of each region across from the larger part of the region are attached to regions that the parts are connected to on land. Specifically, the following changes are made:

- The small, disconnected western part of Bus 2 is added to Bus 27
- The small, disconnected southern part of Bus 3 is added to Bus 10
- The small, disconnected southern part of Bus 11 is added to Bus 13
- The small, disconnected northwestern part of Bus 12 is added to Bus 27
- The small, disconnected northeastern part of Bus 14 is added to Bus 17
- The small, disconnected southern part of Bus 21 is added to Bus 0
- The small, disconnected northern part of Bus 24 is added to Bus 2

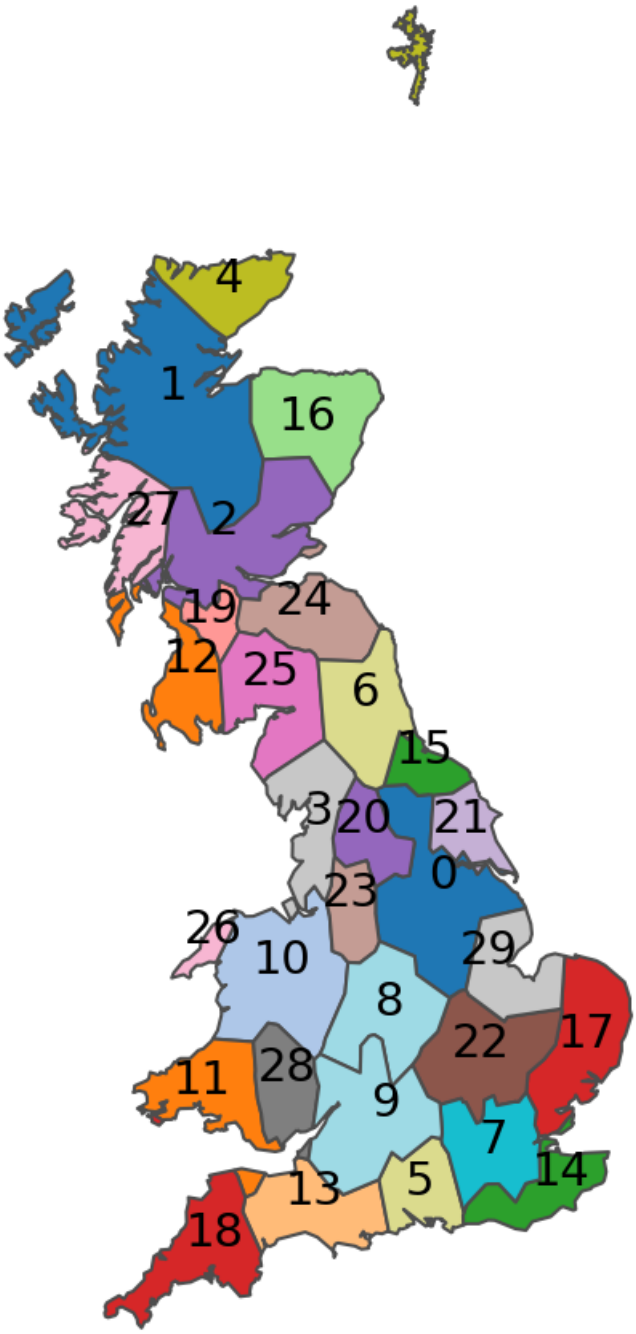

Figure B.1: Map of clustered grid regions with corresponding electric bus number.

Table B.1: Clustered vs. reconnected regional total thermal heating demand

Bus	Clustered regions (TWh)	Re-connected regions (TWh)	Difference (%)
0	28.37	28.45	-0.3
1	1.27	1.27	0.0
2	11.80	11.87	-0.6
3	12.33	10.89	13.2
9	17.72	17.92	-1.2
10	11.67	13.11	-11.0
11	4.15	4.07	2.1
12	2.00	1.99	0.6
13	6.72	6.82	-1.5
14	8.48	8.38	1.2
16	2.55	2.55	0.0
17	11.45	11.55	-0.9
18	5.01	4.99	0.3
21	2.85	2.77	3.1
24	5.57	5.47	1.8
27	0.23	0.29	-20.0
28	7.47	7.26	2.9

- The small, disconnected southern part of Bus 28 is added to Bus 9
- A small part of Scotland clustered to the Northern Irish grid region is added to the southern part of Bus 27

The resulting regions are shown in Figure B.2.

To assess the impact of re-connecting these clustered regions on heating demand, the multi-regional heating demand model introduced in Chapter 3 is applied to the re-connected regions. The resulting regional total thermal heating demand and peak electric heating demand for the re-connected regions is compared to that of the clustered regions in Tables B.1 and B.2, respectively. The percent difference between the re-connected regions and the clustered regions is shown, and only regions with differences in total and peak heating demand are included. While most of the regional differences between the clustered and re-connected regions are small, both total and peak heating demand are much higher for the re-connected Bus 27 and Bus 10 regions and much lower for the Bus 3 region. These larger differences arise because Birkenhead, part of the Liverpool City Region, is moved from Bus 3 to Bus 10, and because many parts from Bus 12, Bus 2, and Northern Ireland are added to the Bus 27 region, a region with relatively low heating demand.

To evaluate the impact of re-connecting these regions on bulk power system planning, the capacity expansion results to meet heating demand without flexibility

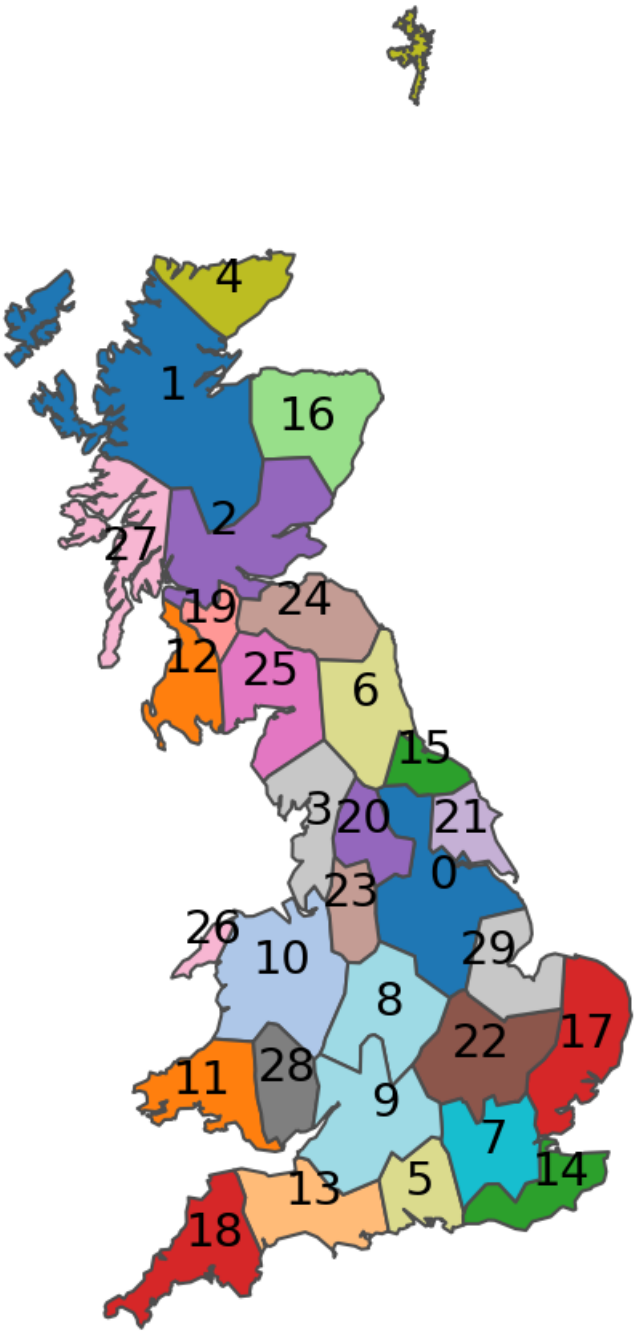

Figure B.2: Map of re-connected grid regions with corresponding electric bus number.

Table B.2: Clustered vs. reconnected regional peak electric heating demand

Bus	Clustered regions (MW)	Re-connected regions (MW)	Difference (%)
0	10,926	10,959	-0.3
1	431	432	0.0
2	4,227	4,252	-0.6
3	4,665	4,105	13.6
9	6,990	7,075	-1.2
10	4,465	5,024	-11.1
11	1,567	1,535	2.1
12	680	676	0.6
13	2,624	2,662	-1.4
14	3,447	3,407	1.2
16	819	819	0.0
17	4,497	4,537	-0.9
18	1,946	1,940	0.3
21	1,088	1,055	3.1
24	1,895	1,861	1.8
27	89	109	-18.0
28	2,868	2,784	3.0

for the clustered regions and the re-connected regions are compared under the central scenario. The capacity expansion results for the clustered regions are the multi-regional results presented in Chapter 4. Figure B.3 compares the generation, storage, and transmission capacity for a power system planned with the re-connected and clustered regions. Infrastructure with an oversized capacity when using the clustered regions compared to the reconnected regions is shown in red, and infrastructure with an undersized capacity is shown in blue. This figure has the same scale as Figure 4.6 to illustrate the magnitude of these differences compared to the difference between using the multi-regional and national heating demand models. Because all storage and generation capacity differences are less than 35 MW, the clustered regions are used in the analysis in this thesis with little impact on the results.

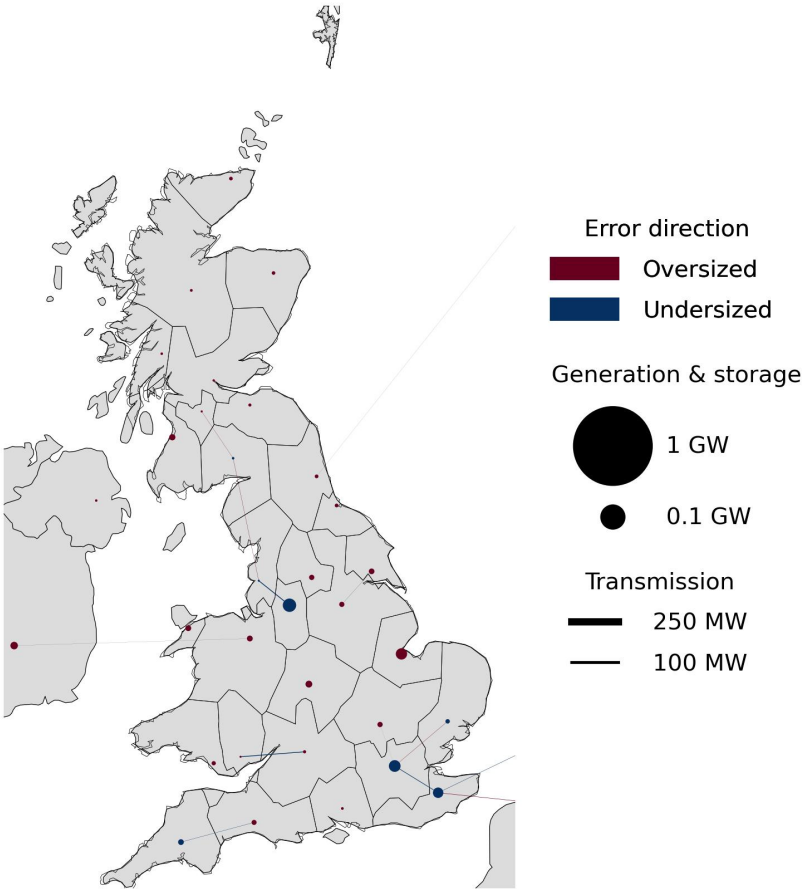

Figure B.3: Generation, storage, and transmission planned capacity differences for multi-regional heating demand for clustered vs. re-connected regions under the central scenario. Infrastructure with an oversized capacity when using clustered regions is shown in red, and infrastructure with an undersized capacity is shown in blue. The legend displays transmission and generation and storage capacities for scale.

Bibliography

[1] International Energy Agency, "The Future of Heat Pumps," International Energy Agency, Paris, Tech. Rep., Dec. 2022. [Online]. Available: https://www.iea.org/reports/the-future-of-heat-pumps

[2] UK Department for Business Energy & Industrial Strategy, "Heat and buildings strategy," Tech. Rep., Oct. 2021. [Online]. Available: https://www.gov.uk/government/publications/heat-and-buildings-strategy

[3] European Environment Agency, "Decarbonising heating and cooling — a climate imperative," Briefing, Feb. 2023. [Online]. Available: https://www.eea.europa.eu/publications/decarbonisation-heating-and-cooling/decarbonising-heating-and-cooling/

[4] International Energy Agency, "Net Zero by 2050 - A Roadmap for the Global Energy Sector," Paris, Tech. Rep., Oct. 2021. [Online]. Available: https://www.iea.org/reports/net-zero-by-2050

[5] UK Climate Change Committee, "The Sixth Carbon Budget: Buildings," Tech. Rep., 2020. [Online]. Available: https://www.theccc.org.uk/wp-content/uploads/2020/12/Sector-summary-Buildings.pdf

[6] F. Harvey and P. Cooke, "Gas boiler lobby trying to delay UK's heat pump plans, leak shows," *The Guardian*, Jul. 2023. [Online]. Available: https://www.theguardian.com/environment/2023/jul/20/gas-boiler-lobby-uk-heat-pump-plans-leak

[7] National Infrastructure Commission, "The Second National Infrastructure Assessment," Tech. Rep., Oct. 2023. [Online]. Available: https://nic.org.uk/studies-reports/national-infrastructure-assessment/second-nia/

[8] Energy Systems Catapult, "Electrification of Heat Demonstration Project: Interim Insights from Heat Pump Performance Data," Tech. Rep., 2023. [Online]. Available: https://doc.ukdataservice.ac.uk/doc/9050/mrdoc/pdf/9050_eoh_Interim_insights_from_heat_pump_performance_data.pdf

[9] J. Lizana, C. E. Halloran, S. Wheeler, N. Amghar, R. Renaldi, M. Killendahl, L. A. Perez-Maqueda, M. McCulloch, and R. Chacartegui, "A national data-based energy modelling to identify optimal heat storage capacity to support heating electrification," *Energy*, vol. 262, p. 125298, Jan. 2023. [Online]. Available: https://linkinghub.elsevier.com/retrieve/pii/S036054422202182X

[10] E. J. Wilson, P. Munankarmi, B. D. Less, J. L. Reyna, and S. Rothgeb, "Heat pumps for all? Distributions of the costs and benefits of residential air-source heat

pumps in the United States," *Joule*, p. S2542435124000497, Feb. 2024. [Online]. Available: https://linkinghub.elsevier.com/retrieve/pii/S2542435124000497

[11] MCS, "The MCS Data Dashboard," 2024. [Online]. Available: https://datadashboard.mcscertified.com/

[12] Air-Conditioning, Heating and Refrigeration Institute, "Central air conditioners and air-source heat pumps," 2024. [Online]. Available: https://www.ahrinet.org/analytics/statistics/historical-data/central-air-conditioners-and-air-source-heat-pumps

[13] I. Staffell and S. Pfenninger, "The increasing impact of weather on electricity supply and demand," *Energy*, vol. 145, pp. 65–78, Feb. 2018. [Online]. Available: https://linkinghub.elsevier.com/retrieve/pii/S0360544217320844

[14] Lazard, "Levelized Cost of Energy+," Tech. Rep., Apr. 2023. [Online]. Available: https://www.lazard.com/research-insights/2023-levelized-cost-of-energyplus/

[15] S. Watson, J. Crawley, K. Lomas, and R. Buswell, "Predicting future GB heat pump electricity demand," *Energy and Buildings*, vol. 286, p. 112917, May 2023. [Online]. Available: https://linkinghub.elsevier.com/retrieve/pii/S0378778823001470

[16] J. Langevin, C. B. Harris, A. Satre-Meloy, H. Chandra-Putra, A. Speake, E. Present, R. Adhikari, E. J. Wilson, and A. J. Satchwell, "US building energy efficiency and flexibility as an electric grid resource," *Joule*, vol. 5, no. 8, pp. 2102–2128, Aug. 2021. [Online]. Available: https://linkinghub.elsevier.com/retrieve/pii/S2542435121002907

[17] M. Waite and V. Modi, "Electricity Load Implications of Space Heating Decarbonization Pathways," *Joule*, vol. 4, no. 2, pp. 376–394, Feb. 2020. [Online]. Available: https://linkinghub.elsevier.com/retrieve/pii/S2542435119305781

[18] S. Bouzarovski and N. Simcock, "Spatializing energy justice," *Energy Policy*, vol. 107, pp. 640–648, Aug. 2017. [Online]. Available: https://linkinghub.elsevier.com/retrieve/pii/S0301421517302185

[19] V. Do, H. McBrien, N. M. Flores, A. J. Northrop, J. Schlegelmilch, M. V. Kiang, and J. A. Casey, "Spatiotemporal distribution of power outages with climate events and social vulnerability in the USA," *Nature Communications*, vol. 14, no. 1, p. 2470, Apr. 2023. [Online]. Available: https://www.nature.com/articles/s41467-023-38084-6

[20] A. Garvey, J. B. Norman, M. Büchs, and J. Barrett, "A "spatially just" transition? A critical review of regional equity in decarbonisation pathways," *Energy Research & Social Science*, vol. 88, p. 102630, Jun. 2022. [Online]. Available: https://linkinghub.elsevier.com/retrieve/pii/S2214629622001347

[21] L. Kotzur, L. Nolting, M. Hoffmann, T. Groß, A. Smolenko, J. Priesmann, H. Büsing, R. Beer, F. Kullmann, B. Singh, A. Praktiknjo, D. Stolten, and M. Robinius, "A modeler's guide to handle complexity in energy systems optimization," *Advances in Applied Energy*, vol. 4, p. 100063, Nov. 2021. [Online]. Available: https://linkinghub.elsevier.com/retrieve/pii/S266679242100055X

[22] National Grid ESO, "Regionalisation of the Future Energy Scenarios," Tech. Rep., Apr. 2022. [Online]. Available: https://www.nationalgrideso.com/future-energy/future-energy-scenarios/regionalisation-fes/explainer

[23] Element Energy, "Spatial GB Clean Heat Pathway Model: Model Overview," Cambridge, Tech. Rep., Mar. 2021. [Online]. Available: https://smarter.energynetworks.org/projects/nia_nggt0154

[24] National Grid ESO, "Regional Breakdown of 2021 FES: Demand (Active Power)." [Online]. Available: https://www.nationalgrideso.com/data-portal/regional-breakdown-fes-data-electricity/regional_breakdown_of_2021_fes_demand_active_power

[25] C. F. Heuberger, P. K. Bains, and N. Mac Dowell, "The EV-olution of the power system: A spatio-temporal optimisation model to investigate the impact of electric vehicle deployment," *Applied Energy*, vol. 257, no. October 2019, p. 113715, 2020. [Online]. Available: https://doi.org/10.1016/j.apenergy.2019.113715

[26] C. Crozier, T. Morstyn, and M. McCulloch, "The opportunity for smart charging to mitigate the impact of electric vehicles on transmission and distribution systems," *Applied Energy*, vol. 268, p. 114973, Jun. 2020. [Online]. Available: https://linkinghub.elsevier.com/retrieve/pii/S0306261920304852

[27] I. Staffell, S. Pfenninger, and N. Johnson, "A global model of hourly space heating and cooling demand at multiple spatial scales," *Nature Energy*, Sep. 2023. [Online]. Available: https://www.nature.com/articles/s41560-023-01341-5

[28] ASHRAE, "ANSI/ASHRAE Standard 169-2021: Climatic Data for Building Design Standards," 2021. [Online]. Available: https://webstore.ansi.org/standards/ashrae/ansiashrae1692021

[29] World Health Organization, "WHO Housing and health guidelines," Tech. Rep., Nov. 2018. [Online]. Available: https://www.who.int/publications/i/item/9789241550376

[30] J. L. Ramirez-Mendiola and J. Torriti, "Energy demand flexibility and the rhythms of everyday life," 2022. [Online]. Available: https://energy-demand-flexibility.co.uk/

[31] Office for National Statistics, "Age of the property is the biggest single factor in energy efficiency of homes," Tech. Rep., Jan. 2022. [Online]. Available: https://www.ons.gov.uk/peoplepopulationandcommunity/housing/articles/ageofthepropertyisthebiggestsinglefactorinenergyefficiencyofhomes/2021-11-01

[32] UK Department for Energy Security & Net Zero, "National Energy Efficiency Data-Framework (NEED): Summary of Analysis, Great Britain, 2024," Tech. Rep., Jun. 2024. [Online]. Available: https://www.gov.uk/government/statistics/national-energy-efficiency-data-framework-need-report-summary-of-analysis-2024

[33] UK Ministry of Housing, Communities & Local Government, "English Housing Survey 2018-19: Size of English homes," Tech. Rep. [Online]. Available: https://assets.publishing.service.gov.uk/media/5f047a01d3bf7f2be8350262/Size_of_English_Homes_Fact_Sheet_EHS_2018.pdf

[34] LCP Delta, "BEIS Electrification of Heat Demonstration Project: Home Surveys and Install Report," Tech. Rep., Dec. 2022. [Online]. Available: https://es.catapult.org.uk/report/electrification-of-heat-home-surveys-and-install-report/

[35] Energy Systems Catapult, "Smart Systems and Heat programme: Phase 2 Summary of key insights and emerging capabilities," Tech. Rep., Sep. 2021. [Online]. Available: https://es.catapult.org.uk/report/smart-energy-services-for-low-carbon-heat/

[36] National Grid, "EQUINOX (Equitable Novel Flexibility Exchange)," Tech. Rep., Nov. 2023. [Online]. Available: https://www.nationalgrid.co.uk/innovation/projects/equinox-equitable-novel-flexibility-exchange

[37] National Grid ESO, "Demand Flexibility Service: Winter 2022/23 review," Tech. Rep., Aug. 2023. [Online]. Available: https://www.nationalgrideso.com/document/287006/download

[38] Centre for Net Zero, "Insights from the UK's Largest Consumer Energy Flexibility Trial: The Demand Flexibility Service and Octopus Energy Saving Sessions," Tech. Rep., May 2023. [Online]. Available: https://www.centrefornetzero.org/wp-content/uploads/2023/05/Centre-for-Net-Zero-Insights-from-the-UKs-largest-consumer-energy-flexibility-trial-May-2023.pdf

[39] UK Department for Energy Security & Net Zero, "Digest of UK Energy Statistics (DUKES) 2023 Chapter 5: electricity," Tech. Rep., Jul. 2023. [Online]. Available: https://www.gov.uk/government/statistics/electricity-chapter-5-digest-of-united-kingdom-energy-statistics-dukes

[40] "Electricity Act 1989." [Online]. Available: https://www.legislation.gov.uk/ukpga/1989/29/contents/enacted

[41] National Grid ESO, "What we do." [Online]. Available: https://www.nationalgrideso.com/what-we-do

[42] National Grid, "National Grid Electricity Transmission." [Online]. Available: https://www.nationalgrid.com/electricity-transmission/

[43] SP Energy Networks, "Our Transmission Network." [Online]. Available: https://www.spenergynetworks.co.uk/pages/our_transmission_network.aspx

[44] SSEN Transmission, "What we do." [Online]. Available: https://www.ssen-transmission.co.uk/about-us/what-we-do-overview/

[45] UK Department for Energy Security & Net Zero, "Digest of UK Energy Statistics (DUKES) Table 5.10.A Plant loads, demand and efficiency of major power producers," Jul. 2023. [Online]. Available: https://www.gov.uk/government/statistics/electricity-chapter-5-digest-of-united-kingdom-energy-statistics-dukes

[46] UK Department for Business Energy & Industrial Strategy, "Energy Consumption in the UK (ECUK) 2022: End use data tables," 2022. [Online]. Available: https://www.gov.uk/government/statistics/energy-consumption-in-the-uk-2022

[47] Office for National Statistics, "Census 2021 Dataset TS046: Central heating," Mar. 2023. [Online]. Available: https://www.ons.gov.uk/datasets/TS046/editions/2021/versions/4/f

[48] National Records of Scotland, "2011 Census Table QS415SC - Central heating," 2014. [Online]. Available: https://www.scotlandscensus.gov.uk/search-the-census#/search-by

[49] M. Kendon, M. McCarthy, S. Jevrejeva, A. Matthews, J. Williams, T. Sparks, and F. West, "State of the UK Climate 2022," *International Journal of Climatology*, vol. 43, no. S1, pp. 1–83, Jul. 2023. [Online]. Available: https://rmets.onlinelibrary.wiley.com/doi/10.1002/joc.8167

[50] BRE Trust, "Housing Conditions in the UK," Tech. Rep., Feb. 2020. [Online]. Available: https://www.bretrust.org.uk/knowledgehub/wellbeing/housing-conditions-in-the-uk/

[51] Department for Levelling Up, Housing and Communities, "English Housing Survey 2022 to 2023: headline report," Tech. Rep., Dec. 2023. [Online]. Available: https://www.gov.uk/government/collections/english-housing-survey-2022-to-2023-headline-report

[52] tado, "UK homes losing heat up to three times faster than European neighbours," Feb. 2020. [Online]. Available: https://www.tado.com/gb-en/press/uk-homes-losing-heat-up-to-three-times-faster-than-european-neighbours

[53] N. Eyre and P. Baruah, "Uncertainties in future energy demand in UK residential heating," *Energy Policy*, vol. 87, pp. 641–653, 2015. [Online]. Available: http://dx.doi.org/10.1016/j.enpol.2014.12.030

[54] National Grid ESO, "Local Authority Level Spatial Heat Model Outputs (FES)," Mar. 2022. [Online]. Available: https://www.nationalgrideso.com/data-portal/local-authority-level-spatial-heat-model-outputs-fes

[55] E. Trutnevyte, "Does cost optimization approximate the real-world energy transition?" *Energy*, vol. 106, pp. 182–193, Jul. 2016. [Online]. Available: https://linkinghub.elsevier.com/retrieve/pii/S0360544216302821

[56] J. DeCarolis, H. Daly, P. Dodds, I. Keppo, F. Li, W. McDowall, S. Pye, N. Strachan, E. Trutnevyte, W. Usher, M. Winning, S. Yeh, and M. Zeyringer, "Formalizing best practice for energy system optimization modelling," *Applied Energy*, vol. 194, pp. 184–198, May 2017. [Online]. Available: https://linkinghub.elsevier.com/retrieve/pii/S0306261917302192

[57] C. E. Halloran, F. Fele, and M. D. McCulloch, "Impact of spatiotemporal heterogeneity in heat pump loads on generation and storage requirements," in *2022 IEEE Power & Energy Society General Meeting (PESGM)*. Denver, CO, USA: IEEE, Jul. 2022, pp. 1–5. [Online]. Available: https://ieeexplore.ieee.org/document/9916794/

[58] C. Halloran, J. Lizana, F. Fele, and M. McCulloch, "Data-based, high spatiotemporal resolution heat pump demand for power system planning," *Applied Energy*, vol. 355, p. 122331, 2024. [Online]. Available: https://www.sciencedirect.com/science/article/pii/S0306261923016951

[59] C. Halloran, J. Lizana, and M. McCulloch, "Quantifying national space heating flexibility potential at high spatial resolution with heating consumption data," 2024. [Online]. Available: https://arxiv.org/abs/2405.10450

[60] A. Bloess, W.-P. Schill, and A. Zerrahn, "Power-to-heat for renewable energy integration: A review of technologies, modeling approaches, and flexibility potentials," *Applied Energy*, vol. 212, pp. 1611–1626, Feb. 2018. [Online]. Available: https://linkinghub.elsevier.com/retrieve/pii/S0306261917317889

[61] National Grid ESO, "FES Modelling Methods 2021," Tech. Rep., Aug. 2021. [Online]. Available: https://www.nationalgrideso.com/document/199916/download

[62] I. G. Wilson, A. J. Rennie, Y. Ding, P. C. Eames, P. J. Hall, and N. J. Kelly, "Historical daily gas and electrical energy flows through Great Britain's transmission networks and the decarbonisation of domestic heat," *Energy Policy*, vol. 61, pp. 301–305, Oct. 2013. [Online]. Available: https://linkinghub.elsevier.com/retrieve/pii/S0301421513004655

[63] S. Tassou, C. Marquand, and D. Wilson, "Energy and economic comparisons of domestic heat pumps and conventional heating systems in the British climate," *Applied Energy*, vol. 24, no. 2, pp. 127–138, Jan. 1986. [Online]. Available: https://linkinghub.elsevier.com/retrieve/pii/0306261986900656

[64] F. Lombardi, M. V. Rocco, L. Belussi, L. Danza, C. Magni, and E. Colombo, "Weather-induced variability of country-scale space heating demand under different refurbishment scenarios for residential buildings," *Energy*, vol. 239, p. 122152, Jan. 2022. [Online]. Available: https://linkinghub.elsevier.com/retrieve/pii/S0360544221024002

[65] P. R. White, J. D. Rhodes, E. J. Wilson, and M. E. Webber, "Quantifying the impact of residential space heating electrification on the Texas electric grid," *Applied Energy*, vol. 298, no. January, p. 117113, 2021. [Online]. Available: https://doi.org/10.1016/j.apenergy.2021.117113

[66] C. Protopapadaki and D. Saelens, "Heat pump and PV impact on residential low-voltage distribution grids as a function of building and district properties," *Applied Energy*, vol. 192, pp. 268–281, Apr. 2017. [Online]. Available: https://linkinghub.elsevier.com/retrieve/pii/S0306261916317329

[67] BRE, "The Government's Standard Assessment Procedure for Energy Rating of Dwellings: 2012 edition," Tech. Rep., 2014. [Online]. Available: https://files.bregroup.com/SAP/SAP-2012_9-92.pdf

[68] E. J. H. Wilson, A. Parker, A. Fontanini, E. Present, J. L. Reyna, R. Adhikari, C. Bianchi, C. CaraDonna, M. Dahlhausen, J. Kim, A. LeBar, L. Liu, M. Praprost, L. Zhang, P. DeWitt, N. Merket, A. Speake, T. Hong, H. Li, N. M. Frick, Z. Wang,

A. Blair, H. Horsey, D. Roberts, K. Trenbath, O. Adekanye, E. Bonnema, R. El Kontar, J. Gonzalez, S. Horowitz, D. Jones, R. T. Muehleisen, S. Platthotam, M. Reynolds, J. Robertson, K. Sayers, and Q. Li, "End-Use Load Profiles for the U.S. Building Stock: Methodology and Results of Model Calibration, Validation, and Uncertainty Quantification," Mar. 2022. [Online]. Available: https://www.osti.gov/biblio/1854582

[69] S. Heinen, W. Turner, L. Cradden, F. McDermott, and M. O'Malley, "Electrification of residential space heating considering coincidental weather events and building thermal inertia: A system-wide planning analysis," *Energy*, vol. 127, pp. 136–154, 2017. [Online]. Available: http://dx.doi.org/10.1016/j.energy.2017.03.102

[70] S. Clegg and P. Mancarella, "Integrated electricity-heat-gas modelling and assessment, with applications to the Great Britain system. Part I: High-resolution spatial and temporal heat demand modelling," *Energy*, vol. 184, pp. 180–190, 2019. [Online]. Available: https://doi.org/10.1016/j.energy.2018.02.079

[71] R. Gelaro, W. McCarty, M. J. Suárez, R. Todling, A. Molod, L. Takacs, C. A. Randles, A. Darmenov, M. G. Bosilovich, R. Reichle, K. Wargan, L. Coy, R. Cullather, C. Draper, S. Akella, V. Buchard, A. Conaty, A. M. Da Silva, W. Gu, G.-K. Kim, R. Koster, R. Lucchesi, D. Merkova, J. E. Nielsen, G. Partyka, S. Pawson, W. Putman, M. Rienecker, S. D. Schubert, M. Sienkiewicz, and B. Zhao, "The Modern-Era Retrospective Analysis for Research and Applications, Version 2 (MERRA-2)," *Journal of Climate*, vol. 30, no. 14, pp. 5419–5454, Jul. 2017. [Online]. Available: https://journals.ametsoc.org/doi/10.1175/JCLI-D-16-0758.1

[72] Copernicus European Centre for Medium-Range Weather Forecasts, "ERA5 dataset," 2022. [Online]. Available: https://www.ecmwf.int/en/forecasts/dataset/ecmwf-reanalysis-v5

[73] UK Department for Energy Security & Net Zero, "LSOA domestic gas 2010 to 2021," Dec. 2022. [Online]. Available: https://www.gov.uk/government/statistics/lower-and-middle-super-output-areas-gas-consumption

[74] M. Hellwig, "Entwicklung und Anwendung parametrisierter Standard-Lastprofile," Ph.D. dissertation, Technischen Universität München, May 2003. [Online]. Available: https://mediatum.ub.tum.de/doc/601557/601557.pdf

[75] O. Ruhnau, L. Hirth, and A. Praktiknjo, "Time series of heat demand and heat pump efficiency for energy system modeling," *Scientific Data*, vol. 6, no. 1, pp. 1–10, 2019. [Online]. Available: http://dx.doi.org/10.1038/s41597-019-0199-y

[76] E. Zeyen, V. Hagenmeyer, and T. Brown, "Mitigating heat demand peaks in buildings in a highly renewable European energy system," *Energy*, vol. 231, p. 120784, Sep. 2021. [Online]. Available: https://linkinghub.elsevier.com/retrieve/pii/S036054422101032X

[77] S. D. Watson, K. J. Lomas, and R. A. Buswell, "How will heat pumps alter national half-hourly heat demands? Empirical modelling based on GB field trials,"

Energy and Buildings, vol. 238, p. 110777, 2021. [Online]. Available: https://doi.org/10.1016/j.enbuild.2021.110777

[78] S. Eggimann, J. W. Hall, and N. Eyre, "A high-resolution spatio-temporal energy demand simulation to explore the potential of heating demand side management with large-scale heat pump diffusion," *Applied Energy*, vol. 236, no. June 2018, pp. 997–1010, 2019. [Online]. Available: https://doi.org/10.1016/j.apenergy.2018.12.052

[79] J. Love, A. Z. Smith, S. Watson, E. Oikonomou, A. Summerfield, C. Gleeson, P. Biddulph, L. F. Chiu, J. Wingfield, C. Martin, A. Stone, and R. Lowe, "The addition of heat pump electricity load profiles to GB electricity demand: Evidence from a heat pump field trial," *Applied Energy*, vol. 204, pp. 332–342, 2017. [Online]. Available: http://dx.doi.org/10.1016/j.apenergy.2017.07.026

[80] Carbon Trust, "Micro Combined Heat and Power (CHP) Accelerator: Final report," Tech. Rep., Mar. 2011. [Online]. Available: https://www.carbontrust.com/our-work-and-impact/guides-reports-and-tools/micro-combined-heat-and-power-chp-accelerator-final-report

[81] R. Sansom, "Decarbonising low grade heat for a low carbon future," Ph.D. dissertation, Imperial College, London, Oct. 2014. [Online]. Available: https://core.ac.uk/download/pdf/77000135.pdf

[82] A. Navarro-Espinosa and P. Mancarella, "Probabilistic modeling and assessment of the impact of electric heat pumps on low voltage distribution networks," *Applied Energy*, vol. 127, pp. 249–266, Aug. 2014. [Online]. Available: https://linkinghub.elsevier.com/retrieve/pii/S030626191400378X

[83] R. Lowe and Department of Energy and Climate Change, "Renewable Heat Premium Payment Scheme: Heat Pump Monitoring: Cleaned Data, 2013-2015," 2017. [Online]. Available: http://doi.org/10.5255/UKDA-SN-8151-1

[84] A. Anderson, B. Stephen, R. Telford, and S. Mcarthur, "Predictive Thermal Relation Model for Synthesizing Low Carbon Heating Load Profiles on Distribution Networks," *IEEE Access*, vol. 8, pp. 195 290–195 304, 2020. [Online]. Available: https://ieeexplore.ieee.org/document/9229416/

[85] O. Ruhnau, L. Lundström, L. Dürr, and F. Hunecke, "Empirical weather dependency of heat pump load: Disentangling the effects of heat demand and efficiency," in *2023 19th International Conference on the European Energy Market (EEM)*. Lappeenranta, Finland: IEEE, Jun. 2023, pp. 1–5. [Online]. Available: https://ieeexplore.ieee.org/document/10161914/

[86] A. Canet, M. Qadrdan, N. Jenkins, and J. Wu, "Spatial and temporal data to study residential heat decarbonisation pathways in England and Wales," *Scientific Data*, vol. 9, no. 1, p. 246, Dec. 2022. [Online]. Available: https://www.nature.com/articles/s41597-022-01356-9

[87] Y. Li, Z. O'Neill, L. Zhang, J. Chen, P. Im, and J. DeGraw, "Grey-box modeling and application for building energy simulations - A critical review," *Renewable and Sustainable Energy Reviews*, vol. 146, p. 111174, Aug. 2021. [Online]. Available: https://linkinghub.elsevier.com/retrieve/pii/S1364032121004639

[88] A. Bampoulas, M. Saffari, F. Pallonetto, E. Mangina, and D. P. Finn, "A fundamental unified framework to quantify and characterise energy flexibility of residential buildings with multiple electrical and thermal energy systems," *Applied Energy*, vol. 282, p. 116096, Jan. 2021. [Online]. Available: https://linkinghub.elsevier.com/retrieve/pii/S0306261920315191

[89] H. Johra, P. Heiselberg, and J. L. Dréau, "Influence of envelope, structural thermal mass and indoor content on the building heating energy flexibility," *Energy and Buildings*, vol. 183, pp. 325–339, Jan. 2019. [Online]. Available: https://linkinghub.elsevier.com/retrieve/pii/S0378778817338562

[90] J. Le Dréau and P. Heiselberg, "Energy flexibility of residential buildings using short term heat storage in the thermal mass," *Energy*, vol. 111, pp. 991–1002, Sep. 2016. [Online]. Available: https://linkinghub.elsevier.com/retrieve/pii/S0360544216306934

[91] G. Reynders, T. Nuytten, and D. Saelens, "Potential of structural thermal mass for demand-side management in dwellings," *Building and Environment*, vol. 64, pp. 187–199, Jun. 2013. [Online]. Available: https://linkinghub.elsevier.com/retrieve/pii/S0360132313000905

[92] G. Reynders, J. Diriken, and D. Saelens, "Generic characterization method for energy flexibility: Applied to structural thermal storage in residential buildings," *Applied Energy*, vol. 198, pp. 192–202, Jul. 2017. [Online]. Available: https://linkinghub.elsevier.com/retrieve/pii/S0306261917304555

[93] A. Arteconi, A. Mugnini, and F. Polonara, "Energy flexible buildings: A methodology for rating the flexibility performance of buildings with electric heating and cooling systems," *Applied Energy*, vol. 251, p. 113387, Oct. 2019. [Online]. Available: https://linkinghub.elsevier.com/retrieve/pii/S030626191931061X

[94] K. Hedegaard and O. Balyk, "Energy system investment model incorporating heat pumps with thermal storage in buildings and buffer tanks," *Energy*, vol. 63, pp. 356–365, 2013. [Online]. Available: http://dx.doi.org/10.1016/j.energy.2013.09.061

[95] D. Patteeuw, K. Bruninx, A. Arteconi, E. Delarue, W. D'haeseleer, and L. Helsen, "Integrated modeling of active demand response with electric heating systems coupled to thermal energy storage systems," *Applied Energy*, vol. 151, pp. 306–319, Aug. 2015. [Online]. Available: https://linkinghub.elsevier.com/retrieve/pii/S0306261915004535

[96] D. Patteeuw, G. Reynders, K. Bruninx, C. Protopapadaki, E. Delarue, W. D'haeseleer, D. Saelens, and L. Helsen, "CO 2 -abatement cost of residential heat pumps with active demand response: demand- and supply-side effects," *Applied Energy*, vol. 156, pp. 490–501, Oct. 2015. [Online]. Available: https://linkinghub.elsevier.com/retrieve/pii/S0306261915008673

[97] J. L. Mathieu, M. E. Dyson, and D. S. Callaway, "Resource and revenue potential of California residential load participation in ancillary services," *Energy Policy*, vol. 80, pp. 76–87, May 2015. [Online]. Available: https://linkinghub.elsevier.com/retrieve/pii/S0301421515000427

[98] X. Xue, S. Wang, Y. Sun, and F. Xiao, "An interactive building power demand management strategy for facilitating smart grid optimization," *Applied Energy*, vol. 116, pp. 297–310, Mar. 2014. [Online]. Available: https://linkinghub.elsevier.com/retrieve/pii/S0306261913009719

[99] X. Chen, X. Lu, M. B. McElroy, C. P. Nielsen, and C. Kang, "Synergies of Wind Power and Electrified Space Heating: Case Study for Beijing," *Environmental Science & Technology*, vol. 48, no. 3, pp. 2016–2024, Feb. 2014. [Online]. Available: https://pubs.acs.org/doi/10.1021/es405653x

[100] A. Bloess, "Impacts of heat sector transformation on Germany's power system through increased use of power-to-heat," *Applied Energy*, vol. 239, no. February, pp. 560–580, 2019. [Online]. Available: https://doi.org/10.1016/j.apenergy.2019.01.101

[101] R. Renaldi, A. Kiprakis, and D. Friedrich, "An optimisation framework for thermal energy storage integration in a residential heat pump heating system," *Applied Energy*, vol. 186, pp. 520–529, Jan. 2017. [Online]. Available: https://linkinghub.elsevier.com/retrieve/pii/S0306261916302045

[102] K. Hedegaard, B. V. Mathiesen, H. Lund, and P. Heiselberg, "Wind power integration using individual heat pumps – Analysis of different heat storage options," *Energy*, vol. 47, no. 1, pp. 284–293, Nov. 2012. [Online]. Available: https://linkinghub.elsevier.com/retrieve/pii/S0360544212007086

[103] G. Papaefthymiou, B. Hasche, and C. Nabe, "Potential of Heat Pumps for Demand Side Management and Wind Power Integration in the German Electricity Market," *IEEE Transactions on Sustainable Energy*, vol. 3, no. 4, pp. 636–642, Oct. 2012. [Online]. Available: http://ieeexplore.ieee.org/document/6246665/

[104] A. Canet and M. Qadrdan, "Quantification of flexibility from the thermal mass of residential buildings in England and Wales," *Applied Energy*, vol. 349, p. 121616, Nov. 2023. [Online]. Available: https://linkinghub.elsevier.com/retrieve/pii/S0306261923009807

[105] J. Lizana, A. Serrano-Jimenez, C. Ortiz, J. A. Becerra, and R. Chacartegui, "Energy assessment method towards low-carbon energy schools," *Energy*, vol. 159, pp. 310–326, Sep. 2018. [Online]. Available: https://linkinghub.elsevier.com/retrieve/pii/S036054421831212X

[106] A. Serrano-Jiménez, J. Lizana, M. Molina-Huelva, and A. Barrios-Padura, "Decision-support method for profitable residential energy retrofitting based on energy-related occupant behaviour," *Journal of Cleaner Production*, vol. 222, pp. 622–632, Jun. 2019. [Online]. Available: https://linkinghub.elsevier.com/retrieve/pii/S0959652619307802

[107] C. Ahern and B. Norton, "Energy Performance Certification: Misassessment due to assuming default heat losses," *Energy and Buildings*, vol. 224, p. 110229, Oct. 2020. [Online]. Available: https://linkinghub.elsevier.com/retrieve/pii/S037877882030880X

[108] J. Few, D. Manouseli, E. McKenna, M. Pullinger, E. Zapata-Webborn, S. Elam, D. Shipworth, and T. Oreszczyn, "The over-prediction of energy use by EPCs in Great Britain: A comparison of EPC-modelled and metered primary energy use intensity," *Energy and Buildings*, vol. 288, p. 113024, Jun. 2023. [Online]. Available: https://linkinghub.elsevier.com/retrieve/pii/S0378778823002542

[109] S. Clegg and P. Mancarella, "Integrated electricity-heat-gas modelling and assessment, with applications to the Great Britain system. Part II: Transmission network analysis and low carbon technology and resilience case studies," *Energy*, vol. 184, pp. 191–203, 2019. [Online]. Available: https://doi.org/10.1016/j.energy.2018.02.078

[110] M. M. Frysztacki, J. Hörsch, V. Hagenmeyer, and T. Brown, "The strong effect of network resolution on electricity system models with high shares of wind and solar," *Applied Energy*, vol. 291, p. 116726, Jun. 2021. [Online]. Available: https://linkinghub.elsevier.com/retrieve/pii/S0306261921002439

[111] F. Jalil-Vega and A. D. Hawkes, "Spatially resolved model for studying decarbonisation pathways for heat supply and infrastructure trade-offs," *Applied Energy*, vol. 210, pp. 1051–1072, 2018. [Online]. Available: https://doi.org/10.1016/j.apenergy.2017.05.091

[112] E. Zhou, E. Hale, and E. Present, "Building flexibility revenue in modeled future bulk power systems with varying levels of renewable energy," *Heliyon*, vol. 8, no. 7, p. e09865, Jul. 2022. [Online]. Available: https://linkinghub.elsevier.com/retrieve/pii/S2405844022011537

[113] R. Earle, E. P. Kahn, and E. Macan, "Measuring the Capacity Impacts of Demand Response," *The Electricity Journal*, vol. 22, no. 6, pp. 47–58, Jul. 2009. [Online]. Available: https://linkinghub.elsevier.com/retrieve/pii/S1040619009001523

[114] J. Kiviluoma and P. Meibom, "Influence of wind power, plug-in electric vehicles, and heat storages on power system investments," *Energy*, vol. 35, no. 3, pp. 1244–1255, 2010. [Online]. Available: http://dx.doi.org/10.1016/j.energy.2009.11.004

[115] K. Hedegaard and M. Münster, "Influence of individual heat pumps on wind power integration – Energy system investments and operation," *Energy Conversion and Management*, vol. 75, pp. 673–684, Nov. 2013. [Online]. Available: https://linkinghub.elsevier.com/retrieve/pii/S0196890413004743

[116] H. Hao, B. M. Sanandaji, K. Poolla, and T. L. Vincent, "Potentials and economics of residential thermal loads providing regulation reserve," *Energy Policy*, vol. 79, pp. 115–126, Apr. 2015. [Online]. Available: https://linkinghub.elsevier.com/retrieve/pii/S0301421515000142

[117] V. Krakowski, E. Assoumou, V. Mazauric, and N. Maïzi, "Feasible path toward 40–100% renewable energy shares for power supply in France by 2050: A prospective analysis," *Applied Energy*, vol. 171, pp. 501–522, Jun. 2016. [Online]. Available: https://linkinghub.elsevier.com/retrieve/pii/S0306261916304251

[118] H. C. Gils, "Economic potential for future demand response in Germany – Modeling approach and case study," *Applied Energy*, vol. 162, pp. 401–415, Jan. 2016. [Online]. Available: https://linkinghub.elsevier.com/retrieve/pii/S0306261915013100

[119] F. Teng, M. Aunedi, and G. Strbac, "Benefits of flexibility from smart electrified transportation and heating in the future UK electricity system," *Applied Energy*, vol. 167, pp. 420–431, Apr. 2016. [Online]. Available: https://linkinghub.elsevier.com/retrieve/pii/S0306261915012556

[120] A. Aryandoust and J. Lilliestam, "The potential and usefulness of demand response to provide electricity system services," *Applied Energy*, vol. 204, pp. 749–766, Oct. 2017. [Online]. Available: https://linkinghub.elsevier.com/retrieve/pii/S0306261917309066

[121] V. Olkkonen, S. Rinne, A. Hast, and S. Syri, "Benefits of DSM measures in the future Finnish energy system," *Energy*, vol. 137, pp. 729–738, Oct. 2017. [Online]. Available: https://linkinghub.elsevier.com/retrieve/pii/S0360544217309829

[122] P.-H. Li and S. Pye, "Assessing the benefits of demand-side flexibility in residential and transport sectors from an integrated energy systems perspective," *Applied Energy*, vol. 228, pp. 965–979, Oct. 2018. [Online]. Available: https://linkinghub.elsevier.com/retrieve/pii/S0306261918310237

[123] T. Brown, D. Schlachtberger, A. Kies, S. Schramm, and M. Greiner, "Synergies of sector coupling and transmission reinforcement in a cost-optimised, highly renewable European energy system," *Energy*, vol. 160, pp. 720–739, Oct. 2018. [Online]. Available: https://linkinghub.elsevier.com/retrieve/pii/S036054421831288X

[124] M. Lynch, S. Nolan, M. T. Devine, and M. O'Malley, "The impacts of demand response participation in capacity markets," *Applied Energy*, vol. 250, pp. 444–451, Sep. 2019. [Online]. Available: https://linkinghub.elsevier.com/retrieve/pii/S0306261919309195

[125] A. Guminski, F. Böing, A. Murmann, and S. Von Roon, "System effects of high demand-side electrification rates: A scenario analysis for Germany in 2030," *WIREs Energy and Environment*, vol. 8, no. 2, p. e327, Mar. 2019. [Online]. Available: https://wires.onlinelibrary.wiley.com/doi/10.1002/wene.327

[126] W.-P. Schill and A. Zerrahn, "Flexible electricity use for heating in markets with renewable energy," *Applied Energy*, vol. 266, no. March, p. 114571, 2020. [Online]. Available: https://doi.org/10.1016/j.apenergy.2020.114571

[127] C. Bernath, G. Deac, and F. Sensfuß, "Impact of sector coupling on the market value of renewable energies – A model-based scenario analysis," *Applied Energy*, vol. 281, p. 115985, Jan. 2021. [Online]. Available: https://linkinghub.elsevier.com/retrieve/pii/S0306261920314331

[128] I. Savelli and T. Morstyn, "The energy flexibility divide: An analysis of whether energy flexibility could help reduce deprivation in Great Britain," *Energy Research*

& Social Science, vol. 100, p. 103083, Jun. 2023. [Online]. Available: https://linkinghub.elsevier.com/retrieve/pii/S2214629623001433

[129] L. Göke, J. Weibezahn, and M. Kendziorski, "How flexible electrification can integrate fluctuating renewables," *Energy*, vol. 278, p. 127832, Sep. 2023. [Online]. Available: https://linkinghub.elsevier.com/retrieve/pii/S0360544223012264

[130] A. Gaur, D. Fitiwi, and J. Curtis, "Deep Electrification of Residential Heating and Possible Implications: An Irish Perspective," in *E3S Web of Conferences*, M. Kolhe, Ed., vol. 173, 2020, p. 03003. [Online]. Available: https://www.e3s-conferences.org/10.1051/e3sconf/202017303003

[131] F. Neumann, "Costs of regional equity and autarky in a renewable European power system," *Energy Strategy Reviews*, vol. 35, p. 100652, May 2021. [Online]. Available: https://linkinghub.elsevier.com/retrieve/pii/S2211467X21000389

[132] T. Tröndle, J. Lilliestam, S. Marelli, and S. Pfenninger, "Trade-Offs between Geographic Scale, Cost, and Infrastructure Requirements for Fully Renewable Electricity in Europe," *Joule*, vol. 4, no. 9, pp. 1929–1948, Sep. 2020. [Online]. Available: https://linkinghub.elsevier.com/retrieve/pii/S2542435120303366

[133] T. Tröndle, S. Pfenninger, and J. Lilliestam, "Home-made or imported: On the possibility for renewable electricity autarky on all scales in Europe," *Energy Strategy Reviews*, vol. 26, p. 100388, Nov. 2019. [Online]. Available: https://linkinghub.elsevier.com/retrieve/pii/S2211467X19300811

[134] E. D. Brill, S.-Y. Chang, and L. D. Hopkins, "Modeling to Generate Alternatives: The HSJ Approach and an Illustration Using a Problem in Land Use Planning," *Management Science*, vol. 28, no. 3, pp. 221–235, Mar. 1982. [Online]. Available: https://pubsonline.informs.org/doi/10.1287/mnsc.28.3.221

[135] J. F. DeCarolis, "Using modeling to generate alternatives (MGA) to expand our thinking on energy futures," *Energy Economics*, vol. 33, no. 2, pp. 145–152, Mar. 2011. [Online]. Available: https://linkinghub.elsevier.com/retrieve/pii/S0140988310000721

[136] J. DeCarolis, S. Babaee, B. Li, and S. Kanungo, "Modelling to generate alternatives with an energy system optimization model," *Environmental Modelling & Software*, vol. 79, pp. 300–310, May 2016. [Online]. Available: https://linkinghub.elsevier.com/retrieve/pii/S1364815215301080

[137] J. Price and I. Keppo, "Modelling to generate alternatives: A technique to explore uncertainty in energy-environment-economy models," *Applied Energy*, vol. 195, pp. 356–369, Jun. 2017. [Online]. Available: https://linkinghub.elsevier.com/retrieve/pii/S0306261917302957

[138] F. G. Li and E. Trutnevyte, "Investment appraisal of cost-optimal and near-optimal pathways for the UK electricity sector transition to 2050," *Applied Energy*, vol. 189, pp. 89–109, Mar. 2017. [Online]. Available: https://linkinghub.elsevier.com/retrieve/pii/S0306261916318104

[139] P. B. Berntsen and E. Trutnevyte, "Ensuring diversity of national energy scenarios: Bottom-up energy system model with Modeling to Generate Alternatives," *Energy*, vol. 126, pp. 886–898, May 2017. [Online]. Available: https://linkinghub.elsevier.com/retrieve/pii/S0360544217304097

[140] J.-P. Sasse and E. Trutnevyte, "Distributional trade-offs between regionally equitable and cost-efficient allocation of renewable electricity generation," *Applied Energy*, vol. 254, p. 113724, Nov. 2019. [Online]. Available: https://linkinghub.elsevier.com/retrieve/pii/S0306261919314114

[141] ——, "Regional impacts of electricity system transition in Central Europe until 2035," *Nature Communications*, vol. 11, no. 1, p. 4972, Oct. 2020. [Online]. Available: https://www.nature.com/articles/s41467-020-18812-y

[142] F. Lombardi, B. Pickering, E. Colombo, and S. Pfenninger, "Policy Decision Support for Renewables Deployment through Spatially Explicit Practically Optimal Alternatives," *Joule*, vol. 4, no. 10, pp. 2185–2207, Oct. 2020. [Online]. Available: https://linkinghub.elsevier.com/retrieve/pii/S2542435120303482

[143] F. Neumann and T. Brown, "The near-optimal feasible space of a renewable power system model," *Electric Power Systems Research*, vol. 190, p. 106690, Jan. 2021. [Online]. Available: https://linkinghub.elsevier.com/retrieve/pii/S0378779620304934

[144] T. T. Pedersen, M. Victoria, M. G. Rasmussen, and G. B. Andresen, "Modeling all alternative solutions for highly renewable energy systems," *Energy*, vol. 234, p. 121294, Nov. 2021. [Online]. Available: https://linkinghub.elsevier.com/retrieve/pii/S0360544221015425

[145] B. Pickering, F. Lombardi, and S. Pfenninger, "Diversity of options to eliminate fossil fuels and reach carbon neutrality across the entire European energy system," *Joule*, vol. 6, no. 6, pp. 1253–1276, Jun. 2022. [Online]. Available: https://linkinghub.elsevier.com/retrieve/pii/S2542435122002367

[146] F. Neumann and T. Brown, "Broad ranges of investment configurations for renewable power systems, robust to cost uncertainty and near-optimality," *iScience*, vol. 26, no. 5, p. 106702, May 2023. [Online]. Available: https://linkinghub.elsevier.com/retrieve/pii/S2589004223007794

[147] F. Lombardi, B. Pickering, and S. Pfenninger, "What is redundant and what is not? Computational trade-offs in modelling to generate alternatives for energy infrastructure deployment," *Applied Energy*, vol. 339, p. 121002, Jun. 2023. [Online]. Available: https://linkinghub.elsevier.com/retrieve/pii/S0306261923003665

[148] N. Patankar, X. Sarkela-Basset, G. Schivley, E. Leslie, and J. Jenkins, "Land use trade-offs in decarbonization of electricity generation in the American West," *Energy and Climate Change*, vol. 4, p. 100107, Dec. 2023. [Online]. Available: https://linkinghub.elsevier.com/retrieve/pii/S2666278723000144

[149] Ipsos MORI, "Consumer Experiences Of Time Of Use Tariffs," Tech. Rep., Oct. 2012. [Online]. Available: https://www.ipsos.com/en-uk/consumer-experiences-time-use-tariffs

[150] National Grid ESO, "Future Energy Scenarios," Tech. Rep., Jul. 2023. [Online]. Available: https://www.nationalgrideso.com/future-energy/future-energy-scenarios-fes

[151] P.-H. Li, I. Keppo, M. Xenitidou, and M. Kamargianni, "Investigating UK consumers' heterogeneous engagement in demand-side response," *Energy Efficiency*, vol. 13, no. 4, pp. 621–648, Apr. 2020. [Online]. Available: http://link.springer.com/10.1007/s12053-020-09847-7

[152] S. Reis, T. Liska, S. Steinle, E. Carnell, D. Leaver, E. Roberts, M. Vieno, R. Beck, and U. Dragosits, "UK gridded population 2011 based on Census 2011 and Land Cover Map 2015," 2017. [Online]. Available: https://doi.org/10.5285/0995e94d-6d42-40c1-8ed4-5090d82471e1

[153] UK Office for National Statistics, "Household and resident characteristics, England and Wales: Census 2021," Tech. Rep., Nov. 2022. [Online]. Available: https://www.ons.gov.uk/peoplepopulationandcommunity/householdcharacteristics/homeinternetandsocialmediausage/bulletins/householdandresidentcharacteristicsenglandandwales/census2021

[154] Open Power System Data, "Data Package Time series." [Online]. Available: https://doi.org/10.25832/time_series/2019-06-05

[155] IEA, *Transition to sustainable buildings: Strategies and opportunities to 2050*. Paris: IEA, 2013. [Online]. Available: https://www.iea.org/reports/transition-to-sustainable-buildings

[156] UK Department for Levelling Up, Housing and Communities, "English Housing Survey 2020 to 2021: headline report," Tech. Rep., 2021. [Online]. Available: https://www.gov.uk/government/statistics/english-housing-survey-2020-to-2021-headline-report

[157] Office for National Statistics, "NUTS, level 1 (January 2018) Boundaries UK BUC," Sep. 2022. [Online]. Available: https://geoportal.statistics.gov.uk/datasets/44c039e762d94a42bf5e0580e8dd9f84/explore

[158] UK Department for Business, Energy, and Industrial Strategy, "Opportunity areas for district heating networks in the UK," Tech. Rep., 2021.

[159] HotMaps, "HotMaps Database and Toolbox." [Online]. Available: https://www.hotmaps.eu/map

[160] A. Müller, M. Hummel, L. Kranzl, M. Fallahnejad, and R. Büchele, "Open Source Data for Gross Floor Area and Heat Demand Density on the Hectare Level for EU 28," *Energies*, vol. 12, no. 24, p. 4789, Dec. 2019. [Online]. Available: https://www.mdpi.com/1996-1073/12/24/4789

[161] Met Office, "Winter 2018/2019," Tech. Rep. [Online]. Available: https://www.metoffice.gov.uk/binaries/content/assets/metofficegovuk/pdf/weather/learn-about/uk-past-events/summaries/uk_monthly_climate_summary_winter_2019.pdf

[162] ——, "Winter 2019/2020," Tech. Rep. [Online]. Available: https://www.metoffice.gov.uk/binaries/content/assets/metofficegovuk/pdf/weather/learn-about/uk-past-events/summaries/uk_monthly_climate_summary_winter_2020.pdf

[163] S. Eggimann, W. Usher, N. Eyre, and J. W. Hall, "How weather affects energy demand variability in the transition towards sustainable heating," *Energy*, vol. 195, p. 116947, 2020. [Online]. Available: https://doi.org/10.1016/j.energy.2020.116947

[164] C. Halloran, "GeoHeat-GB v.0.1.1." [Online]. Available: https://github.com/clairehalloran/GeoHeat-GB/releases/tag/0.1.1

[165] F. Hofmann, J. Hampp, F. Neumann, T. Brown, and J. Hörsch, "atlite: A Lightweight Python Package for Calculating Renewable Power Potentials and Time Series," *Journal of Open Source Software*, vol. 6, no. 62, p. 3294, Jun. 2021. [Online]. Available: https://joss.theoj.org/papers/10.21105/joss.03294

[166] International Energy Agency, "Solar PV," Paris, Tech. Rep., 2023. [Online]. Available: https://www.iea.org/energy-system/renewables/solar-pv

[167] J. Hörsch, F. Hofmann, D. Schlachtberger, and T. Brown, "PyPSA-Eur: An open optimisation model of the European transmission system," *Energy Strategy Reviews*, vol. 22, pp. 207–215, Nov. 2018. [Online]. Available: https://linkinghub.elsevier.com/retrieve/pii/S2211467X18300804

[168] Copernicus Land Monitoring Service, "Corine Land Cover (CLC) 2012, Version 2020_20u1," 2020. [Online]. Available: http://land.copernicus.eu/pan-european/corine-land-cover/clc-2012/view

[169] EEA, "Natura 2000 data - the European network of protected sites," 2016. [Online]. Available: http://www.eea.europa.eu/data-and-maps/data/natura-7

[170] Flanders Marine Institute, "The intersect of the Exclusive Economic Zones and IHO sea areas," 2018.

[171] GEBCO, "The GEBCO_2014 Grid, version 20150318." [Online]. Available: http://www.gebco.net

[172] "ENTSO-E Interactive Transmission System Map," Mar. 2022. [Online]. Available: https://www.entsoe.eu/map/

[173] B. Wiegmans, "GridKit: GridKit 1.0 'for Scientists'," Mar. 2016. [Online]. Available: https://doi.org/10.5281/zenodo.47263

[174] A. Kies, K. Chattopadhyay, L. von Bremen, E. Lorenz, and D. Heinemann, "RESTORE 2050 Work Package Report D12: Simulation of renewable feed- in for power system studies," Technical report, 2016.

[175] B. Pfluger, F. Sensfuß, G. Schubert, and J. Leisentritt, "Tangible ways towards climate protection in the European Union (EU Long-term scenarios 2050)," Fraunhofer ISI, Tech. Rep., Sep. 2011. [Online]. Available: http://www.1aufbau.de/isi-wAssets/docs/x/de/publikationen/Final_Report_EU-Long-term-scenarios-2050_FINAL.pdf

[176] U.S. Energy Information Administration, "Hydroelectricity net generation Europe 2000-2014," 2017. [Online]. Available: http://tinyurl.com/EIA-hydro-gen-EU-2000-2014

[177] GISCO - Eurostat (European Commission), "NUTS (Nomenclature of territorial units for statistics) regions." [Online]. Available: https://ec.europa.eu/eurostat/web/gisco/geodata/reference-data/administrative-units-statistical-units/nuts

[178] European Central Bank, "Pound sterling (GBP)." [Online]. Available: https://www.ecb.europa.eu/stats/policy_and_exchange_rates/euro_reference_exchange_rates/html/eurofxref-graph-gbp.en.html

[179] A. Fairbairn, "Annual Review of the Value of Lost Load (VoLL) and Loss of Load Probability (LoLP)," Elexon, Tech. Rep., Jul. 2022. [Online]. Available: https://www.elexon.co.uk/documents/groups/isg/2022-meetings-isg/255-july/isg255-08-annual-review-of-the-value-of-lost-load-and-loss-of-load-probability-2022/

[180] M. M. Frysztacki, G. Recht, and T. Brown, "A comparison of clustering methods for the spatial reduction of renewable electricity optimisation models of Europe," *Energy Informatics*, vol. 5, no. 1, p. 4, May 2022. [Online]. Available: https://energyinformatics.springeropen.com/articles/10.1186/s42162-022-00187-7

[181] National Grid ESO, "Electricity Ten Year Statement (ETYS)," Tech. Rep., 2022. [Online]. Available: https://www.nationalgrideso.com/research-and-publications/electricity-ten-year-statement-etys/etys-archive

[182] J. Hörsch, T. Brown, F. Hofmann, F. Neumann, M. Frysztacki, J. Hampp, and D. Schlachtberger, "PyPSA-Eur: An open optimisation model of the European transmission system," Sep. 2022. [Online]. Available: https://doi.org/10.5281/zenodo.7097555

[183] F. Neumann, E. Zeyen, M. Victoria, and T. Brown, "The potential role of a hydrogen network in Europe," *Joule*, vol. 7, no. 8, pp. 1793–1817, Aug. 2023. [Online]. Available: https://linkinghub.elsevier.com/retrieve/pii/S2542435123002660

[184] T. Brown, M. Victoria, E. Zeyen, F. Hofmann, F. Neumann, M. Frysztacki, J. Hampp, D. Schlachtberger, and J. Hörsch, "PyPSA-Eur: An open sector-coupled optimisation model of the European energy system," Mar. 2023. [Online]. Available: https://doi.org/10.5281/zenodo.7748803

[185] T. Brown, J. Hörsch, and D. Schlachtberger, "PyPSA: Python for Power System Analysis," *Journal of Open Research Software*, vol. 6, no. 1, p. 4, Jan. 2018. [Online]. Available: https://openresearchsoftware.metajnl.com/article/10.5334/jors.188/

[186] J. Hörsch, H. Ronellenfitsch, D. Witthaut, and T. Brown, "Linear optimal power flow using cycle flows," *Electric Power Systems Research*, vol. 158, pp. 126–135, May 2018. [Online]. Available: https://linkinghub.elsevier.com/retrieve/pii/S0378779617305138

[187] S. Hagspiel, C. Jägemann, D. Lindenberger, T. Brown, S. Cherevatskiy, and E. Tröster, "Cost-optimal power system extension under flow-based market coupling," *Energy*, vol. 66, pp. 654–666, Mar. 2014. [Online]. Available: https://linkinghub.elsevier.com/retrieve/pii/S0360544214000322

[188] N. A. Sepulveda, J. D. Jenkins, F. J. de Sisternes, and R. K. Lester, "The Role of Firm Low-Carbon Electricity Resources in Deep Decarbonization of Power Generation," *Joule*, vol. 2, no. 11, pp. 2403–2420, 2018. [Online]. Available: https://doi.org/10.1016/j.joule.2018.08.006

[189] European Environment Agency, "National emissions reported to the UNFCCC and to the EU Greenhouse Gas Monitoring Mechanism," May 2022. [Online]. Available: https://www.eea.europa.eu/data-and-maps/data/national-emissions-reported-to-the-unfccc-and-to-the-eu-greenhouse-gas-monitoring-mechanism-18

[190] UK Climate Change Committee, "The Sixth Carbon Budget: Electricity generation," Tech. Rep., 2020, iSBN: 9781315065786. [Online]. Available: https://www.theccc.org.uk/publication/sixth-carbon-budget/

[191] UK Department for Business Energy & Industrial Strategy, "Electricity: commodity balances (DUKES 5.1)," 2022. [Online]. Available: https://www.gov.uk/government/statistics/electricity-chapter-5-digest-of-united-kingdom-energy-statistics-dukes

[192] M. Kittel and W.-P. Schill, "Renewable energy targets and unintended storage cycling: Implications for energy modeling," *iScience*, vol. 25, no. 4, p. 104002, Apr. 2022. [Online]. Available: https://linkinghub.elsevier.com/retrieve/pii/S2589004222002723

[193] Energy Systems Catapult, "Electrification of Heat Demonstration Project: Heat Pump Performance Cleansed Data, 2020-2022," 2023. [Online]. Available: https://beta.ukdataservice.ac.uk/datacatalogue/doi/?id=9050#1

[194] C. Halloran, "GeoHeatFlex." [Online]. Available: https://github.com/clairehalloran/GeoHeatFlex

[195] C. Halloran, J. Lizana, and M. McCulloch, "Space heating flexibility potential in British Homes," 2024. [Online]. Available: https://ora.ox.ac.uk/objects/uuid:76f9bb1d-6d1b-4ffd-a238-8eb54f1df69e

[196] UK Department for Energy Security & Net Zero, "Subnational Consumption Statistics: Methodology and guidance booklet," Tech. Rep., Dec. 2023. [Online]. Available: https://assets.publishing.service.gov.uk/media/6580608f5ca017000d734bb6/Sub_national_methodology_and_guidance_booklet_December_2023.pdf

[197] Office for National Statistics, "Lower Layer Super Output Areas (Dec 2011) Boundaries Full Extent (BFE) EW V3," Mar. 2023, contains OS data © Crown copyright and database right 2023. [Online]. Available: https://geoportal.statistics.gov.uk/datasets/ons::lower-layer-super-output-areas-dec-2011-boundaries-full-extent-bfe-ew-v3/about

[198] Government of Scotland, "Data Zone Boundaries 2011," Oct. 2021, copyright Scottish Government, contains Ordnance Survey data © Crown copyright and database right 2021. [Online]. Available: https://spatialdata.gov.scot/geonetwork/srv/eng/catalog.search#/metadata/7d3e8709-98fa-4d71-867c-d5c8293823f2

[199] Met Office, D. Hollis, M. McCarthy, M. Kendon, T. Legg, and I. Simpson, "HadUK-Grid gridded and regional average climate observations for the UK," Nov. 2023. [Online]. Available: http://catalogue.ceda.ac.uk/uuid/4dc8450d889a491ebb20e724debe2dfb

[200] Office for National Statistics, "Census 2011 Table QS407EW: Number of rooms," Jan. 2013. [Online]. Available: https://www.nomisweb.co.uk/census/2011/qs407ew

[201] National Records of Scotland, "2011 Census Table QS407SC - Number of rooms." [Online]. Available: https://www.scotlandscensus.gov.uk/search-the-census#/search-by

[202] M. Kendon, M. McCarthy, S. Jevrejeva, A. Matthews, T. Sparks, and J. Garforth, "State of the UK Climate 2020," *International Journal of Climatology*, vol. 41, no. S2, pp. 1–76, Jul. 2021. [Online]. Available: https://rmets.onlinelibrary.wiley.com/doi/10.1002/joc.7285

[203] Office for National Statistics, "Developing admin-based property floor area statistics for England and Wales: 2021," Tech. Rep., Oct. 2022. [Online]. Available: https://www.ons.gov.uk/peoplepopulationandcommunity/housing/articles/developingadminbasedpropertyfloorareastatisticsforenglandandwales/2021

[204] A. Canet, "Quantification of inherent flexibility from electrified residential heat sector in England and Wales [Data set]," Cardiff University. [Online]. Available: https://data.ukedc.rl.ac.uk/browse/edc/efficiency/residential/Buildings/Flexibility_of_residential_heat_sector

[205] UK Climate Change Committee, "Progress in reducing emissions: 2023 Report to Parliament," Tech. Rep., Jun. 2023. [Online]. Available: https://www.theccc.org.uk/wp-content/uploads/2023/06/Progress-in-reducing-UK-emissions-2023-Report-to-Parliament-1.pdf

[206] N. A. Sepulveda, J. D. Jenkins, A. Edington, D. S. Mallapragada, and R. K. Lester, "The design space for long-duration energy storage in decarbonized power systems," *Nature Energy*, vol. 6, no. 5, pp. 506–516, Mar. 2021. [Online]. Available: https://www.nature.com/articles/s41560-021-00796-8

[207] House of Lords Science and Technology Committee, "Long-duration energy storage: get on with it," London, Tech. Rep., Mar. 2024. [Online]. Available: https://publications.parliament.uk/pa/ld5804/ldselect/ldsctech/68/68.pdf

[208] A. Deroubaix, I. Labuhn, M. Camredon, B. Gaubert, P.-A. Monerie, M. Popp, J. Ramarohetra, Y. Ruprich-Robert, L. G. Silvers, and G. Siour, "Large uncertainties in trends of energy demand for heating and cooling under climate change," *Nature Communications*, vol. 12, no. 1, p. 5197, Dec. 2021. [Online]. Available: https://www.nature.com/articles/s41467-021-25504-8

[209] Danish Energy Agency (DEA), "Technology Data for Generation of Electricity and District Heating," 2019. [Online]. Available: https://ens.dk/en/our-services/projections-and-models/technology-data/technology-data-generation-electricity-and

[210] A. Schröder, F. Kunz, J. Meiss, R. Mendelevitch, and C. von Hirschhausen, "Current and prospective costs of electricity generation until 2050," Deutsches Institut für Wirtschaftsforschung (DIW), Berlin, Tech. Rep. No. 68, 2013. [Online]. Available: http://hdl.handle.net/10419/80348

[211] International Energy Agency, "Renewable Energy Essentials: Hydropower," International Energy Agency, Paris, Tech. Rep., Nov. 2010. [Online]. Available: https://www.iea.org/reports/renewable-energy-essentials-hydropower

[212] Lazard, "Lazard's Levelized Cost of Energy Analysis—Version 13.0," Tech. Rep., 2019. [Online]. Available: https://www.lazard.com/media/o3ln2wve/lazards-levelized-cost-of-energy-version-130-vf.pdf

[213] European Climate Foundation, "Roadmap 2050 - A Practical Guide to a Prosperous Low-Carbon Europe," Tech. Rep., 2010. [Online]. Available: http://www.roadmap2050.eu/attachments/files/Vol1_Appendices.zip

[214] Danish Energy Agency (DEA), "Technology Data for Energy Storage," 2019. [Online]. Available: https://ens.dk/en/our-services/projections-and-models/technology-data/technology-data-energy-storage

[215] A. Purvins, L. Sereno, M. Ardelean, C.-F. Covrig, T. Efthimiadis, and P. Minnebo, "Submarine power cable between Europe and North America: A techno-economic analysis," *Journal of Cleaner Production*, vol. 186, pp. 131–145, Jun. 2018. [Online]. Available: https://linkinghub.elsevier.com/retrieve/pii/S0959652618307522

[216] Danish Energy Agency (DEA), "Technology Data," 2019. [Online]. Available: https://ens.dk/en/our-services/projections-and-models/technology-data

[217] S. Cole, P. Martinot, S. Rapoport, G. Papaefthymiou, and V. Gori, "Study of the Benefits of a Meshed Offshore Grid in the Northern Seas Region: Final Report," European Commission, Tech. Rep., Jul. 2014.

[218] P. Härtel, T. K. Vrana, T. Hennig, M. Von Bonin, E. J. Wiggelinkhuizen, and F. D. Nieuwenhout, "Review of investment model cost parameters for VSC HVDC transmission infrastructure," *Electric Power Systems Research*, vol. 151, pp. 419–431, Oct. 2017. [Online]. Available: https://linkinghub.elsevier.com/retrieve/pii/S0378779617302572

[219] BP, "BP Statistical Review of World Energy," Tech. Rep. 68th edition, 2019. [Online]. Available: https://www.bp.com/content/dam/bp/business-sites/en/global/corporate/pdfs/energy-economics/statistical-review/bp-stats-review-2019-full-report.pdf

[220] P. Icha, Geschäftsstelle der AGEE Stat, and G. Kuhs, "Entwicklung der spezifischen Kohlendioxid-Emissionen des deutschen Strommix in den Jahren 1990 - 2018 [Development of specific carbon dioxide emissions from the German electricity

mix in 1990 - 2018]," Umweltbundesamt, Tech. Rep., Apr. 2019. [Online]. Available: https://www.umweltbundesamt.de/publikationen/entwicklung-der-spezifischen-kohlendioxid-5

[221] International Energy Agency, "Potential for Biomass and Carbon Dioxide Capture and Storage," Tech. Rep., Jul. 2011. [Online]. Available: https://ieaghg.org/publications/technical-reports/reports-list/9-technical-reports/1033-2011-06-potential-for-biomass-and-carbon-dioxide-capture-and-storage

[222] ——, "World Energy Outlook 2017," Tech. Rep., 2017.